

University of Alberta

Identification and Characterization of *mel-43* in *C. elegans*

by

Maryam Ataeian

A thesis submitted to the Faculty of Graduate Studies and Research
in partial fulfilment of the requirements for the degree of

Master of Science

in

Molecular Biology and Genetics

Department of Biological Sciences

©Maryam Ataeian

Spring 2013

Edmonton, Alberta

Permission is hereby granted to the University of Alberta Libraries to reproduce single copies of this thesis and to lend or sell such copies for private, scholarly or scientific research purposes only.

Where the thesis is converted to, or otherwise made available in digital form, the University of Alberta will advise potential users of the thesis of these terms.

The author reserves all other publication and other rights in association with the copyright in the thesis and, except as herein before provided, neither the thesis nor any substantial portion thereof may be printed or otherwise reproduced in any material form whatsoever without the author's prior written permission.

Abstract

In the newly fertilized embryo, meiotic and mitotic spindles form consecutively within the same egg cytoplasm. The order of events during this transition is controlled, in part, via the regulation of the microtubule cytoskeleton. Herein, I show that *mel-43* is part of a small paralogous gene family that is required to specify the meiosis II program of cell division in the fertilized egg. RNAi of *mel-43* and paralogues resulted in failed meiosis I polar body extrusion, followed by direct entry into mitotic prophase. Furthermore, the dominant maternal-effect mutation *mel-43(sb41)* showed a meiosis-to-mitosis transition delay and a failure to segregate chromatids that exhibited persistent REC-8/kleisin immunostaining. Anti-MEL-43 antibodies showed that the MEL-43 proteins exhibited high cytoplasmic levels in meiosis as well as a fibrous staining pattern in the midzone of the anaphase spindle. The protein levels were reduced after meiosis, and this was dependent on the CUL-2/ZYG-11 E3 ligase complex.

Acknowledgment

The accomplishment of this M.Sc would never be possible without the support from many individuals. I would like to express my gratitude to all the people who have been instrumental in the successful completion of this project.

First and foremost, I would like to thank my supervisor, Dr. Martin Srayko, for all his support, encouragement and guidance during the course of my M.Sc at the University of Alberta. His expertise, insight, and attitude have been an endless source of inspiration. I am really glad I had the chance to work with him.

I am deeply grateful to Dr. Shelagh Campbell for her kindness and constant support from the first day I came to the University of Alberta.

I would also like to thank my labmates Tegha, Cheryl, Karen, Megha, Kelly, Eva and my amazing friends especially Farshad for all the friendship and support throughout these years.

Lastly, I extend special thanks to my husband, Ali, and my parents for their constant love and support. This thesis is dedicated to them.

Table of Contents

1. Introduction:	1
1.1 Reproduction	1
1.2 <i>C. elegans</i> as a model to study germline function and post-fertilization events	2
1.3 Oocyte maturation and fertilization	4
1.4 Microtubules	8
1.5 The Centrosome	9
1.6 Meiosis and female meiotic spindle assembly	11
1.6.1 Meiotic chromosome segregation and polar body formation	13
1.6.2 Meiotic spindle positioning.....	14
1.6.3 Cohesins: controlling the segregation of chromosomes	15
1.6.4 Eggshell formation and polarity establishment after fertilization	17
1.7 Mitosis and mitotic spindle assembly	18
1.7.1 Segregation of chromosomes in mitosis.....	20
1.8 The meiosis-to-mitosis transition	21
1.9 Regulation of meiosis I	22
1.10 Regulation of meiosis II	23
1.11 Goals of this thesis	24
1.12 Summary of the thesis	24
2. Materials and Methods	26
2.1 <i>Caenorhabditis elegans</i> nomenclature	26
2.2 <i>C. elegans</i> strains and maintenance	27
2.3 Worm lysis and sequencing	30
2.4 RNAi by feeding	33
2.5 RNAi by injection	34
2.6 Immunostaining	35
2.7 Antibody production	37
2.8 Ex-utero and in-utero confocal imaging	38
2.9 Western blotting for MEL-43	39
3. Results	42

3.1	Characterization of <i>mel-43(sb41)</i>	42
3.1.1	Live imaging characterization of <i>mel-43(sb41)</i> embryos	42
3.1.2	Centrosome maturation in <i>mel-43(sb41)</i> mutants	45
3.1.3	Timing of the events in <i>mel-43(sb41)</i> one cell embryo	48
3.1.4	Chromatid congression and segregation in <i>mel-43(sb41)</i> mutants .	49
3.2	Mapping of <i>mel-43</i>	52
3.2.1	Sequencing of candidate genes	52
3.2.2	Duplication analysis	53
3.2.3	Genomic sequencing of <i>mel-43(sb41)</i> worms	59
3.3	Characterization of two closely-related paralogues of <i>mel-43</i>	63
3.4	Subcellular distribution of <i>mel-43</i>	67
3.4.1	Towards constructing a MEL-43::GFP fusion protein	68
3.4.2	MEL-43 antibody production	70
3.5	Investigating the relationship between MEL-43 and pathways of post-meiotic protein degradation	75
3.5.1	Cyclin B1 degradation in <i>mel-43&mpar-1/2(RNAi)</i> embryos	76
3.5.2	Katanin degradation in <i>mel-43&mpar-1/2(RNAi)</i> embryos	78
3.5.3	Investigation of the APC and cullin-based E3 ligase complex on MEL-43 degradation.....	80
3.6	Assessing REC-8 location in <i>mel-43(sb41)</i> mutants	82
4.	Discussion	86
4.1	<i>mel-43</i> is part of a novel protein family.....	86
4.2	<i>mel-43</i> is required for the meiosis II program	87
4.3	MEL-43 and pathways of post-meiotic protein degradation	90
4.4	<i>mel-43</i> and chromosome segregation	92
4.5	<i>mel-43</i> role in transition from meiosis to mitosis	94
4.6	Mel-43 and cytokinesis	98
4.7	Summary.....	99
5.	Bibliography	100

List of Figures

1-1	The <i>C. elegans</i> reproductive system.....	4
1-2	Early events in the one cell embryo.....	18
2-1	Crossing scheme for generating the double deletion strains.....	30
2-2	Bacterial contamination assessment of the <i>mel-43(sb41)</i> genomic DNA using gel electrophoresis.....	32
2-3	Schematic drawing of the method used for MEL-43 cytoplasmic signal measurements.....	37
3-1	Live imaging of <i>mel-43(sb41)</i> mutants.....	45
3-2	Aurora A kinase is recruited to centrosomes in <i>mel-43(sb41)</i> and wild-type embryos.....	47
3-3	Timing of the events in <i>mel-43(sb41)</i> and wild-type embryos.....	49
3-4	Analysis of meiosis II chromatid congression and segregation in <i>mel-43(sb41)</i> and wild-type embryos.....	51
3-5	Diagram showing regions of two candidate genes (<i>pcn-1</i> and <i>ubc-1</i>) that were sequenced.....	53
3-6	A schematic of the <i>mDp4</i> duplication coverage of chromosome IV.....	54
3-7	Duplication <i>mDp4</i> crossing scheme.....	55
3-8	The duplication <i>mDp4</i> is detected by scoring Dpy-13 in the F2 generation.....	56
3-9	Comparison of the embryonic lethality between embryos heterozygous for <i>mel-43(sb41)</i> and embryos with <i>mDp4</i> duplication over the heterozygous <i>mel-43(sb41)</i>	59
3-10	The map position of <i>mel-43</i> and two paralogues (H02I12.5 and Y62E10A.14) on chromosome IV.....	61
3-11	Identification of <i>mel-43</i> and two paralogues.....	62

3-12 Amino acid sequence alignment of MEL-43 and two closely- related paralogues MPAR-1 and MPAR-2 using CLUSTAL O(1.1.0).....	63
3-13 The MEL-43 paralogue family are required for the female meiosis II program.....	65
3-14 Timing of events in wild-type (red; n = 4) and <i>mel-43&mpar-1/2(RNAi)</i> (green; n = 6) embryos.....	66
3-15 Embryonic viability assessment of different strains having deletions for one or more <i>mel-43</i> paralogues.....	67
3-16 Western blot of worm lysates probed with anti-MEL-43.....	71
3-17 Western blot of wild-type worm lysate, mitotic embryos and males probed with anti-MEL-43.....	72
3-18 Immunofluorescence staining with anti-MEL-43 antibodies....	73
3-19 Immunofluorescence staining of the <i>mel-43&mpar-1/2(RNAi)</i> embryos confirmed the specificity of the antibody.....	74
3-20 Quantification of MEL-43 cytoplasmic levels in meiosis and mitosis of wild-type, <i>mel-43&mpar-1/2(RNAi)</i> and <i>mel-43(sb41)</i> embryos.....	74
3-21 Cyclin B1 degradation in wild-type and <i>mel-43&mpar-1/2 (RNAi)</i> embryos.....	77
3-22 Measurement of the CYB- 1::GFP fluorescence intensity over time.....	78
3-23 MEI-1 degradation in wild-type and <i>mel-43&mpar-1/2 (RNAi)</i> embryos.....	79
3-24 MEL-43 antibody staining of wild-type, <i>mat-3(RNAi)</i> and <i>zyg-11(RNAi)</i> embryos.	81
3-25 Quantification of cytoplasmic levels of MEL-43 in wild-type, <i>zyg-11(RNAi)</i> , <i>mat-2(RNAi)</i> and <i>mat-3(RNAi)</i>	82
3-26 Immunofluorescence staining with anti-REC-8	

antibody on wild- type and <i>mel-43(sb41)</i> embryos.....	85
4-1 MEL-43 and chromatid segregation.....	94
4-2 Fertilization and meiosis II spindle assembly.....	97

List of Tables

2-1 <i>Caenorhabditis elegans</i> strains used in this thesis.....	27
2-2 Primers generated and used for sequencing of candidate genes	33
2-3 Primers generated and used for making dsRNAs.	35
3-1 Observed lethality percentage of progeny from F2 generation with or without mDp4.	58
3-2 Five mutations predicted to alter coding sequence were found in whole genomic sequencing of mel-43(sb41) mutants on chromosome IV.....	60
3-3 Primers generated and used for making MEL-43::GFP transgene.....	69
3-4 Primers generated and used for making a ,<i>mel-43::gfp</i> transgene by the MosSCI technique.....	70

List of Symbols, Abbreviations and Nomenclature

°C	Degrees Celsius
AB	Anterior daughter cell
AIR	Aurora/Ipl1-related serine/threonine kinase
AP	Anterior-posterior
APC/C	Anaphase promoting complex/cyclosome
ATP	Adenosine triphosphate
bp	Base pair
CDK	Cyclin-dependent kinase
CHS	Chitin synthase
CKI	Cyclin-dependent kinase inhibitor
COH	COHesin family
CUL	Cullin
CYB	Cyclin B
DIC	Differential interference contrast
DNA	Deoxyribonucleic acid
DPY	Dumpy
DTC	Distal tip cell
EGG	Egg non-fertilizable
ELC	Elongin C
EMB	Abnormal embryogenesis
GDP	Guanine diphosphate
GFP	Green fluorescent protein
GSP	Glc-seven-like phosphatase
HECT	Homologous to the E6-AP carboxyl terminus
γ TuRC	γ -tubulin ring complex
GTP	Guanosine triphosphate
IPTG	Isopropyl β -D-1-thiogalactopyranoside
KLP	Kinesin-like protein

LAB	long arms of bivalent
L4	larval instar stage 4
LB	Luria Bertani broth
MAP	Microtubule-associated protein
MAPK	Mitogen-activated protein kinase
MAS	Martin A. Srayko (lab designation for <i>C. elegans</i> strains)
MAT	Metaphase-to-anaphase transition defective
MEL	Maternal effect embryonic lethal
MEI	Defective meiosis
MPAR	MEL-43 paralogue
mRNA	Messenger ribonucleic acid
MSP	Major sperm protein
MT	Microtubule
MTOC	Microtubule-organizing center
NEBD	Nuclear envelope breakdown
NGM	Nematode growth medium
P1	Posterior daughter cell
PAGE	Polyacrylamide gel electrophoresis
Par	Partitioning defective
PB	Polar body
PBS	Phosphate buffered saline
PCM	Pericentriolar material
PCR	Polymerase chain reaction
PLK	Polo-like kinase
PP2A	Protein phosphatase 2 A
RanGTP	Ras-related nuclear protein bound to GTP
RBX	Ring-box
RE	Restriction enzyme
REC	Recombination defective
RNA	Ribonucleic acid
RNAi	Ribonucleic acid interference

RSA	Regulator of Spindle Assembly
SAS	Spindle ASsembly abnormal
SDS-PAGE	Sodium dodecyl sulfate polyacrylamide gel electrophoresis
SMC	Structural maintenance of chromosomes
SNP	Single nucleotide polymorphism
SP	Spermatheca
SPD	Spindle defective
SPE	Defective spermatogenesis
TAC	Transforming acid coiled coil protein family
TBST	Tris buffered saline tween 20
TPXL	Targeting protein for xenopus Klp2-like
U Box	Ubiquitination box
UNC	Uncoordinated
UT	Uterus
VU	Vulva
WT	Wild-type
ZYG	Zygote defective

1. Introduction:

1.1 Reproduction

Each individual organism in the world exists as a result of either sexual or asexual reproduction. Asexual reproduction is the process of creating an individual from one cell; therefore the offspring is genetically identical to the parent. This form of reproduction is very simple and it does not involve meiosis or fertilization. Single-celled organisms such as bacteria, archaea and protists reproduce asexually. However asexual reproduction is not limited to single-celled organisms, as many plants and fungi are able to reproduce asexually.

Sexual reproduction is a process that involves the combination of genetic material from two cells, usually contributed by two organisms of different sex, to produce a new individual. This kind of reproduction is more complicated and is used by most animals and plants. Because it involves the combination of genetic material from two cells, the cells that combine to form the new individual undergo a specialized series of cell divisions to reduce the genetic material by half. With diploid organisms, each of the parents divide their genetic material into half and create haploid gametes through a process called meiosis. In animals the haploid gamete from the male sex is called the sperm and the female gamete is the egg. After meiosis, fertilization of the egg by the sperm results in a

fusion of the haploid gametes to create the diploid zygote. The zygote then divides mitotically to produce a new offspring, which has a combination of the parents' genes. Many mechanisms are required to control each stage of the reproductive process, and this thesis addresses the problem of how organisms regulate the transition between the end of female meiosis and the first zygotic cell division after fertilization.

1.2 *C. elegans* as a model to study germline function and post-fertilization events

The *Caenorhabditis elegans* embryo is a powerful experimental system to study cell division mechanisms due to its rapid and highly stereotypical mitotic division and the ease of observing oocyte development and meiotic maturation in anesthetized animals. Some other advantages of this model include simple genetics, the ability to generate strains expressing fluorescent fusion proteins, and the effectiveness of RNA-mediated interference (RNAi).

This nematode has two sexes: self-fertilizing hermaphrodites and males. The time required for an adult hermaphrodite to develop from the egg requires about three days at 20°C. The length of the life cycle is temperature-dependent and worms tolerate a wide temperature range from 25°C to 15°C. Hermaphrodites have two sex chromosomes (XX) and mostly produce hermaphrodite progeny, however mating between male (XO) and hermaphrodite results in 50% males in the offspring. Males are

generated spontaneously in hermaphrodite populations through nondisjunction of the X chromosome during meiosis. Although most of the experiments are conducted with the hermaphrodites, males can be used for generating new heterozygous strains by crossing them into the desired strain. Upon mating, the male-derived sperm is selected over the hermaphrodite sperm, thus allowing straight-forward genetics and logical interpretation of phenotypes resulting from successful mating.

The reproductive system of the adult hermaphrodite is composed of two U-shaped gonads, each having a syncitium of germline nuclei (Figure 1-1). In hermaphrodites, the germline nuclei are born in the distal portion of the gonad and they gradually migrate proximally, whereupon they mature into sperm in the L4 larval stage, or into oocytes in the adult stage. The production and maturation of the germ cells is controlled by the distal tip cell (DTC) (Kimble and White, 1981). After the nuclei move far enough from the DTC and reach the transition zone, the nuclei enter meiotic prophase (Figure 1-1). The meiotic cells briefly arrest in pachytene before continuing to diplotene. After condensation of the chromosomes, the cells enter diakinesis and arrest for a second time in the female germline. During sperm production, these cells exit pachytene without delay and complete gametogenesis. In both oocyte and sperm, activation of the mitogen-activated protein kinase (MAPK) causes the exit from pachytene (Church et al., 1995). At the most proximal part of each gonad arm is a specialized sac called the spermathecae, which stores the sperm (Figure

1-1). Once fully mature, the oocytes travel through the spermatheca, become fertilized, and enter the uterus, located between the two spermathecae. Young embryos complete the very early stages of development in the uterus before exiting through the vulva.

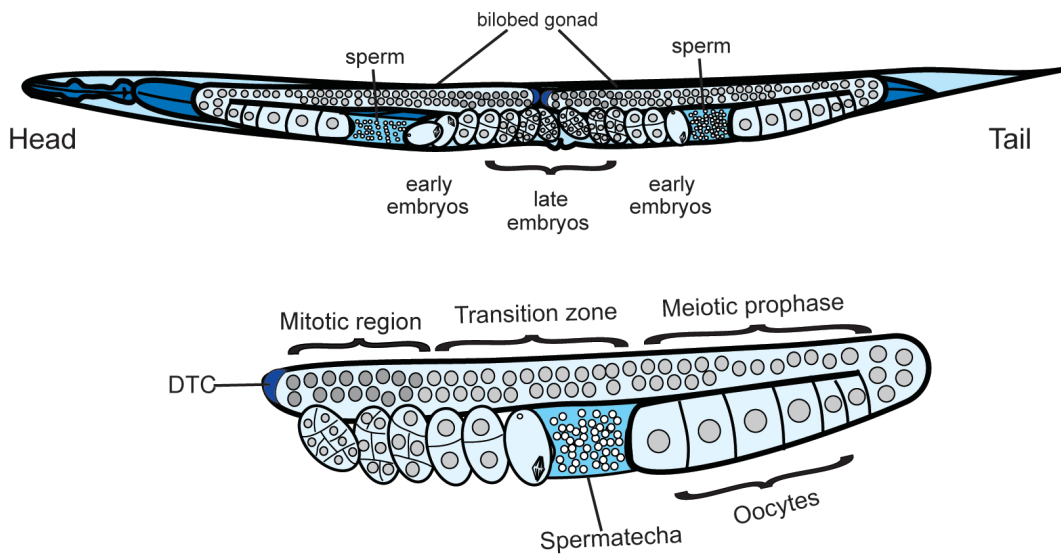


Figure1-1: The *C. elegans* reproductive system. On top is a schematic drawing of an adult hermaphrodite. The reproductive system consists of two U-shaped gonads with a distal tip cell (DTC) at the distal end to the spermatheca at the proximal end. On bottom is a drawing of one gonad arm. The DTC sends a signal for mitotic proliferation of the germ nuclei. As the nuclei move away from the distal tip, they enter the transition zone and begin meiotic development. Their progress through meiotic prophase continues as they move proximally and become encased in a plasma membrane. The oocytes grow in size and enter the spermatheca for fertilization by sperm. The fertilized embryos undergo early stages of development within the uterus, until they exit via the vulva.

1.3 Oocyte maturation and fertilization

Oocytes provide the maternal components essential for the developing zygote after fertilization, and sperm needs to be motile and

capable of penetrating the egg, therefore, each gamete has a unique maturation process. Although the end product of maturation for both oocytes and spermatocytes are haploid gametes, meiosis is regulated differently in these germ cells. Typically, spermatocyte meiosis proceeds uninterrupted, however, oocytes arrest once or twice during meiosis, depending on the species.

The distinct stages of arrest for oocytes during meiosis allow different phases of growth and differentiation. The first arrest occurs at prophase I and can remain for several weeks in lower animals and for years in higher vertebrates. In most of the animals, release from this first arrest requires hormones such as progesterone in *Xenopus* and 1-methyladenine in starfish. The release from prophase I and the transition from diakinesis to metaphase of meiosis I is called oocyte meiotic maturation and leads to nuclear envelope breakdown, cortical cytoskeleton rearrangements and the formation of the meiosis I spindle. This maturation process depends on the activity of cyclin B/cdk1. Active cyclin B/cdk1 phosphorylates proteins required for germinal vesicle breakdown and the transition from prophase into metaphase (Kishimoto, 1998; Abrieu et al., 2001). The second arrest allows the coordination between fertilization and the completion of meiosis. Most vertebrate oocytes arrest at meiosis II in anticipation of fertilization (Tunquist and Maller, 2003), whereas insects arrest at meiosis I and starfish in G1 after completion of both meioses. Fertilization in vertebrates activates the

anaphase-promoting complex, which targets cyclin B for degradation and inactivates cdk1 (Nixon et al., 2002). Inactivation of cdk1 allows the exit from meiotic metaphase II and promotes the formation of a nuclear envelope around the male and female chromatin, visualized as pronuclei.

In *C. elegans*, sperm signaling through the major sperm protein (MSP) is responsible for final maturation of the oocytes. MSP is the ligand that regulates maturation of the oocytes, reorganization of the microtubules, actin-based cytoplasmic streaming in the oocyte, and contraction of the sheath cells (Miller et al., 2001; Harris et al., 2006; Govindan et al., 2009). Almost every 23 minutes, meiotic maturation occurs for the oldest oocyte in the gonad (McCarter et al., 1999) due to the secreted MSP from sperm in the neighboring spermatheca. Upon receiving the MSP signal, the oocyte exhibits nuclear envelope breakdown (NEBD) and microtubules accumulate around the meiotic chromatin. The contraction of the sheath cell causes the opening of the spermatheca and the oocyte enters the spermatheca, allowing fertilization (McCarter et al., 1999). Cyclin/cdk is required for phosphorylation of the substrates that have a role in meiotic maturation including nuclear envelope breakdown, condensation of the chromosomes and assembly of the spindle (Boxem et al., 1999; Burrows et al., 2006). Often, meiosis I spindle assembly initiates before the oocyte enters the spermatheca and continues after the zygote enters the uterus (Yang et al., 2003). In the uterus, the embryo completes meiosis and begins the early stages of embryogenesis.

Fertilization is critical for the successful development of the worm, but also for the behaviour of cell-cycle dependent events in the one-cell embryo. Mature, unfertilized oocytes still assemble a functional meiosis I spindle, which segregates chromosomes in anaphase I at the right time. However, these unfertilized embryos fail to extrude the first polar body and they do not form the second meiotic spindle (McNally and McNally, 2005). Therefore, the sperm contributes to the maturation of the oocyte (via MSP signalling before fertilization) as well as to the execution of the female meiotic programme (via a mechanism that requires sperm entry).

In *C. elegans*, the APC (anaphase promoting complex; see below) is required for the completion of meiosis I (Golden et al., 2000). Since unfertilized embryos are able to complete the metaphase-to-anaphase transition in meiosis I, it can be concluded that APC activation and function is independent of fertilization.

SPE-11 is one of the key proteins required for the completion of meiosis and formation of the eggshell in the embryo. The sperm provides SPE-11 after fertilization (Hill et al., 1989). Embryos fertilized by sperm devoid of SPE-11 are able to assemble the second meiotic spindle, however they fail to complete the first cytokinesis and extrude the first polar body (McNally and McNally, 2005). These observations reveal that sperm-derived proteins regulate the extrusion of the first polar body and formation of the second meiotic spindle through two different pathways.

Chromosome segregation in both meiosis and mitosis depends on the formation of a specialized structure termed the spindle apparatus. Some important features of this cellular machine, as well as specific structural and functional distinctions between female meiotic spindles and their mitotic counterparts are discussed.

1.4 Microtubules

Microtubules, one of the main components of meiotic and mitotic spindles, are long polymeric cytoskeletal fibres that can be found throughout the cytoplasm. Microtubules have multiple roles in the cell, for instance, they are important for cell structure, transport of vesicles and organelles, and cell division. The microtubule polymer is composed of α - and β - tubulin dimers, and the fibre grows by addition (polymerization) or removal (depolymerization) of these dimers (Mitchison and Kirschner, 1984; Kirschner and Mitchison, 1986). Microtubules exhibit dynamic instability, whereby they switch between periods of growth and shrinkage. This dynamic instability depends on GTP hydrolysis. Most of the tubulin dimers have GTP bound to their β subunit. Hydrolysis of the GTP to GDP at the tip of the microtubules causes the depolymerization and fibre shrinkage, termed a catastrophe (Hyman et al., 1992; Drechsel and Kirschner, 1994). During cell division microtubules organise into a spindle apparatus, which facilitates the segregation of genetic material and specifies the cleavage plane of the cell during cytokinesis.

Polymerization of the microtubules occurs by addition of the α -subunit of one dimer to the β -subunit of the other one, which causes a polarity to the fibre. Therefore, one end will have exposed α -subunits (the minus end) while the other end will have a β -subunit exposed (the plus end). This polarity has consequences for microtubule dynamics since heterodimers are added or removed preferentially from the plus end, which makes this end faster growing and more dynamic (Mitchison and Kirschner, 1984). The minus end is usually relatively static and often anchored to specific subcellular organelles, termed microtubule-organizing centers (MTOCs).

In the cell, the MTOC contributes to the overall polarity of the microtubule network. Directed transport of intracellular cargo can occur along the microtubule network. Microtubule motor proteins utilize ATP hydrolysis to physically move cargo along the microtubules. Two important motor proteins are kinesin, which moves toward the + end of the microtubules, and dynein, which moves toward the – end.

1.5 The Centrosome

The centrosome is the primary MTOC in most animal cells. Each cell has a pair of centrosomes that act as two poles of the spindle (Doxsey et al., 2005). They also participate in mitotic spindle positioning, chromosome segregation, and cytokinesis (Piel et al., 2001; Manneville and Etienne-Manneville, 2006).

The basic structure of the centrosome is conserved in different species, although centrosome morphology can vary. One important structural feature is the centriole, which resides at the centre of the centrosome. Depending on the stage of the cell cycle, centrosomes will have a single centriole or a pair of centrioles (one mother centriole and one daughter centriole) (Bobinnec et al., 1998; Luders and Stearns, 2007). *C. elegans* centrioles are barrel-shaped structures composed of nine singlet symmetric microtubules. Although the mechanism is unknown, centrioles are necessary to recruit and organize pericentriolar material (PCM), which is a microtubule nucleation and anchoring scaffold comprising many different proteins (Strome et al., 2001; Azimzadeh and Bornens, 2007).

To build a bipolar spindle, centrosomes must duplicate exactly once per cell cycle during S phase. When the sperm enters the egg in *C. elegans*, it brings a pair of centrioles. Soon after fertilization, centrioles start to recruit pericentriolar material and each centriole separates to form two centrosomes, each having a single centriole (O'Connell, 2000; Pelletier et al., 2004). After that, the new daughter centrioles begin to grow out from the mother centrioles in an orthogonal arrangement. During centrosome maturation, recruitment of additional PCM causes an increase in size and microtubule-nucleating capacity (Hannak et al., 2001). In telophase centriole pairs split and by cytokinesis two small centrosomes can be observed in each daughter cell.

The pericentriolar material consists of many different proteins. One group is known as the centromatrix proteins (Bornens, 2002), which are required to recruit other PCM components. Coiled coil proteins, SPD-5 and SPD-2, as well as AIR-1 protein kinase are members of this group and they are necessary for the maturation of the PCM. The next set of proteins are γ -tubulin, CeGrip-1, and CeGrip-2 which are involved in the microtubule nucleating and anchoring activity of the PCM (Hannak et al., 2002; O'Toole et al., 2012). Growth of microtubules depends on two conserved proteins, ZYG-9 (XMAP-215 MT-polymerization factor homolog) and TAC-1 (TACC, transforming acidic coiled-coil protein) (Srayko et al., 2003). Centrosome duplication requires a distinct set of proteins including SAS-4, SAS-5, SAS-6, and the polo-like kinase ZYG-1 (O'Connell et al., 2001; Leidel and Gonczy, 2003; Delattre et al., 2004; Leidel et al., 2005), all of which are required for daughter centriole formation. Depletion of any single protein from the maternal cytoplasm results in a monopolar spindle in each of the two daughter cells after the first division. SPD-2 (Kemp et al., 2004), SPD-5 and γ -tubulin (Dammermann et al., 2004; O'Toole et al., 2012) also have a role in centriole assembly as well as a function in PCM recruitment and microtubule nucleation.

1.6 Meiosis and female meiotic spindle assembly

Although the centrosomes are clearly essential for most animal mitosis, plant cells and some specialized animal cells do not have them. In

C. elegans the female germ cells eliminate their centrioles during diplotene of the oocyte maturation process (Zhou et al., 2009; Mikeladze-Dvali et al., 2012). This process is likely regulated by the cyclin-dependent kinase inhibitor-2 (*cki-2*). In *cki-2* mutants, failure in elimination of the centrosomes results in multipolar mitotic spindles (Kim and Roy, 2006). Because the oocytes are normally devoid of centrioles, a specialized pathway is used for nucleating and organising microtubules during female meiotic spindle assembly. Microtubules initially coalesce around the meiotic chromatin and the microtubules subsequently organize into a barrel-like spindle structure that is both acentriolar and anastral (Albertson and Thomson, 1982; Howe et al., 2001; Yang et al., 2003). The small GTPase Ran has been implicated in stabilizing microtubules near chromatin (Kalab and Heald, 2008). The guanine exchange factor RCC-1 is located at chromatin and generates a Ran-GTP concentration gradient around chromatin, which results in stabilization of microtubules near the chromatin (Bischoff and Ponstingl, 1991). However, in *C. elegans*, Ran-GTP is not required for female meiotic spindle assembly and it seems to have a role in assembly of the mitotic spindle suggesting a different mechanism for microtubule nucleation when centrosomes are absent (Askjaer et al., 2002).

Among the components required for meiotic spindle assembly, one class of microtubule regulators seems to play an important role specifically during female meiotic spindle assembly. *mei-1* and *mei-2* encode subunits

of the microtubule-severing protein called katanin (Srayko et al., 2000). Katanin was first purified from sea *urchin* eggs (McNally and Vale, 1993) based on its ability to sever microtubules into short fragments (Vale, 1991). Meiotic spindle length and shortening is also controlled with katanin (McNally et al., 2006). In *mei-1* mutants, chromatin is surrounded with fewer microtubules, which are very long and not organized into a bipolar spindle (Srayko et al., 2006). This work suggested that, in acentrosomal female meiosis, relatively inefficient microtubule-nucleating chromatin generates a few long microtubules, which are converted into many short fragments by katanin, and that this is necessary to assemble the female meiotic spindle. At the end of female meiosis, degradation of katanin must occur through ubiquitin-mediated proteolysis (Pintard et al., 2003a), as persistence of katanin in mitosis results in mitotic defects, including short spindles, errors in chromosome segregation and cytokinesis (Clark-Maguire and Mains, 1994). Therefore, katanin seems to facilitate acentrosomal meiotic spindle assembly by increasing the number of microtubules and promoting their organization (Srayko et al., 2006).

1.6.1 Meiotic chromosome segregation and polar body formation

Each of the two female meiotic divisions takes about 20 minutes to complete. Although the structures and behaviours of the two meiotic spindles are very similar, they accomplish different tasks with respect to chromosome segregation. In anaphase I, segregation of the homologous

chromosomes occurs and extrusion of one set of homologues near the cortex produces the first polar body (Figure 1-2). This meiotic division is reductional, since the genetic information is halved. Immediately after the first meiotic division and extrusion of the first polar body, the second meiotic spindle forms near the cortex. At anaphase II, sister chromatids segregate to form the second polar body and a haploid female pronucleus that is ready for fusion with the male haploid counterpart (Figure 1-2).

1.6.2 Meiotic spindle positioning

In both of the meiotic divisions, the small size of the spindles and their association with the cortex result in an extremely asymmetric division culminating in the extrusion of small polar bodies. Therefore, minimal cytoplasm is lost during the meiosis divisions. The first meiotic spindle initially forms parallel to the cortex and then rotates until the spindle axis is orthogonal to the cortical surface. Cortical localization of the meiotic spindle is controlled through two mechanisms. Early translocation occurs before nuclear envelope breakdown (McCarter et al., 1999; McNally et al., 2010). This first oocyte nuclear migration requires *mpk-1* (Lee et al., 2007) and *kinesin-1* (McNally et al., 2010) functions and fertilization is not required for this process. In the second translocation, the meiotic spindle rotates 90° prior to anaphase to facilitate the extrusion of polar bodies. This late translocation requires the APC (Yang et al., 2005) in addition to the motor protein dynein (Ellefson and McNally, 2009). NUMA-related LIN-5, ASPM-1 and calmodulin CMD-1 are also involved in this translocation

(van der Voet et al., 2009). It has been shown that active cyclinB/CDK1 is able to inhibit the rotation and shortening of the meiotic spindle. Degradation of the cyclin B results in the function of the APC complex for rotation of the spindle and segregation of the chromosomes (Ellefson and McNally, 2011).

1.6.3 Cohesins: controlling the segregation of chromosomes

Failure to segregate the sister chromatids in either mitosis or meiosis results in aneuploidy with significant consequences such as tumorigenesis and congenital defects (Hassold and Hunt, 2001; Kops et al., 2005). The cohesins are proteins that physically link homologues and sister chromatids, and they play an important role in controlling how chromosomes separate in the two meiotic divisions. The cohesin complex is composed of two SMC (structural maintenance of chromosomes) core proteins (Smc1 and Smc3) and two non-SMC proteins (Scc1/Rad21/kleisin and Scc3, an accessory protein) (Michaelis et al., 1997). The kleisin subunit links the ends of the Smc1/Smc3 heterodimers to form a ring-like structure, which joins the chromosomes together (Nasmyth and Haering, 2005). In many organisms such as *C. elegans*, the Scc1/Rad21/kleisin is replaced by its paralogue, REC-8, in meiosis (Watanabe and Nurse, 1999). To allow the segregation of chromosomes at anaphase, cohesin must be removed through the degradation of the kleisin subunit (Uhlmann et al., 1999; Buonomo et al., 2000).

This process is especially complex during the first meiosis, because homologues must segregate without allowing their associated sister chromatids to be released. *C. elegans* has holocentric chromosomes and attachment of microtubules to chromosomes is through both lateral and poleward ends (Albertson and Thomson, 1982). It has been shown that during meiosis I, LAB-1 (Long Arm of the Bivalent) binds to the chromosomes to protect sister chromatids from AIR-2 Aurora B kinase phosphorylation, via the opposing activity of GSP-2 phosphatase (Kaitna et al., 2000; Rogers et al., 2002; de Carvalho et al., 2008). Therefore, during meiosis I, AIR-2 has access only to the interface between homologous chromosomes where it phosphorylates the meiosis-specific cohesin subunit, REC-8/kleisin. This phosphorylation results in removal of REC-8 specifically between homologues, and cleavage of the cohesin ring by separase at anaphase I. In *C. elegans* there are three meiosis-specific kleisin paralogues, REC-8, COH-3, and COH-4 (Severson et al., 2009). However, among these, REC-8 is specifically retained for sister chromatid cohesion (Severson et al., 2009). In anaphase II, removal of REC-8 from sister chromatids allows their segregation.

1.6.4 Eggshell formation and polarity establishment after fertilization

Coincident with meiotic spindle assembly, a number of other important transformations occur after fertilization of the egg. For example, a chitinous eggshell forms around the developing zygote after fertilization, providing physical and osmotic protection during embryonic development. Formation of the eggshell requires EGG-3, EGG-4, and EGG-5 (tyrosine phosphatase-like proteins) and chitin synthetase, CHS-1 (Johnston et al., 2006; Maruyama et al., 2007; Parry et al., 2009). These proteins are also required for completion of meiosis, formation of the polar body and prevention of polyspermy.

Polarization of the embryo also begins at fertilization and is evidenced by the distribution of anterior and posterior cortical PAR proteins (partitioning defective). The point of sperm entry specifies the future posterior half of the embryo.

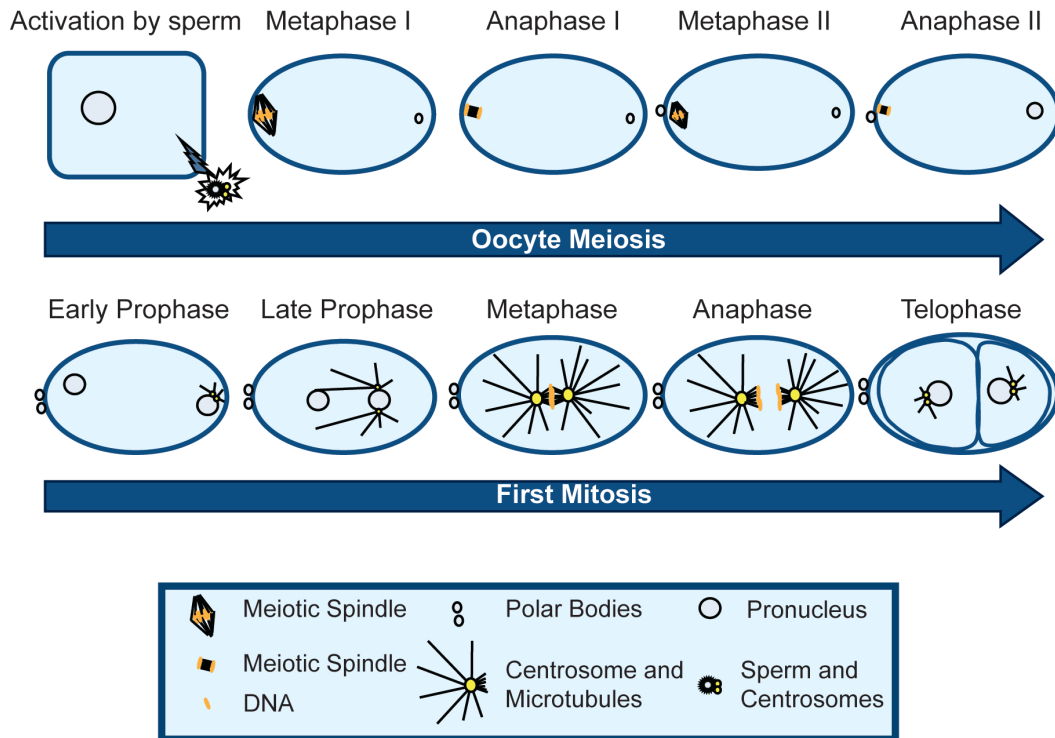


Figure 1-2: Early events in the one cell embryo. (On top row from left) sperm activates the oocyte and brings two centrioles into the oocyte by fertilization. Sperm entry triggers the meiotic spindle assembly in metaphase I and then it follows by the extrusion of first polar body in anaphase I and second polar body in anaphase II. (On bottom row from left) after completion of meiosis, sperm centrosomes start nucleating the microtubules. Then the female pronucleus migrate slowly toward the posterior end of the embryo and then it gets faster when centrosomal microtubules reach the pronucleus. After rotation and centring of the two pronuclei, the nuclear envelope breakdown facilitates the congression of the chromosomes in metaphase, which follows by anaphase. In telophase, an asymmetric division creates a smaller posterior cell (P1) and larger anterior cell (AB).

1.7 Mitosis and mitotic spindle assembly

The sperm provides a haploid pronucleus as well as the pair of centrioles to the oocyte. However these centrioles do not mature until after the completion of meiotic division when centrosomes start to mature and

nucleate microtubules (Figure 1-2). The presence of centrosomal microtubules prior to completion of the meiotic division would interfere with the meiotic spindle and affect the chromosome segregation. After completion of meiosis, the chromosomes of the haploid pronuclei condense and increase in size. Then the two centrioles of the sperm separate from each other and produce a pair of mature centrosomes. The two centrosomes stay tightly associated with the sperm pronucleus but move to opposite sides of the pronuclear envelope as they separate. Cytoplasmic flows caused by polarity-induced cortical contractions of the embryo help push the oocyte pronucleus towards the posterior end of the embryo where it can make contact with the centrosomal microtubules of the sperm pronucleus. These microtubules facilitate faster migration of the female pronucleus toward the sperm. After meeting of the two pronuclei they come to the centre of the embryo and rotate so that the centrosomes are placed along the long axis of the embryo. At this point nuclear envelope breakdown (NEBD) occurs and microtubules attach to the chromosomes (Figure 1-2). Then the mitotic spindle skews towards the posterior side of the embryo. After that, in anaphase, chromosomes segregate and an asymmetric cytokinesis results in one larger anterior daughter cell (AB) and one smaller posterior daughter cell (P1) (Figure 1-2). Therefore, despite their morphological and functional differences, meiotic and mitotic spindles are assembled sequentially in the same cytoplasm.

Several proteins that play key roles in spindle assembly in mitosis have been identified. Most of them locate to the centrosomes or the spindle microtubules. Aurora kinases are important regulators of mitotic spindle assembly as they have roles in centrosome maturation, spindle assembly, chromosome segregation and cytokinesis (Glover et al., 1995; Gopalan et al., 1997; Andrews et al., 2003). Two different Aurora kinases exists in metazoans, Aurora A and Aurora B (AIR-1 and AIR-2 in *C. elegans*) (Schumacher et al., 1998a; Schumacher et al., 1998b). Aurora B is a chromosomal passenger complex member and associates with the kinetochores until anaphase (Ruchaud et al., 2007). Aurora A localizes to the centrosomes and spindle microtubules, and in *C. elegans*, AIR-1 promotes centrosome maturation and microtubule nucleation, spindle assembly and nuclear envelope breakdown (Schumacher et al., 1998a; Ozlu et al., 2005; Portier et al., 2007). A PP2A protein phosphatase complex RSA (regulator of spindle assembly) is also important for mitotic spindle assembly, however it acts downstream of centrosome maturation. RSA promotes centrosomal microtubule outgrowth and stability during mitotic spindle assembly, likely through a combination of down-regulating the microtubule depolymerase KLP-7 and up-regulating the microtubule-stabilizing protein TPXL-1 (Schlaitz et al., 2007).

1.7.1 Segregation of chromosomes in mitosis

In most eukaryotes, segregation of chromosomes in mitosis is achieved by removal of the cohesion through phosphorylation events.

Activity of a Polo-like kinase (Plk1/Cdc5) prior to entry into metaphase releases the cohesin from chromosome arms (Sumara et al., 2002). During the transition from metaphase to anaphase PLK1 releases the cohesin complex around the centromeres (Hornig and Uhlmann, 2004).

1.8 The meiosis-to-mitosis transition

Once activated by the MSP, the oocyte proceeds past diakinesis and begins meiotic spindle assembly to segregate homologous chromosomes. Normally the sperm also enters at this time, which creates a special problem for the cell. The two acentrosomal meiotic divisions must occur even though sperm DNA and centrioles are present in the same cytoplasm. In the absence of zygotic transcription, regulation of the proteins required to assemble the two meiotic spindles as well as the subsequent first mitotic spindle is vital. For instance, katanin is only required during meiosis and it must be removed or inactivated prior to mitosis. On the other hand, mitosis-specific proteins must be inhibited until after meiosis, otherwise the mitotic spindle would assemble before the completion of meiosis. Therefore, coordination between the stages of meiosis and mitosis is crucial in the one-cell embryo.

Ubiquitination of substrates and their destruction via the proteasome is a process used by the cell to degrade proteins, and this is an important method of regulating protein activity during the meiosis-to-mitosis transition. Meiotic and mitotic phenotypes observed in some mutants can be directly related to this degradation pathway. For example,

degradation of katanin at the end of meiosis requires the E3 ubiquitin-protein ligase complex (Pintard et al., 2003a; Pintard et al., 2003b). In *C. elegans*, the ubiquitin-mediated proteolysis machinery consists of a single 26S proteasome, ubiquitin, one ubiquitin-activating enzyme (E1), over 20 ubiquitin-conjugating enzymes (E2s), and hundreds of ubiquitin-protein ligases (E3s). The protein ligases can be grouped into four categories: U-box proteins, monomeric RING finger proteins, HECT-domain proteins, and multimeric complexes with a RING finger protein (Kipreos, E. T., 2005, wormbook). The multimeric RING finger complex class can be grouped into cullin-based complexes and the anaphase-promoting complex (APC).

1.9 Regulation of meiosis I

Separation of the chromosomes during anaphase of mitosis is dependent on the Anaphase Promoting Complex (APC) and in *C. elegans*, the first meiotic division is dependent on the APC, which promotes the metaphase I to anaphase I transition (Golden et al., 2000; Davis et al., 2002). One of the proteins targeted for destruction is securin, the loss of which releases the cysteine protease separase from inhibition, allowing cleavage of cohesin (Davis et al., 2002). In addition, degradation of B-type cyclins by the APC in metaphase results in inactivation of the cyclin-dependent kinase (CDKs) and exit from metaphase (Liu et al., 2004; Sonnevile and Gonczy, 2004). Loss of APC function prevents segregation of homologous chromosomes and no polar body extrusion; these embryos arrest at the one-cell stage (Golden et al., 2000). At least five different

genes found to encode components of the APC: *mat-1*, *mat-2*, *mat-3*, *emb-27* and *emb-30* (Golden et al., 2000). It also has been suggested that the APC and the CUL-2 pathway have partially redundant functions during meiosis I, since *cul-2(RNAi)* enhanced the meiosis I defects of a temperature-sensitive allele of *mat-1* at the permissive temperature of 15°C (Sonneville and Gonczy, 2004).

1.10 Regulation of meiosis II

At least one other E3 ligase has been implicated in progression through meiosis II (Liu et al., 2004; Sonneville and Gonczy, 2004). This cullin-based E3 ligase complex contains four important subunits: adaptor protein elongin C (ELC-1), ring-box 1 protein (RBX-1), substrate recognition subunit (ZYG-11), and the protein ligase (CUL-2). ZYG-11 binds elongin C to directly interact with the CUL-2 E3 complex (Vasudevan et al., 2007). Knock out of *cul-2* results in metaphase II delays and failure to complete anaphase. *zyg-11* embryos exhibit meiosis II delays and although most of them eventually go through anaphase, they do not extrude the second polar body. The meiosis II delay in these mutants could be rescued by removal of CYB-1, which shows that degradation of B-type cyclins is a major substrate of the CUL-2 pathway and that high levels of CYB-1 are responsible for the delay (Liu et al., 2004).

1.11 Goals of this thesis

This thesis started with three main goals that centred on understanding the phenotypes caused by *mel-43(sb41)*, a mutation that perturbs the meiosis-to-mitosis transition in *C. elegans*. The first aim was to identify the *mel-43* gene using genetic and molecular approaches. The second aim was to further characterize the phenotypes caused by the *mel-43(sb41)* mutation. The third aim was to determine the subcellular distribution of the MEL-43 protein in the embryos and relate this information to MEL-43 function during the meiosis-to-mitosis transition.

1.12 Summary of the thesis

mel-43(sb41) is a dominant, temperature-sensitive, maternal-effect mutation that is required for early embryonic viability (Mitenko et al., 1997). Through in vivo imaging, I have found that these mutants exhibit abnormal first cell division as well as microtubule cytoskeleton defects at the end of meiosis II. Consequently, the mutant embryos fail to extrude the second polar body and display a significant delay during the transition from metaphase II to mitosis. These embryos exhibited extensive cytoplasmic blebbing as well as improper polarity establishment; however, the centrosome maturation seemed to occur normally. Chromosomal duplication analysis suggested that *mel-43(sb41)* was a hypermorphic gain-of-function mutation. Genomic sequencing revealed a missense mutation in the coding region of the *y17g9b.9* gene and RNAi against this

gene rescued the *mel-43(sb41)* mutant phenotype. *mel-43* is predicted to encode a novel, potentially nematode-specific protein. *mel-43* has two very similar paralogues, called in this thesis *mpar-1* and *mpar-2*. *mel-43(RNAi)* and *mel-43(deletion)* embryos were phenotypically wild type, however, RNAi predicted to target all three paralogues resulted in a highly penetrant embryonic lethal phenotype. Interestingly, these embryos did not extrude the polar body at the end of meiosis I, and rather than assemble a meiosis II spindle, they proceeded directly into mitosis. Immunostaining revealed high cytoplasmic levels for MEL-43 in meiosis as well as a fibrous staining pattern in the midzone of the anaphase spindle that was most obvious in meiosis II. MEL-43 and paralogues were not required for the normal degradation of cyclin B1 and katanin, however, *zyg-11(RNAi)* resulted in persistent high cytoplasmic levels of MEL-43 protein in mitosis, suggesting that the cullin-based E3 ligase complex degrades MEL-43 at the end of meiosis. Chromosome segregation analysis in the hypermorphic mutant *mel-43(sb41)* embryos showed that the persistence of the REC-8/kleisin on sister chromatids correlates with the failure of anaphase II in *mel-43(sb41)* mutants, suggesting that down-regulation of *mel-43* is required for proper exit from meiosis. This work has revealed a novel protein family that specifies the female meiosis II programme.

2. Materials and Methods

2.1 *Caenorhabditis elegans* nomenclature

C. elegans genes are designated by an italicized three or four letter name that typically describes gene function or mutant phenotype (Horvitz et al., 1979), followed by a hyphen and an Arabic number. For instance, *dpy-20* is one of many genes so labelled because they result in a Dumpy phenotype when mutated. A specific allele of the gene is placed in parentheses after the gene name using a unique laboratory code of one to three letters (e.g. “*abc*” refers to alleles discovered in the Srayko laboratory; AB, Canada). Phenotypes caused by RNAi methods can also be written as genetic alleles. For example, *zyg-11(RNAi)* indicates double stranded RNA-mediated interference of *zyg-11*. Protein products of a gene are written in capitals and non-italicized letters (e.g. DPY-20). Phenotypes can be described using the complete word (e.g. Dumpy) or a three-letter abbreviation (e.g. Dpy). Strain designations comprise two or three uppercase letters followed by a number and are named by laboratory of origin (e.g. the Srayko laboratory strain designation is MAS).

2.2 *C. elegans* strains and maintenance

Table 2-1: *Caenorhabditis elegans* strains used in this thesis.

Strain	Genotype
MAS89	<i>mel-43(sb41) dpy-20(e1282)/nT1[unc(n754dm) let] IV; +/nT1 V; pie-1::GFP::cyb-1</i>
MAS91	<i>mcherry::histone IV; GFP::βtubulin</i>
MAS100	<i>mel-43(sb41) dpy-20(e1282)/ dpy-13(e184) unc-24(e138) IV; mDp4 [unc-17(e245)</i>
MAS123	<i>y17g9b.9(tm3099), y62e10a.14(tm2638) IV</i>
MAS131	<i>y17g9b.9(tm3099) IV</i>
MAS132	<i>y62e10a.14(tm2638) IV</i>
MAS133	<i>h02i12.5(tm3158) IV</i>
MAS134	<i>y17g9b.9(tm3099), h02i12.5(tm3158) IV</i>
MAS135	<i>y62e10a.14(tm2638), h02i12.5(tm3158) IV</i>
MAS137	<i>mel-43(sb41) dpy-20(e1282) IV</i>
MAS138	<i>mel-43(sb41), mcherry::histone IV; GFP::βtubulin</i>
DR1786	<i>dpy-13(e184) unc-24(e138) IV; mDp4[unc-17(e245) IV</i>
EU1060	<i>unc-119(+);pei-1::GFP-mei-1</i>
ET113	<i>pie-1::GFP-cyb-1</i>
FX03099	<i>y17g9b.9(tm3099)IV</i>
FX03158	<i>ho2i12.5(tm3158) IV</i>
FX02638	<i>y62e10a.14(tm2638) IV</i>
HR592	<i>mel-43(sb41) dpy-20(e1282)/nT1[unc(n754dm) let] IV; +/nT1 V</i>

All *C. elegans* strains were cultured on Nematode Growth Medium (NGM) plates and were seeded with a uracil auxotrophic *Escherichia coli* strain referred to as OP50 (Brenner, 1974). HR592 was obtained directly from Dr. Paul Mains' laboratory (University of Calgary), strain ET113 was kindly sent by Dr. Edward Kipreos (University of Georgia), FX03099,

FX03158 and FX02638 were received from National Bioresource Project (Tokyo, Japan). All the other strains were either obtained from the Caenorhabditis Genetics Centre (CGC) or generated within the Srayko laboratory (MAS-designated strains).

N2, ET113, DR1786 and EU1060 were maintained at 25°C, while HR592, MAS137 and MAS138 were maintained at 15°C, due to temperature-sensitivity at 25°C. The rest of the strains were kept at 20°C. HR592 was maintained by picking individual Unc worms and checking for proper segregation of parental heterozygotes. For HR592, the following segregants are expected: Uncs, *mel-43(sb41) dpy-20/nT1[unc(n754dm) let]*, Dpys (*mel-43(sb41) dpy-20* homozygotes) and dead eggs (*nT1[unc(n754dm) let]* homozygotes). DR1786 strain contains an *mDp4* duplication and maintained by picking wild-types and checking for proper segregation of the progeny: wild type, Dpy-13, Unc-24, Dpy-13 Unc-24 and dead eggs (*mDp4[unc-17(e245)* homozygotes). The GFP and mCherry transgenes are expressed under control of the germline promoter, *pie-1* (Praitis et al., 2001). FX03099 is deleted for *mel-43*. FX03158 and FX02638 contain the deletion mutation of *mpar-1* and *mpar-2* respectively.

MAS100 was made by crossing DR1786 hermaphrodites to *mel-43(sb41) dpy-20(e1282)/ + males*. In the course of constructing a *mel-43(sb41)* strain that expressed mCherry::histone and GFP::tubulin, I noticed that the mCherry::histone transgene exhibited genetic linkage with the *mel-43(sb41)* mutation. Therefore, MAS138 was made in two steps.

First, N2 males were crossed to the MAS91 strain homozygous for both transgenes to generate heterozygous males, which were crossed to HR592 hermaphrodites to generate *nonGFP* and *GFP::tubulin/+* males that were also heterozygous for *mel-43(sb41)* and *dpy-20*. Individual males were mated with HR592 to generate hermaphrodites homozygous for *mel-43(sb41) dpy-20* and heterozygous for *GFP::tubulin*. Self-fertilization generated a strain homozygous for both *mel-43(sb41) dpy-20* and *GFP::tubulin*. In the next step, these homozygous hermaphrodites were crossed to *GFP::tubulin; mCherry::histone* heterozygous males to generate the strain heterozygous for *mCherry::histone* and *mel-43(sb41) dpy-20* and homozygous for *GFP tubulin*. These were allowed to self-fertilize and crossover products were screened for strong mCherry fluorescence (evidence of homozygosity) via microscopy.

Double-deletion strains (MAS123, MAS134, MAS135) were made by crossing two single deletion strains and generating trans-heterozygotes for each of the deletions. All three genes are on the same chromosome (Figure 2-1), thus the trans-heterozygotes were allowed to self-fertilize, and crossovers that created a double deletion *in cis* on chromosome IV was screened via single worm PCR (Figure 2-1). Selfing produced homozygous double-deletion strains; each double-deletion strain was viable.

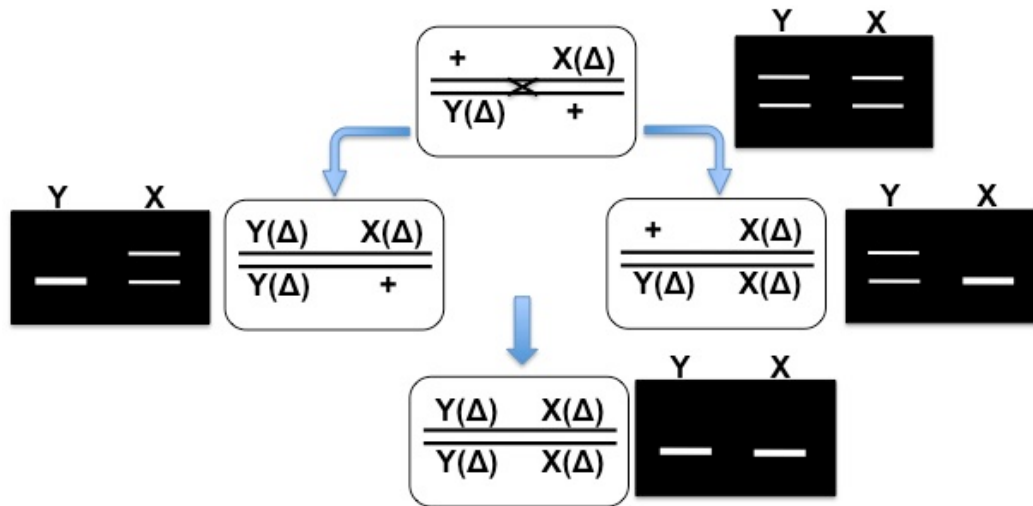


Figure 2-1: Crossing scheme for generating the double deletion strains. X and Y represent two paralogues. White lines in the black boxes are showing the bands observed after gel electrophoresis of the single worm PCR. The upper band in each column represents the wild type copy of the gene and the lower band represents the deleted form of the gene.

2.3 Worm lysis and sequencing

Candidate gene sequencing was performed on genomic DNA. For preparation of the DNA, 20-30 gravid hermaphrodites were picked into a small volume of Worm Lysis Buffer (50mM KCl, 10mM Tris pH 8.3, 2.5mM MgCl₂, 0.45% NP-40, 0.45% Tween-20, 0.01% Gelatin) with a final concentration of 1 mg/mL of Proteinase K. The mixture was heated to 65°C for 60 minutes and 95°C for 15 minutes to inactivate the Proteinase K. Then the sequencing reactions were done with prepared BigDye sequencing mixture for 25 cycles with the following PCR program: 96°C X

30" - 50°C X 15" - 60°C X 2'. Sequencing analysis was performed by the Molecular Biology Service Unit (MBSU) at the University of Alberta.

For whole genomic sequencing of *mel-43(sb41)* worms, MAS137 strain was cultured on 10 NGM-agarose plates with OP50, to avoid potential agar-based inhibition of sequencing reactions. Worms were maintained at 15°C until almost all the bacteria were eaten. Worms were washed off of the plates with M9 (22mM KH₂PO₄, 42mM Na₂HPO₄, 85mM NaCl, 1mM MgSO₄) followed by two centrifugation and washing steps, resulting in a pellet of washed gravid worms. The pellet was resuspended in 0.5 mL of lysis buffer (10mM Tris-Cl, 0.1M EDTA, 0.5% SDS, 20 µg/ml DNase-free RNase) followed by 25 µL of 10% SDS and 2.5 µL of proteinase K (20 mg/mL) and incubated at 50°C for 1 hour. Another 2.5 µL of 20 mg/mL of proteinase K was added and incubated at 50°C for 1 more hour. Nucleic acid was extracted with 0.5 mL of phenol followed by 0.5 mL 1:1 phenol/chloroform and then chloroform (0.5 mL). DNA was isolated by ethanol precipitation and the pellet was dissolved in H₂O. The DNA was checked by restriction enzyme digestion and agarose gel electrophoresis to verify the purity of the DNA for sequencing. Since all the worms used for the extraction were washed from culture plates, bacterial DNA (from the *C. elegans* food source) was also likely present in the DNA preparation. Although the worms were starved before preparation, some residual bacteria were likely present. Therefore, a series of PCRs using random *E. coli* -specific primers were performed in different dilutions of the *mel-*

43(*sb41*) DNA to determine the amount of bacterial contamination (Figure 2-2). Inspection of the PCR products via gel electrophoresis indicated that the bacterial contamination was low and not likely to interfere with genomic DNA sequencing.

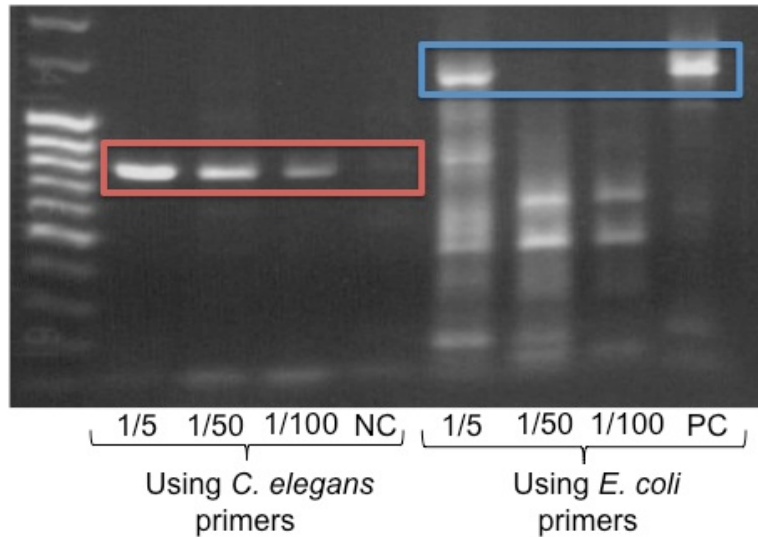


Figure 2-2: Bacterial contamination assessment of the *mel-43(sb41)* genomic DNA using gel electrophoresis. 1/5, 1/50, and 1/100 dilutions of the genomic DNA was used in the PCR reactions. Red box represents the bands using a *C. elegans*-specific primers and blue box represents the bands using *E. coli*-specific primers. NC (negative control) is a PCR reaction with no genomic DNA and PC (positive control) is a PCR reaction on only a bacterial DNA. In 1/50 and 1/100 dilutions, *C. elegans*-specific bands are visible but no band could be detected for the *E. coli*-specific primers.

A total of 5 μ g of the genomic DNA was sent to UBC *C. elegans* Gene Knockout Laboratory for sequencing and BC Cancer Agency Genomic Sciences Center for analysis.

Table 2-2: Primers generated and used for sequencing of candidate genes

Primer Name	Primer Sequence
<i>pcn-1-s1</i>	5'-CATCGTCAGTGTTGGAAGATG -3'
<i>pcn-1-s2</i>	5'-AATGCTGATTTCCGCCAA -3'
<i>pcn-1-s3</i>	5'-GTTGAACATCACCGCCA -3'
<i>pcn-1-s4</i>	5'-TGTGGTTTTTCGGTAGTC -3'
<i>pcn-1-s5</i>	5'-CGCTGTCAATGTCCATC -3'
<i>pcn-1-s6</i>	5'-TTAGGCCGAAATAGTCTG -3'
<i>ubc-1-s1</i>	5'-TTGAACATTAGAGAACATTTGCAAC -3'
<i>ubc-1-s2</i>	5'-CCAAAAAAAAAATCACTTAAAAATTACC -3'
<i>ubc-1-s3</i>	5'-CACTTGCCGCACAGCTTTAT -3'
<i>ubc-1-s4</i>	5'-TGCTGAATTTTGGCTGAAAAT -3'
<i>ubc-1-s5</i>	5'-TCTACCCCCAAAATCATCTGA -3'
<i>ubc-1-s6</i>	5'-TAGACCCAAAATTTGTGAAAATCTG -3'

2.4 RNAi by feeding

RNAi by feeding was performed as previously described (Kamath and Ahringer, 2003). RNAi plates were NGM agar with 0.001M IPTG (isopropyl β -D- 1- thiogalactopyranoside) and 25 mg/mL carbenicillin. Plates were kept at 4°C no longer than one week before use. The RNAi vector, L4440, has a T7 promoter on each side of the MCS driving transcription of the gene of interest (Timmons and Fire, 1998). These clones are transferred into an RNase III-deficient strain of *E. coli* (HT115 (DE3)) that carries an IPTG-inducible T7 polymerase (Timmons et al., 2001). HT115 bacteria (+ the desired RNAi vector) were grown in LB broth

(1.0 mg/mL Bacto-Tryptone, 0.5 mg/mL Bacto-Yeast extract, 0.5 mg/mL NaCl) with 50 mg/mL ampicillin at 37°C for at least 6 hours. The resulting RNAi bacterial culture was used to seed RNAi NGM plates overnight at room temperature to induce the production of double-stranded RNA. The next day, L4 *C. elegans* larvae were transferred to an empty plate for 1 hour to remove the OP50 bacteria from the outside of the worms. Then they were placed onto the RNAi plate and incubated overnight. A maximum of 50 worms were plated on a single RNAi plate. For scoring the effect of RNAi on viability of the worms, only 5 worms were plated on each RNAi plate. For each experiment *mel-26(RNAi)* was used as a positive control and an empty L4440 vector was the negative control.

2.5 RNAi by injection

To produce dsRNA for microinjection into worms, genomic DNA was amplified via PCR. The gene-specific primers used for the PCR contained T3 and T7 bacterial polymerase promoter sequences at each end. After purification of the PCR fragment, a transcription reaction was set up using MEGAscript RNAi kit (Invitrogen). Each T3 and T7 reaction products were mixed and annealed and TURBO DNase1 was used to remove the template DNA. The dsRNA was purified with QIAGEN RNeasy. 400 ng/μL of purified dsRNA was injected into the gonad of L4 *C. elegans* larvae. The injected worms were incubated at 25°C overnight prior to use in further experiments.

Table 2-3: Primers generated and used for making dsRNAs.

Primer Name	Primer Sequence
y17g9b.9_T3F1	5'-AAT TAA CCC TCA CTA AAG GGT CGA GCA CGT GTT TCT TCA -3'
y17g9b.9_T7R1	5'-TAA TAC GAC TCA CTA TAG GGC AGT GTG TGG TTC TCA GGA -3'
y17g9b.9_T3F2	5'-AAT TAA CCC TCA CTA AAG GGC TGA CAC TCA CAA AAA CTG -3'
y17g9b.9_T7R2	5'-TAA TAC GAC TCA CTA TAG GGT TGC GGT GGG AAA ATA AC -3'

2.6 Immunostaining

Between 30 to 40 gravid hermaphrodites were picked into 5 μ L of water on polylysine-coated slides. An 18X18mm cover slip was placed on top of the worms and gentle pressure was applied to squeeze the embryos out of the worms. Slides were immediately frozen in liquid nitrogen for 5 minutes. A razor blade was used to flick the cover slips off the slides to crack the eggshells. The slides were fixed for 15 minutes in -20°C methanol (for REC-8 staining, slides were fixed in methanol (5 min.) and then in 1:1 acetone/methanol (5 min.) followed by acetone (5 min.) until they were transferred to phosphate-buffered saline (PBS) for at least 5 minutes. The embryos were blocked with 25% goat serum (in PBS) for at least 30 minutes. Slides were incubated in humid conditions with the primary antibody solution (5% goat serum, 0.01% Triton-X100 and 1-10 $\mu\text{g}/\text{mL}$ of primary antibodies) for 1 hour. Slides were washed with PBS twice and then incubated with secondary solution (5% goat serum, 0.01% Triton-X100 and 1 $\mu\text{g}/\text{mL}$ secondary antibody) for 1 hour. Goat anti-rabbit

or goat anti-mouse secondary antibodies covalently linked to one of three fluorophores (Alexa488, Alexa546, Alexa647) were used for visualization via fluorescence microscopy. The slides were washed with PBS again and DAPI was applied (5 $\mu\text{g}/\text{mL}$ for 5 minutes) to visualize chromatin. Slides were then washed with PBS twice and 8 μL mounting media (0.5% p-phenylenediamine, 20 mM Tris-Cl, pH 8.8, 90% glycerol) was used to mount the embryos. A 22 mm cover slip was placed over the embryos and sealed with nail polish. In order to compare the intensity signals between two types of worms, each of them were picked into separate drops of water on the same slides.

Microscopy was performed on an Olympus IX81 motorized inverted microscope fitted with a Yokogawa CSU-10 spinning disc confocal head modified with a condenser lens in the optical path (Quorum Technologies). Images were acquired using a 60X oil objective lens (NA 1.42) and captured with a Hamamatsu Orca R2 camera controlled by MetaMorph® software. Multiple image planes were acquired for each embryo, at an increment of 0.2 μm , for a total depth of approximately 12 μm . Image files were analyzed using MetaMorph® software. For some figures, out-of-focus planes were removed from 3D stacks prior to projecting the images.

Primary antibodies were mouse anti-tubulin (DM1A; 1:100; Sigma), rabbit anti-AIR-1 (1:200), and mouse anti-REC-8 (1/100; Abcam).

For quantifying MEL-43 cytoplasmic fluorescence levels, the average of integrated intensity of three circles drawn within the cytoplasm

of each embryo was calculated (Figure 2-3). The intensity of each embryo was compared to N2 controls and displayed as relative fluorescence levels for the graphs.

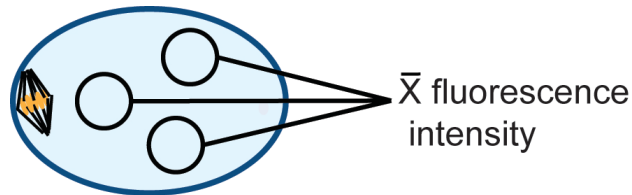


Figure 2-3: Schematic drawing of the method used for MEL-43 cytoplasmic signal measurements.

2.7 Antibody production

The MEL-43 antibodies were generated in rabbits against full-length MEL-43 fused to glutathione S-transferase after expressing them in Rosetta 2 (DE3) bacteria. A bacterially-expressed GST-fusion of the full-length MEL-43 was injected into rabbits (Karen Cheung, Srayko laboratory; Bioscience Animal Services, University of Alberta). MEL-43 antisera were affinity-purified using full-length MEL-43 fused to maltose binding protein. A bacterial powder from OP50 and Rosetta strains was made using acetone. The bacterial acetone powder cleaning method was used to remove antibodies against the bacterial proteins from polyclonal antisera. 25 mg of the powder / mL of serum were vortexed for 5 min, followed by 5 min high-speed centrifugation. The supernatant was used for western blot and immunostaining.

2.8 Ex-utero and in-utero confocal imaging

For *ex utero* imaging, three to five worms were dissected in 5 μ L of egg buffer (118 mM NaCl, 48 mM KCl, 2 mM CaCl₂, 2 mM MgCl₂, and 25 mM Hepes, pH 7.4) on poly-L-lysine slides to release the embryos from the gonad and were covered with a glass lid to reduce the dryness. Live time-lapse imaging was performed on an Olympus IX81 microscope as described above.

For *in utero* imaging, worms were picked into 7 μ L of egg buffer solution containing 5 mM tetramisole hydrochloride to immobilize the worms prior to imaging. Tetramisole is an acetylcholine agonist that paralyzes the adult worms while allowing normal metabolic and developmental processes (Aceves et al., 1970). When the worms stopped moving, the cover slip was mounted on a 2% agarose pad surrounded by a thin silicone bead.

For the MAS138 (GFP::tubulin; mCherry::histone; *mel43-(sb41)* *dpy-20*) strain, 5 planes (2 μ m spacing) were taken every 20 sec from the time that the oocyte entered the spermatheca until the embryo completed the first mitosis division. The image stacks were projected prior to making the movie. A single DIC picture was taken at the end of mitosis for analyzing the cytokinesis. For comparing the timing of cell cycle events, the following landmarks were used: anaphase I, shortening of MII spindle, anaphase II, meeting of the pronuclei, mitosis metaphase, and mitosis anaphase.

To analyse chromatid segregation in meiosis II, image stacks of metaphase II and anaphase II were projected. A 10 μm line (width of 15 pixels) from one pole to the other pole of the spindle was drawn and the pixel intensity of the red (histone) and green (tubulin) signal along the line was measured.

For cyclin B (CYB-1::GFP) measurements, 3 planes were taken every one-minute to limit photo bleaching. Integrated intensity was calculated from a defined circular region of interest, from a projected stack at each time point. In order to account for background photobleaching, integrated intensity was also calculated for a multicellular embryo in the uterus and then a ratio of fluorescence intensity over time was determined.

For MEI-1::GFP imaging, after finding the right stage of meiotic and mitotic embryos with DIC optics, fluorescence stacks of 41 planes in a range of 10 μm were acquired. Projection of the eight planes in the centre of the stacks was used to make the figures.

For *mel-43&mpar-1/2(RNAi)* worms, imaging was performed 24 hours after the dsRNA injection. Since one of the two gonad arms was often damaged during the injection procedure, only the non-injected gonad was imaged.

2.9 Western blotting for MEL-43

Western blotting of MEL-43 was performed on both whole worm and collected embryo lysates (Hannak et al., 2002). For preparing the embryos, 100 worms were picked into tubes with 100 μL M9 buffer (22mM

KH_2PO_4 , 42mM Na_2HPO_4 , 85mM NaCl, 1mM MgSO_4). Worms were pelleted at 1,000 g for 1 min and washed 3X in H_2O , leaving a final volume of 50 μL . 50 μL of a 2Xbleach solution (27.5 μL H_2O , 5 μL of 10M NaOH, and 17.5 μL NaOCl) was added to each tube and vortexed for 3 min to dissolve the hermaphrodite worms. Embryos were pelleted at 1,000 g for 1 min and washed 3X with 400 μL of embryo wash buffer (0.1 M Tris, pH 7.5, 100 mM NaCl, and 0.1% Tween 20), leaving a final volume of 10 μL . For whole worm lysates, worms were pelleted at 1,000 g for 1 min and washed 3X in H_2O and they were left with a final volume of 10 μL . For both whole worm and embryo lysates, an equal volume of 2X Laemmli sample buffer (Sigma-Aldrich) was added to each tube, and the tubes were placed in a water bath sonicator for 5 min at RT followed by boiling at 95°C for 5 min. Samples were loaded into a 10% SDS-PAGE resolving gel. A prestained protein marker (7–175 kDa; New England Biolabs, Inc.) was used to determine the relative mass of the proteins. After electrophoresis, the proteins were transferred to a nitrocellulose membrane (Hybond-N, GE Healthcare) at 100 V for 2 hours. The membrane was blocked in 8% skim milk in TBST for 1 h (Tris buffer saline Tween 20; 20 mM Tris-HCl, pH 7.4, 500 mM NaCl, and 0.05% Tween 20). The anti-MEL-43 and anti-tubulin antibodies were used at 1:200 and 1:400 respectively in TBST + 4% skim milk and incubated for 1 h at RT. The membrane was washed 3X 10 minutes with TBST at room temperature. Goat anti-rabbit and goat anti-mouse HRP-bound secondary antibodies (Bio-Rad Laboratories) were

used at 1:5,000 in TBST + 4% skim milk and incubated with the membrane for 1 hour at RT. The membrane was washed 3X 10 minutes with TBST at room temperature. The secondary antibodies were detected via an ECL kit (SuperSignal West Pico; Thermo Fisher Scientific). Detection reagents were added in a 1:1 ratio and incubated with the membrane for 5 minutes. The membrane was exposed to the X-ray film for about 3 minutes and the signal was detected.

3. Results

3.1 Characterization of *mel-43(sb41)*

The *mel-43(sb41)* mutation was originally identified in a large-scale genetic screen for redundant genes affecting embryonic development (Mitenko et al., 1997). *mel-43(sb41)* was reported as a dominant, temperature-sensitive, maternal-effect, embryonic-lethal mutation (Mitenko et al., 1997). The homozygous *mel-43(sb41)* animals were viable, however, they displayed only 2% hatching at the permissive temperature of 15°C and no hatching at the restrictive temperature of 25°C.

3.1.1 Live imaging characterization of *mel-43(sb41)* embryos

In the original report, conventional DIC light microscopy showed that *mel-43(sb41)* resulted in multiple cellular defects in the first cell division, including excessive membrane blebbing and cytokinesis failure in the first mitosis (Mitenko et al., 1997). In wild type, the newly fertilized oocyte completes meiosis I and meiosis II (producing polar bodies 1 and 2 respectively) and then it enters the first mitosis. Thus, any defects observed during the first mitosis could mask earlier meiotic defects. In order to address the phenotypes associated with *mel-43(sb41)* in more detail, and to observe the progression through female meiosis and the first mitosis, I created a *mel-43(sb41)* mutant strain (MAS138) that expresses both GFP::tubulin (to observe microtubules) and mCherry::histone (to

observe chromatin). This strain was imaged using DIC optics and fluorescence time-lapse microscopy. In *mel-43(sb41)* embryos, the female meiosis I spindle appeared normal. Segregation of homologous chromosomes in anaphase I and extrusion of the first polar body occurred as in wild type. During meiosis II, *mel-43(sb41)* embryos exhibited normal spindle assembly, however, 80% of the embryos (16/20) did not segregate sister chromatids and they failed to extrude the second polar body (Figure 3-1). The meiosis II spindle persisted in these embryos until mitotic prophase, at which time, the spindle migrated away from the cortex, often with irregular and unpredictable movements (Figure 3-1). In rare cases the chromatids separated in anaphase II and polar body extrusion occurred, however, the resulting polar body was often grossly enlarged and had an abnormal morphology. In wild-type embryos, the sperm-derived centrosomal microtubule asters appear only after the completion of meiosis II. However, in *mel-43(sb41)* embryos microtubule fibres, consistent with centrosome-based microtubule asters, were observed near the condensed sperm DNA, even though the meiosis II spindle was also present (Figure 3-1). In most embryos, the condensed sperm DNA migrated towards the anterior and joined the meiotic spindle (Figure 3-1). After this, the meiotic spindle became less discernible due to the increased microtubule levels from centrosomes and the formation of the mitotic spindle around the chromatin. Despite the severe *mel-43(sb41)* defects present during the transition between meiosis and mitosis, a

mitotic spindle eventually assembled and chromatids usually segregated in mitotic anaphase, suggesting that kinetochores and mitotic anaphase forces are functional in these embryos (12/16). At the end of mitosis *mel-43(sb41)* mutants exhibited relatively dynamic cortical contractility, but usually failed to complete cytokinesis after the first cell division, as observed by DIC (12/16 embryos; Figure 3-1).

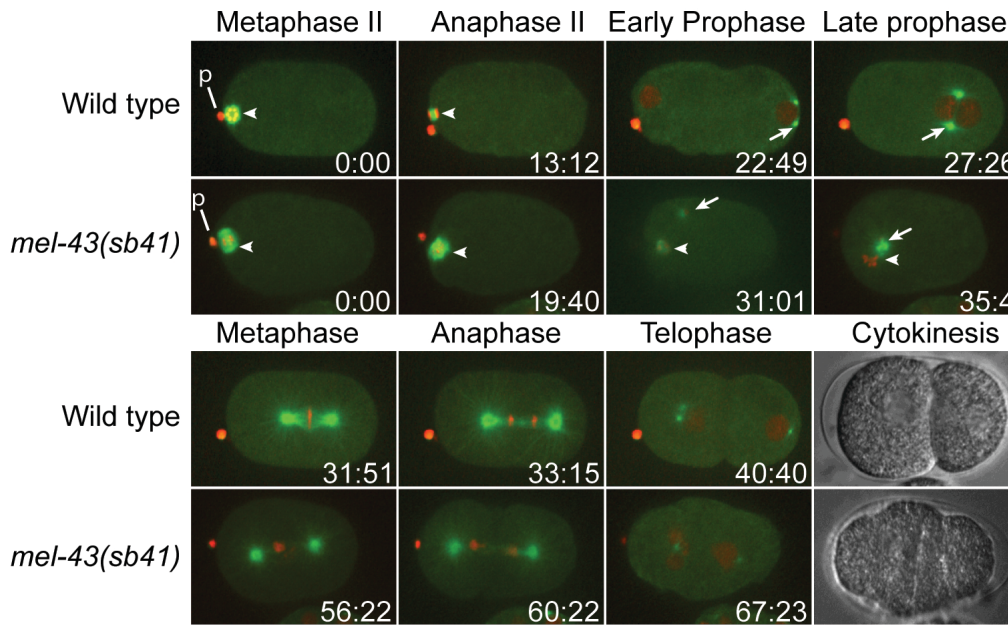


Figure 3-1: Live imaging of *mel-43(sb41)* mutants. *Ex-utero* time-lapse images of wild-type and *mel-43(sb41)* embryos expressing mCherry::Histone and GFP::Tubulin are shown. Images start from the second meiotic metaphase (t=0). The meiosis I division was successful in *mel-43(sb41)* embryos (not shown), as evidenced by the first polar body (p). In *mel-43(sb41)* meiosis II embryos, chromatin usually does not segregate and polar body extrusion fails (t=19.40). A mitotic spindle eventually forms in *mel-43(sb41)* embryos. A DIC image shows the end of the first division, in which *mel-43(sb41)* cytokinesis usually fails (the visible crease at the mid-point of the mutant embryo is a remnant of a non-productive cortical furrow). Meiotic spindle and centrosomes are shown with arrowheads and arrows respectively.

3.1.2 Centrosome maturation in *mel-43(sb41)* mutants

In wild-type embryos, meiosis II completes prior to the appearance of centrosomal asters, which are required for the fusion of the male and female pronuclei in late mitotic prophase, and positioning the nuclei at the

centre of the cell prior to mitotic spindle assembly. The observations of *mel-43(sb41)* embryos indicated that meiotic and mitotic processes were occurring within the same cytoplasm at the same time. In order to assess the maturation state of the centrosomes in *mel-43(sb41)* embryos, antibodies against the aurora A kinase, AIR-1, were used. AIR-1 is required for many steps leading to the full maturation of the centrosomes, including the recruitment of gamma-tubulin, the gamma-tubulin ring complex protein, CeGrip, as well as the TAC-1/ZYG-9 complex, implicated in promoting microtubule growth (Hannak et al., 2001; Srayko et al., 2005). Aurora A kinase is also required for centrosome separation, and mitotic spindle assembly (Furuta et al., 2002). In wild type, AIR-1 was detected on the centrosomes as very small foci only after anaphase II was completed. In mitosis, AIR-1 levels at centrosomes increased in intensity with the cell-cycle. This trend was also observed in *mel-43(sb41)* embryos, with two important differences. First, centrosomal AIR-1 was detected in embryos that still had a meiosis II spindle present, something which was never observed in wild-type. Second, *mel-43(sb41)* embryos in early mitotic prophase often exhibited a fragmented pattern of AIR-1 (Figure 3-2). Based on live GFP::tubulin imaging, this fragmentation occurred as the centrosome sperm complex migrated towards the meiotic spindle (Figure 3-2).

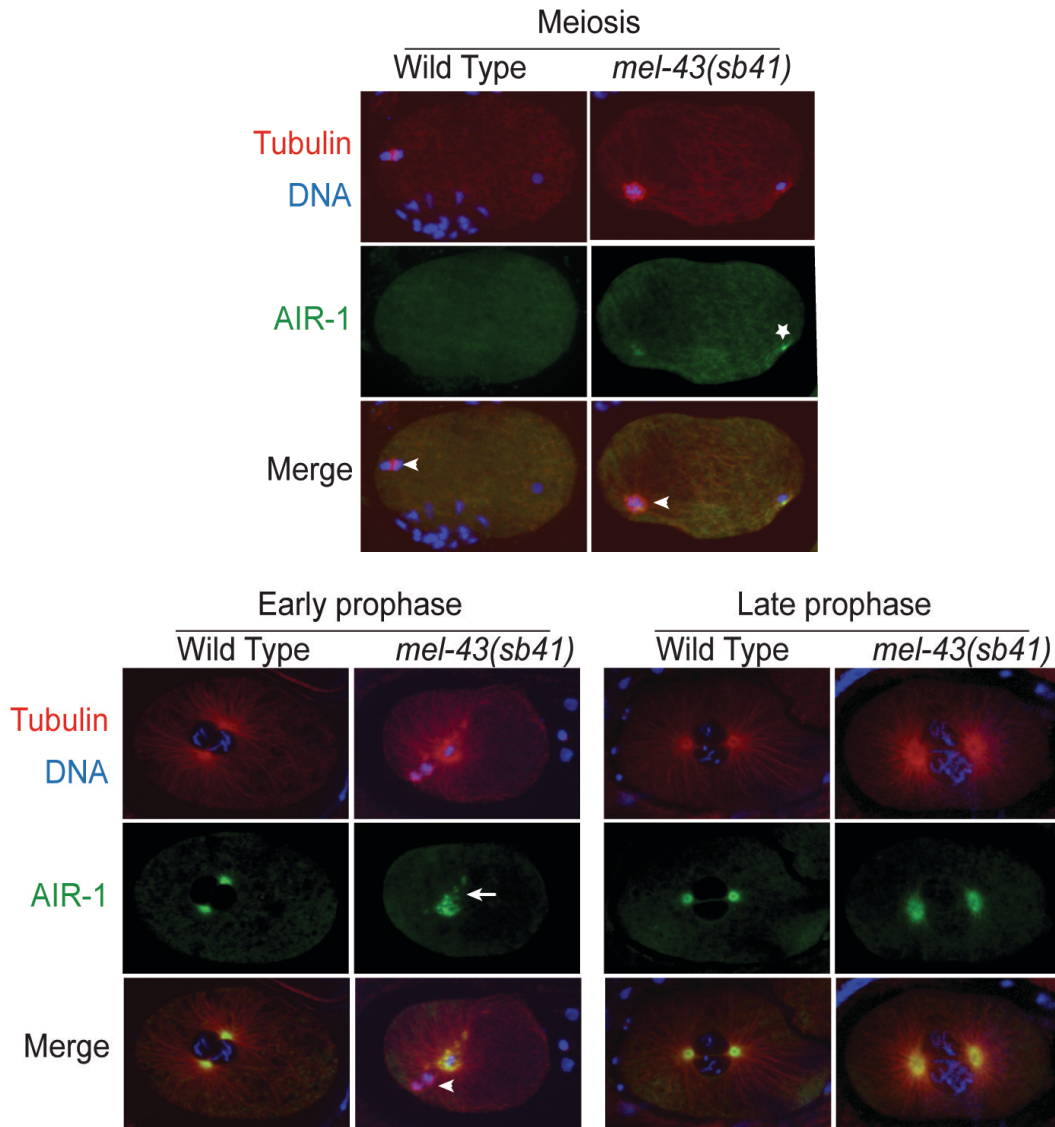


Figure 3-2: Aurora A kinase is recruited to centrosomes in *mel-43(sb41)* and wild-type embryos. Immunofluorescence is used to detect the localization of microtubules (Red), DNA (Blue) and the centrosomal aurora A kinase AIR-1 (Green). Centrosome maturation is observed in metaphase of meiosis in *mel-43(sb41)* mutants (star). Centrosome fragmentation is observed during early prophase of mitosis in many *mel-43(sb41)* embryos (arrow). Often centrosome fragments join the persistent meiosis II spindle (arrowhead) before separating to opposite sides of the nuclear envelope.

3.1.3 Timing of the events in *mel-43(sb41)* one cell embryo

Our initial analysis indicated that *mel-43(sb41)* embryos are slow to complete the meiosis-mitosis program (Figure 3-3). In order to determine the specific events affected, *in utero* time-lapse imaging was performed. No obvious delays were evident prior to meiotic metaphase II. However, the transition from meiotic metaphase to meeting of the nuclei in prophase of mitosis was delayed by about 10 minutes (Figure 3-3). Because nuclei were not discernible, and the sperm DNA remained condensed in *mel-43(sb41)* embryos, mitotic prophase for these embryos was defined as the stage when the sperm DNA migrated to meet the meiotic spindle/meiotic chromatin. Based on this criterion, the transition from mitotic prophase to metaphase was also significantly delayed in mutant embryos. However, the subsequent mitotic metaphase-to-anaphase transition occurred at a rate similar to wild type (Figure 3-3). These results showed that *mel-43(sb41)* mutants exhibited a cell-cycle delay specifically between meiosis II metaphase and mitotic metaphase.

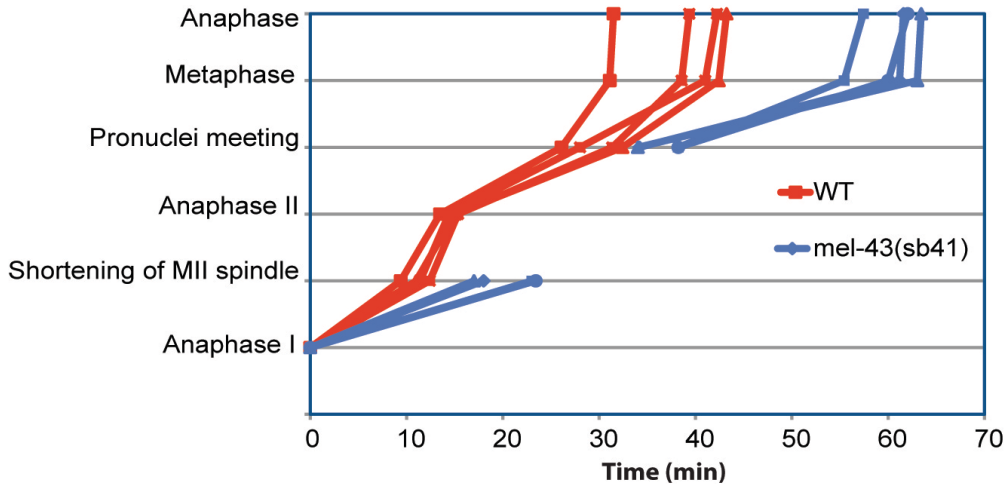


Figure 3-3: Timing of the events in *mel-43(sb41)* and wild-type embryos. Four wild-type (red) and four *mel-43(sb41)* (blue) embryos are analyzed from anaphase I (t=0) until the end of mitosis. The four *mel-43(sb41)* embryos shown did not undergo anaphase II.

3.1.4 Chromatid congression and segregation in *mel-43(sb41)* mutants

mel-43(sb41) embryos exhibited normal meiosis II spindle assembly but they usually failed to extrude a second polar body. In order to analyze the positions of the chromosomes in meiosis II, line scan intensity plots of fluorescence intensity for mCherry::histone and GFP:: β -tubulin in wild-type and *mel-43(sb41)* mutant embryos were performed. Embryos were analyzed in metaphase II for congression of the chromosomes and in anaphase II for segregation of the chromatids. In metaphase, both *mel-43(sb41)* and wild-type embryos exhibited a similar profile of tubulin and chromatin distribution along the spindle axis, based on fluorescence intensity. Specifically, tubulin was concentrated at the spindle poles, and the chromatin was aligned in the spindle midzone, suggesting that

chromosomes congress normally in the mutants (Figure 3-4). In anaphase, wild-type meiotic spindles undergo a change in the distribution of tubulin such that microtubules appear between the separating masses of chromatin (Figure 3-4). In the *mel-43(sb41)* embryos, chromatin exhibited a more random distribution along the presumed spindle axis, (11/15). Importantly, the peak of tubulin fluorescence was never observed centrally between chromatin masses. In a few embryos, chromatin separated within the meiotic spindle (4/15), but tubulin fluorescence levels were more uniformly distributed along the pole-pole axis, suggesting that these embryos did not execute a normal program of anaphase (Figure 3-4). Based on these observations, it can be concluded that congression of chromatids is normal in meiosis II in *mel-43(sb41)* embryos, however microtubule reorganization does not occur in anaphase, and this could be the primary defect leading to the observed defects in chromatid segregation in anaphase II.

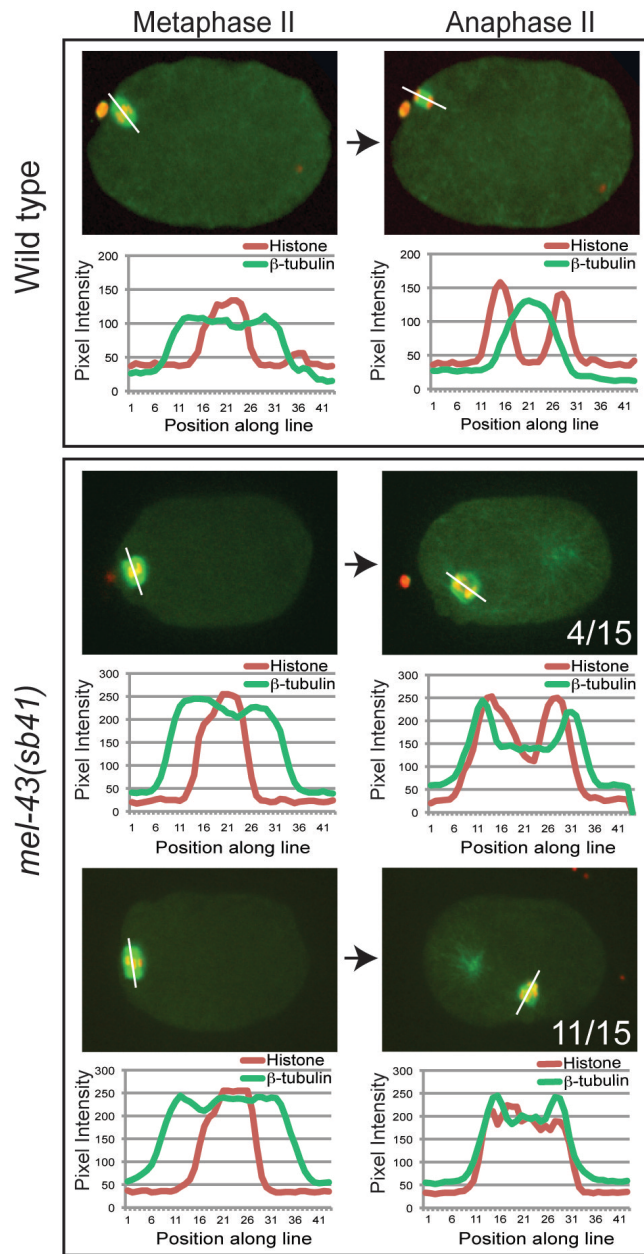


Figure 3-4: Analysis of meiosis II chromatin congression and segregation in *mel-43(sb41)* and wild-type embryos. Single plane confocal images of metaphase II and anaphase II of a wild-type embryo and two *mel-43(sb41)* embryos are shown with line-scan intensity plots of fluorescence intensity for Histone (Red) and β -tubulin (Green) along the marked line in the corresponding image. In *mel-43(sb41)* chromatin segregation fails and microtubule reorganization to the central region, characteristic of meiotic anaphase, does not occur.

3.2 Mapping of *mel-43*

mel-43 was originally mapped to chromosome IV between *unc-24* and *fem-3*, a range of approximately 1 Mbp (Mitenko et al., 1997), however recent evidence from SNIP-SNP mapping in the Srayko lab indicated that *mel-43* resides four map units away from the originally-published location, likely between *unc-17* and *dpy-13* (Pahara, 2010). Although *mel-43* had been mapped to a relatively small genetic interval, further approaches were implemented to identify the *mel-43* locus.

3.2.1 Sequencing of candidate genes

In order to find the *mel-43* locus, the indicated region was scanned for candidate genes based on their RNAi phenotype in Phenobank. Two genes, *pcn-1* and *ubc-1*, fit the criteria based on their functions. *pcn-1* interacts with CKI-2, a cyclin-dependent kinase inhibitor homolog that may be required for cell cycle progression during embryogenesis and *ubc-1* encodes an E2 ubiquitin-conjugating enzyme (Leggett et al., 1995), with the rationale that ubiquitin-mediated protein degradation is important during cell-cycle transitions. Primers were designed to amplify the respective coding sequences, and both candidates were sequenced completely in wild-type and homozygous *mel-43(sb41)* worms and no differences were detected (Figure 3-5). Therefore this approach did not identify any lesions in the *mel-43(sb41)* strain.

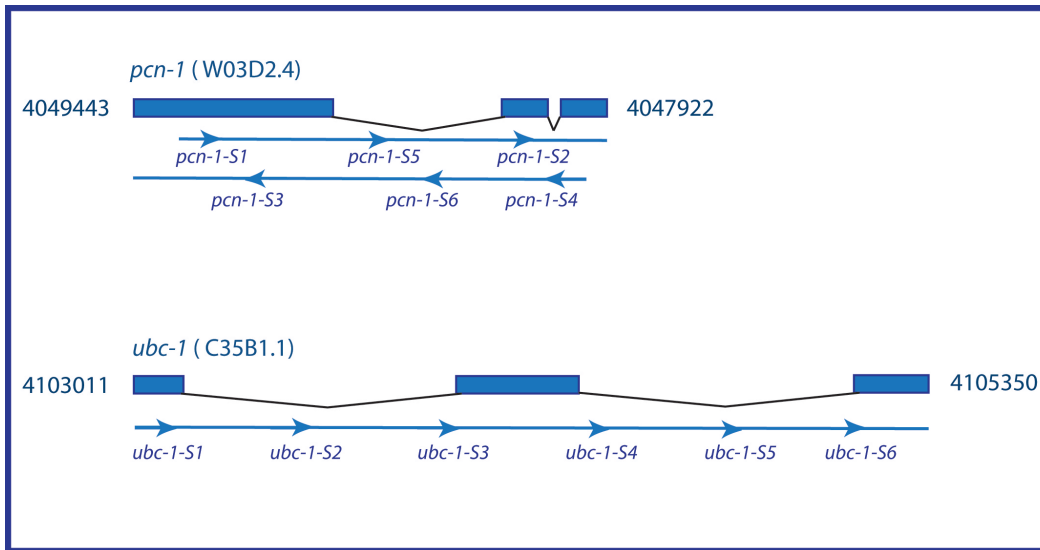


Figure 3-5: Diagram showing regions of two candidate genes (*pcn-1* and *ubc-1*) that were sequenced.

3.2.2 Duplication analysis

Transformation rescue by microinjection is one of the standard approaches used for identifying genes in *C. elegans* (Mello et al., 1991; Mello and Fire, 1995). This technique exploits the available library of cosmid or fosmid vectors that contain overlapping fragments of DNA that span the entire *C. elegans* genome. Purified fosmid DNA can be microinjected into the mutant worms to identify rescuing clones, and thus, the gene of interest. If more than one gene is present on the rescuing fosmid, subcloning smaller fragments for injection would identify the gene of interest. This approach is predicted to work well for recessive loss-of-function mutations. Since the *mel-43(sb41)* mutation is dominant, it could be a gain-of-function mutation. In this case, adding more wild type copies to the mutant would not necessarily be helpful. Therefore, I performed a

genetic analysis using a chromosomal duplication to first characterize the behaviour of the mutation and see whether the transformation rescue would be useful or not.

In *C. elegans*, many large-scale duplications collectively cover a large proportion of the genome. On chromosome IV, there is one duplication (*mDp4*) that spans a region from -26.5871 to 4.70371 and was predicted to cover the *mel-43* region (Figure 3-6). In order to determine the effect of the duplication on the phenotype, *mDp4* was added to *mel-43(sb41) / +* and plates were scored for embryonic lethality. If a duplication that spans the *mel-43* region is able to rescue the *mel-43(sb41)* lethality at 15°C, the transformation rescue technique could be used to identify the *mel-43* gene.

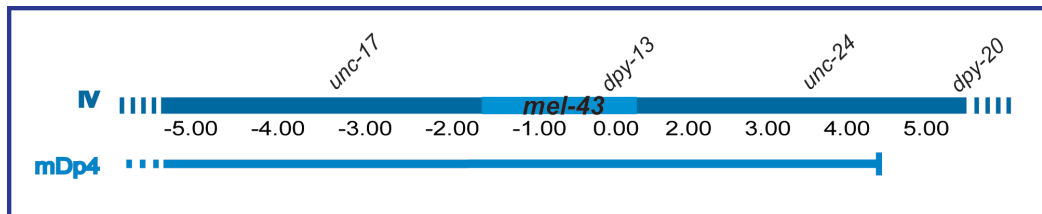


Figure 3-6: A schematic of the *mDp4* duplication coverage of chromosome IV.

After crossing *mel-43(sb41), dpy-20(e1282)/+* heterozygous males to DR1786 (*dpy-13(e184) unc-24(e138) IV; mDp4[unc-17(e245) IV]*), fifty F1 progeny were plated and allowed to self-fertilize at 15°C (Figure 3-7). The reason for this cross was to compare the embryonic lethality of the progeny from: *mel-43(sb41) dpy-20(e1282) / dpy-13(e184) unc-24(e138)*

vs. *mel-43(sb41) dpy-20(e1282) / dpy-13(e184) unc-24(e138) / mDp4* genotype. Since *dpy-20(e1282)* and *dpy-13(e134)* exhibit completely different Dumpy phenotypes, I was able to genotype the F1 worms by examining the surviving F2 progeny. Among the 50 plates of F1 progeny only 10 plates, which had both types of dumpy in the F2 generation were selected. In order to make sure that the *dpy-20* worms still have the *mel-43(sb41)* mutation, three *dpy-20* worms from each plate were transferred to 25°C and scored for lethality.

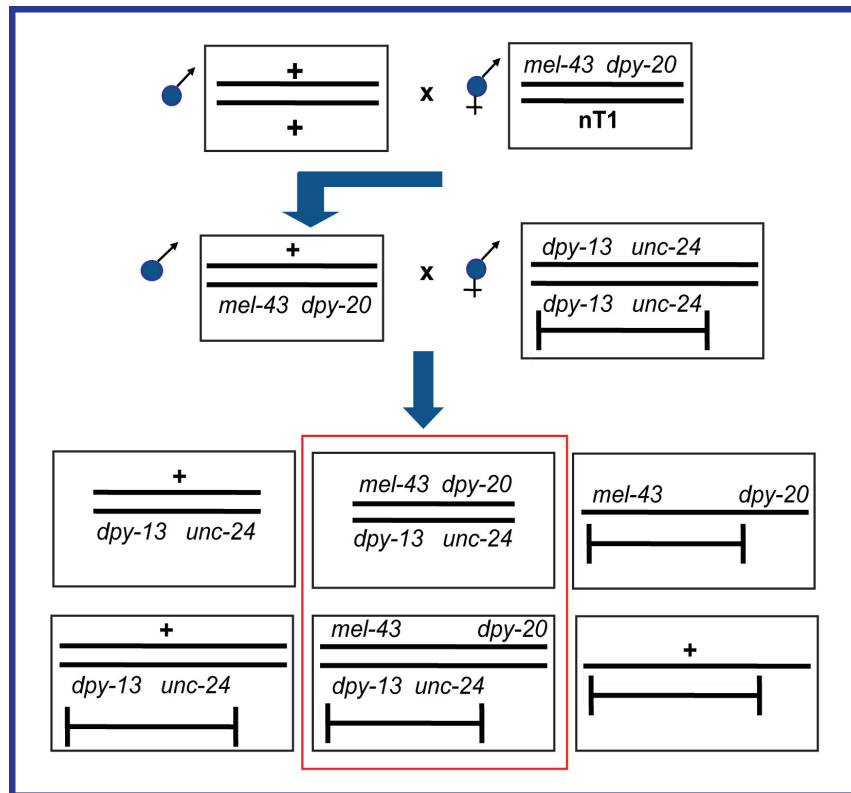


Figure 3-7: Duplication *mDp4* crossing scheme. Males heterozygous for *mel-43(sb41)* and *dpy-20(e1282)* were crossed to DR1876 strain. Progeny shown in the red box were used for embryonic lethality comparison.

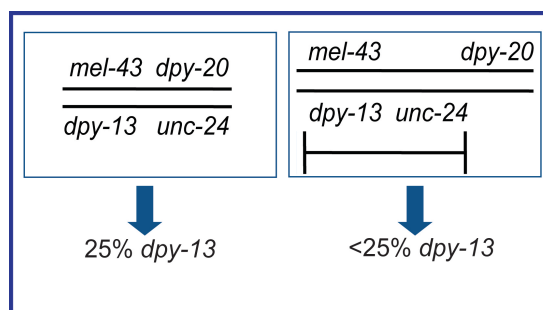


Figure 3-8: The duplication *mDp4* is detected by scoring *Dpy-13* in the F2 generation. Mendelian segregation of *dpy-13* from a heterozygous parent is expected to yield 25% *Dpy-13* progeny, whereas the presence of a duplication that covers *dpy-13* would be expected to significantly lower the proportion of *Dpy-13* progeny.

In order to score egg viability, the gravid hermaphrodites were transferred off of the plates one day prior to scoring. The *mel-43(sb41) dpy-20(e1282) / +* heterozygotes revealed 23.5% lethality at 15°C, and the *mDp4* duplication on its own caused 11% embryonic lethality at 15°C (scored from five DR1786 worms). Since the *mel-43(sb41)* mutation and *mDp4* duplication are two independent causes of the embryonic lethality, the expected percent of embryonic lethality for worms having both *mel-43(sb41)* and *mDp4* was calculated as 32% ($1 - 0.89 \times 0.765$). Among the 10 plates of F1 progeny, the range of 10% to 39% lethality was observed in the F2 generation, which was not helpful for distinguishing between two expected genotypes. Therefore, five wild-type worms were picked from five plates with different lethality and allowed to self-fertilize at 15°C. This time all progeny observed on the plates were scored and the percentage of *Dpy-13* progeny was used to distinguish between the two genotypes. Based on Mendelian genetics, worms with *mel-43(sb41) dpy-20(e1282) /*

dpy-13(e184 unc-24(e138)) genotype are expected to give 25% homozygous *dpy-13(e184) unc-24(e138)* progeny (Figure 3-8). However, having the duplication over the same genotype would result in less than 25% homozygous *dpy-13(e184) unc-24(e138)* progeny (Figure 3-8). Using this method it was possible to separate all 25 hermaphrodites into two classes. Two out of twenty-five plates exhibited only 9% *dpy-13*, which means the parent of these worms had the *mDp4* duplication. From each of these two plates, 10 wild-type progeny were plated individually and allowed to self-fertilize and again seven out of seventeen plates revealed less than 13% of *dpy-13* (Table 3-1).

Table 3-1: Observed lethality percentage of progeny from F2 generation with or without mDp4. Percentages in red represent the worms with *mDp4* over the heterozygous *mel-43(sb41)* worms. Percentages in the left column represent the number of Dpy-13 progeny, which was used to identify worms with or without the duplication.

No. of plates	<i>dpy-13 unc-24</i>	Embryonic lethality
1	7%	76%
2	11%	65%
3	23%	25%
4	21%	8%
5	17%	21%
6	21%	30%
7	21%	26%
8	13%	66%
9	18%	19%
10	11%	53%
11	17%	8%
12	11%	53%
13	17%	22%
14	9%	57%
15	14%	23%
16	24%	12%
17	13%	41%

Since both types of progeny were distinguishable, I was able to score their embryonic lethality and compare it with the expected 32%. As a result, all the worms with the duplication revealed more than 41% dead eggs, which is higher than the expected 32% (Figure 3-9). These observations determined that the duplication *mDp4* was not able to rescue the *mel-43(sb41)* mutation, rather it increased the severity of the phenotype. Therefore, this analysis revealed a hypermorphic behaviour for

the *mel-43(sb41)* mutant and suggested that cosmid rescue would not likely work to identify *mel-43*.

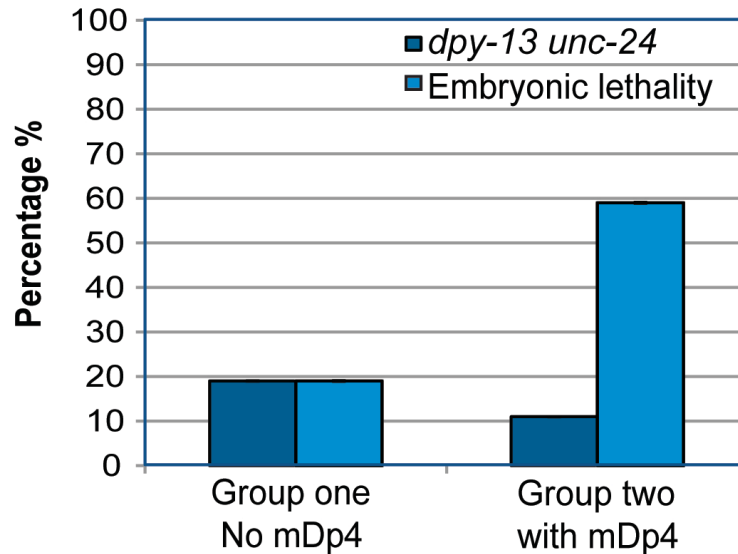


Figure 3-9: Comparison of the embryonic lethality between embryos heterozygous for *mel-43(sb41)* and embryos with *mDp4* duplication over the heterozygous *mel-43(sb41)*. Percentage of Dpy-13 worms on the plates was used as a marker to separate the two genotypes. An inverse correlation was observed between the proportion of Dpy-13 progeny and the proportion of dead embryos, suggesting that *mDp4* was responsible for increased lethality (beyond that which was expected from the duplication alone; refer to text for details).

3.2.3 Genomic sequencing of *mel-43(sb41)* worms

Since a wild-type copy of the *mel-43* region was unable to rescue the mutation, identification of the gene was pursued by genomic sequencing of *mel-43(sb41)* mutants. Therefore, genomic DNA was extracted from the 10 plates of gravid *mel-43(sb41)* hermaphrodites worms and 5 µg of DNA was sent to UBC *C. elegans* Gene Knockout Laboratory for sequencing. After analysis of the DNA by the *C. elegans*

Knockout Facility (kindly provided by Dr. Don Moerman, UBC, Vancouver), five mutations near the expected region were found, however only one, Y17G9B.9, was within the expected map position (Table 3-2). Searches of the *C. elegans* database (Wormbase) indicated that Y17G9B.9 was uncharacterized. The predicted Y17G9B.9 protein contains no recognizable protein domains and no obvious homologues outside of nematodes. The identified mutation is expected to cause a P74S substitution in the protein. Information from Phenobank (a database of RNAi phenotypes) indicated no obvious RNAi phenotype for this gene. In addition, we tested worms homozygous for a Y17G9B.9 deletion of nucleotides 420 to 616 (National Bioresource Project; Tokyo, Japan) and observed no obvious phenotype. These results suggested that Y17G9B.9 was functionally redundant. Consistent with this idea, database searches revealed the existence of two paralogues in *C. elegans*, Y62E10.A and H02112.5, each having 87% sequence identity at the DNA level.

Table 3-2: Five mutations predicted to alter coding sequence were found in whole genomic sequencing of *mel-43(sb41)* mutants on chromosome IV. Only Y17G9B.9 resided within the expected genetic interval of *mel-43(sb41)*.

Chromosome	Nucleotide change	Gene	AA change
IV	3304040 A to G	W08E12.3	I to V29
IV	3304068 G to A	W08E12.3	G to E98
IV	4760199 G to A	Y17G9B.9	P to S74
IV	4990262 C to A	E03H12.9	V to F50
IV	5179199 G to A	W03F8.5	A to T58

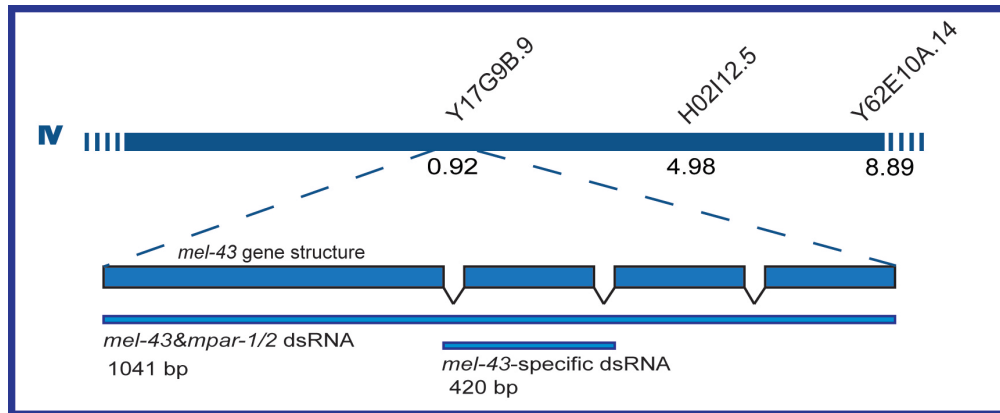


Figure 3-10: The map position of *mel-43* and two paralogues (H02I12.5 and Y62E10A.14) on chromosome IV. *mel-43* gene structure is shown with a region used to make dsRNA that is maximally divergent from *mpar-1* (Y62E10A.14) and *mpar-2* (H02I12.5) (termed *mel-43(RNAi)*). Full-length RNA is predicted to be 87% identical (overall) and is expected to efficiently target all three genes (termed *mel-43&mpar-1/2(RNAi)*).

If the three genes were functionally redundant, I hypothesized that removing the function of all three genes should result in a phenotype. In order to determine the consequence of knocking down Y17G9B.9 and its paralogues, a 1041 bp dsRNA derived from the entire Y17G9B.9 gene was generated, with the idea that 87% identity should confer RNAi-based knockdown of all three genes (Figure 3-10). The RNAi directed against all three related genes resulted in 100% embryonic lethality at 25°C (Figure 3-11). A 420 bp dsRNA predicted to be more specific to Y17G9B.9 (80% identity with paralogues) injected into WT did not cause any obvious defects (Figure 3-11). The duplication analysis described above indicated that *mel-43(sb41)* was likely a hypermorphic mutation. Therefore, I predicted that, if Y17G9B.9 is *mel-43*, then removal of Y17G9B.9 activity

should rescue *mel-43(sb41)* worms. To perform this experiment, the 420 bp dsRNA specific to Y17G9B.9 was injected into the mutants and their lethality was scored at 25°C. As predicted, the maternal-effect lethality of *mel-43(sb41)* worms was completely rescued by *Y17G9B.9(RNAi)* (Figure 3-11). This provided strong evidence that I had identified *mel-43* and that the original mutation was likely not a simple loss-of-function allele. I refer to Y62E10.A and H02I12.5 as *mpar-1* (*mel-43* paralogue) and *mpar-2* respectively.

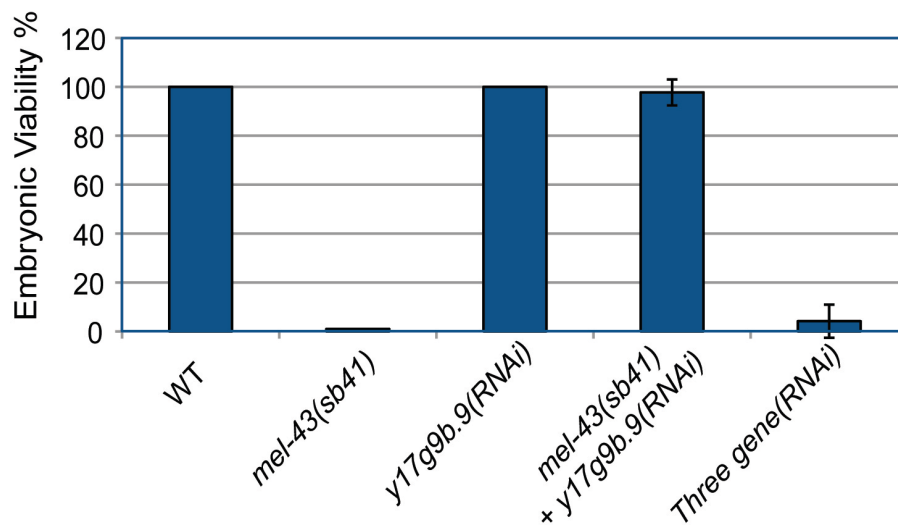


Figure 3-11: Identification of *mel-43* and two paralogues. Percent viability of progeny for each worm is shown. ($n > 600$ progeny from > 3 hermaphrodites for each). Embryonic viability of *mel-43(sb41)* is rescued by *Y17G9B.9(RNAi)*. “Three gene RNAi” represents full-length RNA from *mel-43* expected to target *mel-43* and the two closely-related paralogues. Bars show SD.



Figure 3-12: Amino acid sequence alignment of MEL-43 and two closely-related paralogues MPAR-1 and MPAR-2 using CLUSTAL O(1.1.0). Asterisks indicate a fully conserved residue. Colons indicate groups with strongly similar properties. Periods indicate groups with weakly similar properties. The *sb41* lesion is outlined in red.

3.3 Characterization of two closely-related paralogues of *mel-43*

mel-43(sb41) mutants have defective anaphase II as well as failure to extrude the second polar body. The chromosomal aneuploidy resulting from failed meiosis II, as well as the cytokinesis defects observed in mitosis, are likely responsible for the 100% embryonic lethality at 25°C. Although *mel-43(null)* is wild type, *mel-43&mpar-1/2(RNAi)* results in

100% lethality at 25°C (Figure 3-11). In order to analyze the cellular phenotypes of embryos lacking all 3 paralogues, *in utero* fluorescence time-lapse microscopy on a strain expressing GFP::tubulin and mCherry::histone (MAS138) was performed. *mel-43&mpar-1/2(RNAi)* embryos exhibited normal meiosis I spindle assembly, metaphase I, as well as segregation of homologous chromosomes in anaphase I. However, cytokinesis did not occur at the end of anaphase I, resulting in a failure to extrude the first polar body (Figure 3-13). Surprisingly, *mel-43&mpar-1/2(RNAi)* embryos did not assemble a meiosis II spindle, but instead exhibited decondensation of sperm DNA and the maturation of the centrosomes, hallmarks of mitotic prophase (Figure 3-13, arrows and arrowhead). Therefore, after failure in cytokinesis of meiosis I, *mel-43&mpar-1/2(RNAi)* embryos proceed to mitosis without forming a meiosis II spindle. Chromosome segregation occurred in mitosis (Figure 3-13) and cytokinesis was initiated but did not complete, resulting in a multinucleate cell. The cell-cycle length between meiosis and mitosis was variable in the RNA-treated embryos; however, most of them entered mitosis sooner than wild-type embryos. Therefore, the *mel-43&mpar-1/2(RNAi)* embryos exhibit some delay between meiosis I and mitosis, but this time is shorter than expected for a typical meiosis II program (Figure 3-14).

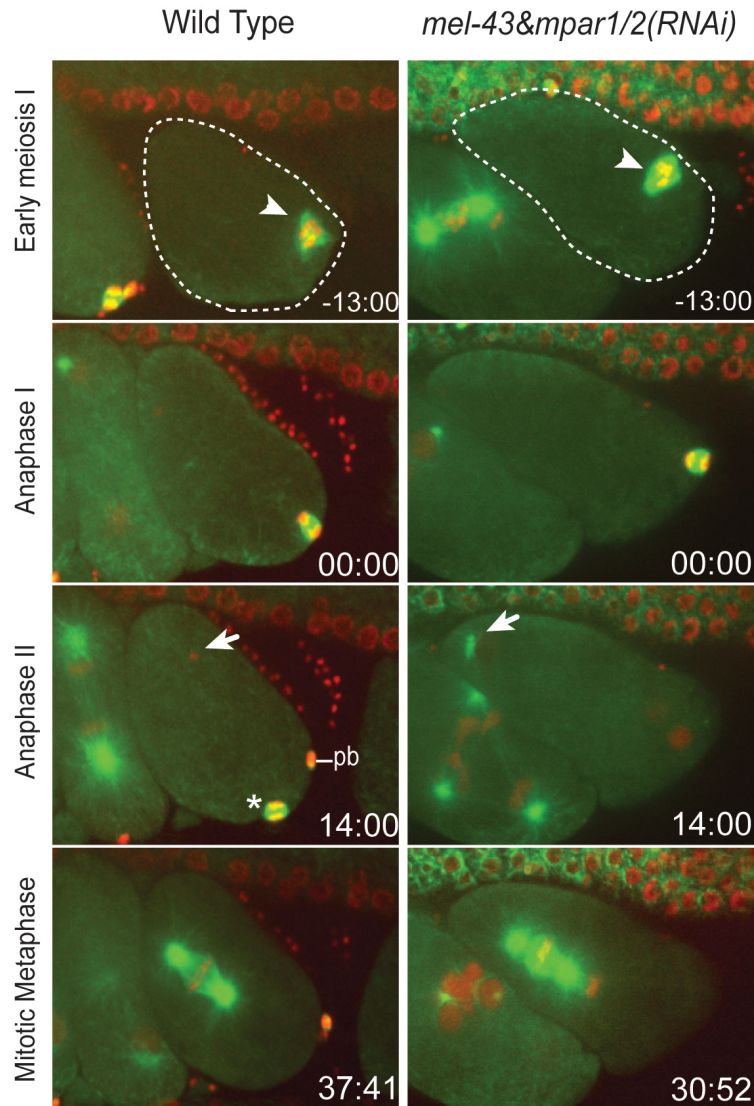


Figure 3-13: The MEL-43 paralogue family are required for the female meiosis II program. Selected frames from a time-lapse movie of wild-type and *mel-43&mpar1/2(RNAi)* embryos expressing GFP::tubulin (microtubules; green) and mCherry::histone (DNA; red) are shown. Anaphase I is time=0. The meiosis I spindle assembles normally (arrowhead) in the fertilized oocytes (outlined) in both wild-type and RNAi-treated samples. Wild-type embryos segregate sister chromatids in anaphase II (asterisk), however, RNAi-treated embryos exhibit mitotic, rather than meiosis II structures. The sperm-derived centrosomes are quiescent in WT; in the RNAi sample, the centrosomes nucleate microtubules prematurely (compare arrows).

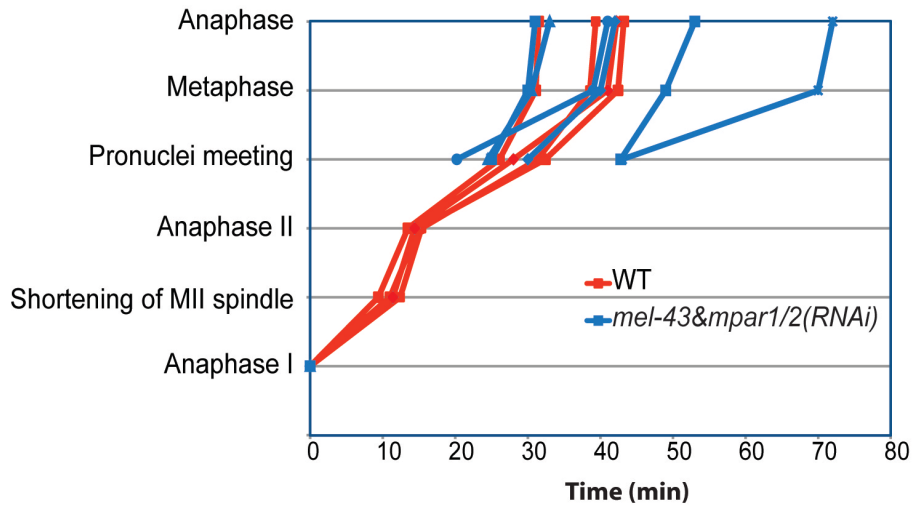


Figure 3-14: Timing of events in wild-type (red; n = 4) and *mel-43&mpar-1/2(RNAi)* (green; n = 6) embryos. Anaphase I is t=0.

Since *mel-43* and the paralogues are together involved in meiosis II spindle assembly, I sought to determine the contributions of individual paralogues to this process. Therefore, viable strains containing each single deletion were obtained and single worm PCR genotyping was used to make double-deletion homozygotes.

All of the single deletion and double-deletion worms were scored for lethality at three temperatures, 15°C, 20°C and 25°C. Single deletions of *mel-43*, *mpar-1*, or *mpar-2* appeared wild type, however, different double-deletion combinations exhibited some lethality, depending on the genes deleted (Figure 3-15). The *mel-43(Δ); mpar-1(Δ)* combination resulted in the most severe phenotype (as low as 50% hatching) (Figure 3-15). Using DIC light microscopy, we observed impenetrant defects that were reminiscent of the *mel-43(sb41)* and *mel-43&mpar-1/2(RNAi)* phenotypes, such as extra female pronuclei likely resulting from meiotic failure and/or

polar body extrusion defects, as well as failure in cytokinesis at the end of the mitosis. The double deletion mutants indicated that each single gene was capable of providing at least partial function for survival of most embryos, and that each of these genes normally plays a role in early embryonic processes. A triple mutant was not recovered, suggesting that loss of all three genes results in embryonic lethality, as suggested from the RNAi experiments.

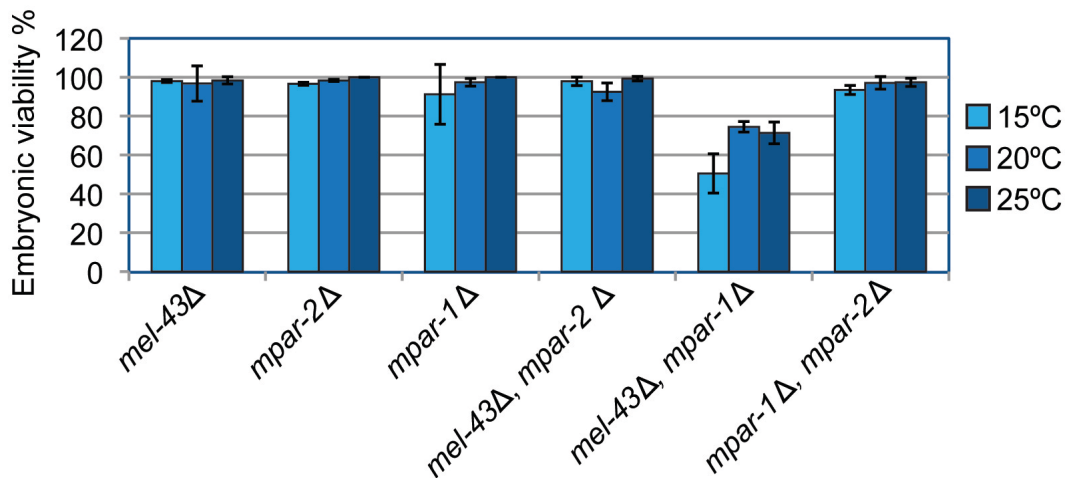


Figure 3-15: Embryonic viability assessment of different strains having deletions for one or more *mel-43* paralogues. Viabilities were calculated from at least three hermaphrodites and >200 progeny at three different temperatures. Bars show SD.

3.4 Subcellular distribution of *mel-43*

Since *mel-43(sb41)* mutants are defective in exiting meiosis II and *mel-43&mpar-1/2(RNAi)* embryos skip the meiosis II division, *mel-43* might be involved in regulating the cell cycle progression during the meiosis-to-

mitosis transition. In order to determine the function of *mel-43* in the early stages of development, it was necessary to assess the subcellular distribution of the MEL-43 protein. Since MEL-43 is a novel protein, no commercial antibody or GFP fusion transgenes were available. Therefore, two parallel procedures were performed to determine the location of the MEL-43 protein in the cell; 1) constructing MEL-43::GFP transgenic embryos and 2) making antibodies directed against MEL-43.

3.4.1 Towards constructing a MEL-43::GFP fusion protein

Making MEL-43::GFP transgenic embryos would be very useful for investigating the location of MEL-43 protein throughout the cell cycle. In order to make the transgene, *mel-43* was cloned into a PAZ-GFP(Amp) vector containing a functional copy of the *unc-119* (uncoordinated) gene with a selection marker of ampicillin resistance. Sequencing of the cloned *gfp::mel-43* fusion construct was performed to make sure that the DNA was free of mutations. The plasmid was adhered to gold beads and the high-speed particle bombardment technique was used to transfer the plasmid into the *unc-119(ed3)* mutant worms, which have paralyzing neuronal defects that prevent dauer formation and cause the death of the worms in the absence of food (Maduro and Pilgrim, 1995). Worms that move well and survive starvation are selected for and identified as successful transformants. Individual worms exhibiting 100% transmission of *unc-119* rescue indicate likely insertion of the DNA into the worm

genome (Praitis et al., 2001). Unfortunately, after performing thirty bombardment reactions, none of the *unc-119(ed3)* worms were rescued and no transgenic animals were isolated.

Table 3-3: Primers generated and used for making MEL-43::GFP transgene.

Primer Name	Primer Sequence
y17g9b.9_spe1-F1	5'-TTA CTA GTT CAG CTC CAT CTC GCA CC-3'
y17g9b.9_xma1-R1	5'-AAG GGC CCAAT GCG GGC AAT ATA CA-3'

In addition to the microparticle bombardment technique, another technique called MosSCI (Mos1-mediated Single Copy Insertion; (Frokjaer-Jensen et al., 2008; Zeiser et al., 2011) was attempted. For the MosSCI technique, the gateway cloning system was used to clone *mel-43* into the destination vector. Gateway cloning requires successive recombination reactions to transfer the DNA fragments between different cloning vectors without changing the reading frame. The destination vector, which contained *mel-43* and a functional copy of *unc-119*, was made using BP clonase and LR clonase during two rounds of gateway recombination reactions. The final vector was sequenced to confirm the absence of mutations and 80 *unc-119(ed3)* worms were injected. In this technique, mobilization of the Mos1 transposon is used to generate a double-strand break in a specific non-coding DNA. The injected transgenic DNA provides a template from which repair of the dsDNA break can occur (Frokjaer-Jensen et al., 2008; Zeiser et al., 2011). As with the bombardment

technique, the selection scheme also involves *unc-119* rescue. Unfortunately, no rescuing lines were recovered with this approach.

Table 3-4: Primers generated and used for making a ,*mel-43::gfp* transgene by the MosSCI technique.

Primer Name	Primer Sequence
y17g9b.9_mos_N_F1	5'-GGG GAC AAG TTT GTA CAA AAA AGC AGG CTC ATC AGC TCC ATC TCG CAC CGT C -3'
y17g9b.9_mos_N_R1	5'-GGG GAC CAC TTT GTA CAA GAA AGC TGG GTA TTA CTC GTC CTC TTC ATC CAG -3'
y17g9b.9_mos_C_F1	5'-GGG GAC AAG TTT GTA CAA AAA AGC AGG CTC AAT GTC AGC TCC ATC TCG CAC C-3'
y17g9b.9_mos_C_R1	5'-GGG GAC CAC TTT GTA CAA GAA AGC TGG GTA CTC GTC CTC TTC ATC CAG TTC-3'

3.4.2 MEL-43 antibody production

Because of the difficulties encountered in generating a GFP fusion protein, rabbit antibodies were generated against MEL-43 to investigate the subcellular distribution of the protein. In order to make antibodies against MEL-43, a bacterially-expressed GST-fusion of the full-length MEL-43 was made. In order to assess the purified antibodies and to determine the behaviour of the protein *in vivo*, Western blots were performed on hermaphrodite worm lysates made from wild type and each of the deletion mutants. The purified antibodies detected three proteins, which ranged in size from 45 to 52 kDa (Figure 3-16). The predicted size for all three paralogues was 40 kDa, however, the deletion mutants revealed the identity of each species on the blot, and provided a

confirmation that the antibodies recognize all three paralogous proteins. All three proteins were also detected in *mel-43(sb41)* mutant lysate (Figure 3-16), indicating that *sb41* does not significantly alter the levels of MEL-43 or the two paralogues. The apparent lack of protein bands in worm lysates derived from adult males was consistent with MEL-43 having a maternal function (Figure 3-17). Using the same blotting and probing conditions as above, bands were not detected on Western blots of lysates prepared from embryos. This result suggests that MEL-43 and the paralogous proteins are likely degraded sometime after the completion of meiosis.

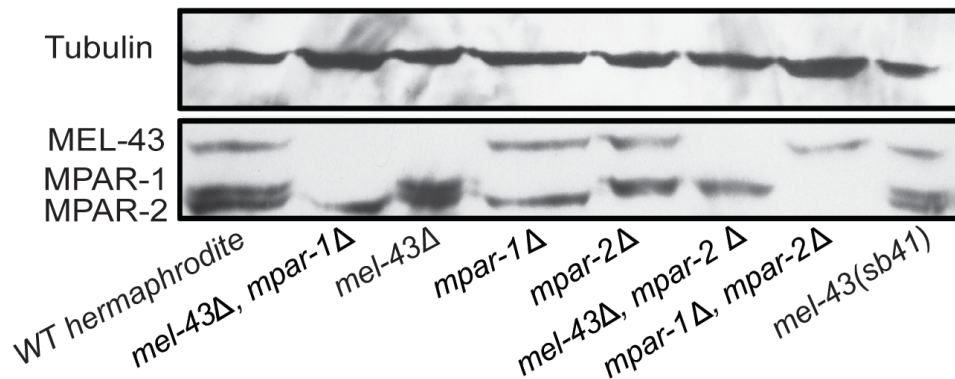


Figure 3-16: Western blot of worm lysates probed with anti-MEL-43. MEL-43 antiserum detects MEL-43 and two closely-related paralogues. Worm strains homozygous for different deletion mutant combinations indicate the identity of each protein and the specificity of the antibodies. All three proteins are present in *mel-43(sb41)* mutants. Tubulin is used as a loading control.

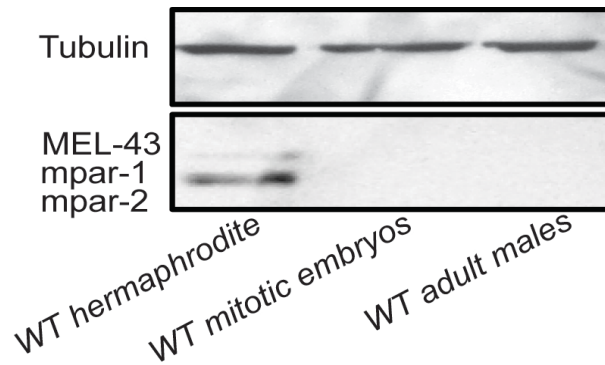


Figure 3-17: Western blot of wild-type worm lysate, mitotic embryos and males probed with anti-MEL-43. MEL-43, MPAR-1 and MPAR-2 proteins are enriched in WT hermaphrodite total lysate, but are not evident in male worm lysate, or embryo lysate, which contains mostly late-stage embryos.

In order to determine the location of MEL-43 and paralogues, meiotic and mitotic embryos were fixed and immunostained with rabbit anti-MEL-43, mouse anti-tubulin to visualize microtubules, and DAPI to visualize DNA. Indirect immunofluorescence of MEL-43 revealed a strong cytoplasmic signal in meiosis I and in some meiosis I embryos a signal slightly above cytoplasmic background was observed at the midzone of the meiosis I spindle (Figure 3-18). In meiosis II embryos, the cytoplasmic signal was slightly reduced, however a prominent fibrous staining pattern was usually observed at the midzone of the meiosis II spindle (Figure 3-18). The high cytoplasmic levels present in meiosis I embryos probably decrease the signal-to-noise ratio of any specific subcellular region of interest, thus it is difficult to ascertain the nature of the weak midzone signal observed in some of the meiosis I spindles. Quantification of the cytoplasmic fluorescence intensity revealed that the cytoplasmic signal

drops considerably by the start of mitosis (Figure 3-20). *mel-43&mpar-1/2(RNAi)* significantly reduced staining of all structures in meiosis, confirming the specificity of the antibody (Figure 3-19 and 3-20). In *mel-43(sb41)* embryos, the cytoplasmic signal was more variable, possibly due to observed delays in meiosis (Figure 3-19 and 3-20).

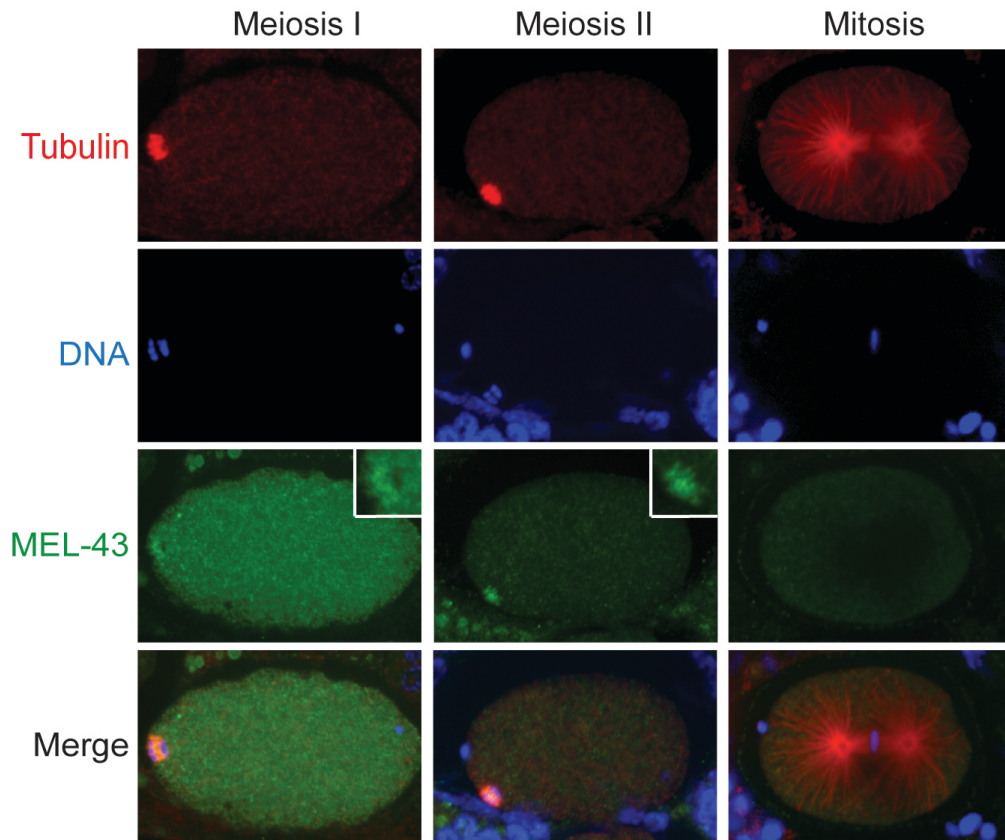


Figure 3-18: Immunofluorescence staining with anti-MEL-43 antibodies. MEL-43 antibody staining of wild-type embryos indicated high cytoplasmic levels in meiosis as well as a fibrous staining pattern in the midzone of the meiosis II spindle, and possibly meiosis I spindle (insets). Microtubules in red, DNA in blue and MEL-43 in green.

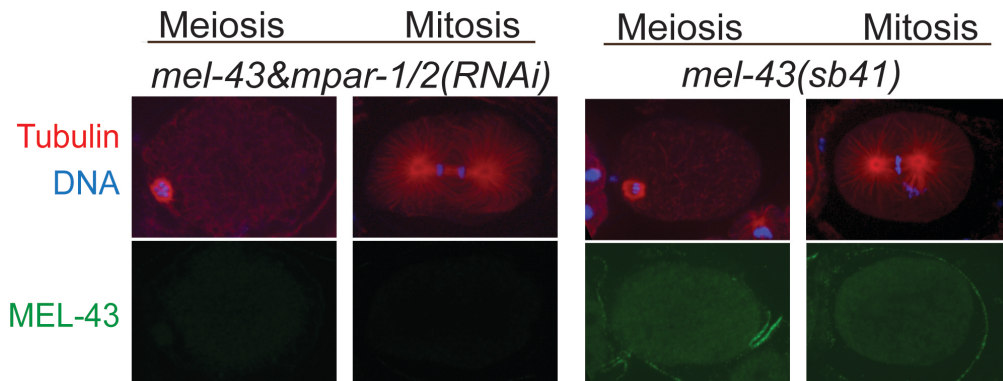


Figure 3-19: Immunofluorescence staining of the *mel-43&mpar-1/2(RNAi)* embryos confirmed the specificity of the antibody. *mel-43(sb41)* embryos exhibited higher cytoplasmic fluorescence in meiosis, similar to wild type.

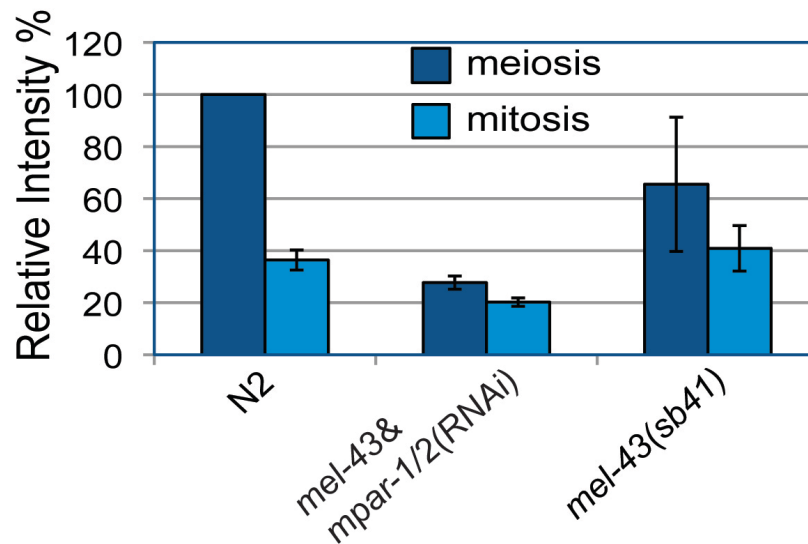


Figure 3-20: Quantification of MEL-43 cytoplasmic levels in meiosis and mitosis of wild-type, *mel-43&mpar-1/2(RNAi)* and *mel-43(sb41)* embryos. Data indicates a decrease from meiosis stage embryos to mitosis. These levels are greatly reduced in the RNAi samples but seem more variable in the *mel-43(sb41)* mutant, possibly due to observed delays in meiosis II. Bars show SD.

3.5 Investigating the relationship between MEL-43 and pathways of post-meiotic protein degradation

mel-43(sb41) embryos have severe delays in metaphase of meiosis II and they are unable to complete anaphase II. In *C. elegans*, two different complexes have been shown to be required for the progression through meiosis I and meiosis II. The anaphase promoting complex (APC) functions as an E3 ligase for ubiquitin-mediated proteolysis and in *C. elegans*, is required for exit from female meiosis I (Golden et al., 2000). Knock-out of any subunits of this complex results in an arrest in metaphase of meiosis I. Like the APC for meiosis I, another specific E3 ligase complex containing CUL-2 (cullin-ring ubiquitin-ligase) has been shown to be essential for meiosis II metaphase-to-anaphase transition (Liu et al., 2004; Vasudevan et al., 2007). This complex ubiquitinates substrates such as cyclins CYB-1 and CYB-3 and primes them for destruction. Loss of components of this complex result in a delay in metaphase of meiosis II, which is caused by the cyclin B accumulation. *zyg-11(RNAi)* embryos eventually go through anaphase II but they fail to extrude the second polar body. The 26S proteasome degrades the proteins and causes progression through metaphase II (Pickart, 2001).

3.5.1 Cyclin B1 degradation in *mel-43&mpar-1/2(RNAi)* embryos

Since the phenotype of *zyg-11(RNAi)* resembles *mel-43(sb41)* embryos at least in part, MEL-43 might be affecting the function of an E3-ligase like ZYG-11. In order to test whether MEL-43 is required for the degradation of cyclin during the meiosis–mitosis transition, I examined the behaviour of cyclin B1, one of two cyclins that are degraded at this cell-cycle stage. Degradation of CYB-1 is required for progression through meiosis. It gets degraded primarily by the APC complex at the end of meiosis I and by the cullin-based E3 ligase complex at the end of meiosis II. Defects in any of these pathways cause persistence of Cyclin B in the embryo (Golden et al., 2000; Sonnevile and Gonczy, 2004). Therefore, the degradation of CYB-1 was assessed by injecting *mel-43&mpar-1/2* dsRNA into worms that express GFP::CYB-1. In wild type, oocytes have high GFP::CYB-1 fluorescence levels and by fertilization, levels begin to decrease due to function of the regulatory complexes (Liu et al., 2004; Sonnevile and Gonczy, 2004). Four embryos for each of the wild type and *mel-43&mpar-1/2(RNAi)* embryos were used. Photobleaching was controlled by calculating the ratio of the fluorescence signal in the desired one-cell embryo to an adjacent multicellular embryo in the uterus.

In both wild type and *mel-43&mpar-1/2(RNAi)* embryos, CYB-1 levels were observed to decline similarly from time 0 after exit from the spermatheca (Figure 3-21). The fluorescence ratio gradually decreased,

reaching a value of approximately 1.2 times above background at 35 minutes post-spermatheca exit (Figure 3-22). The lack of any obvious difference in the rate of cyclin B degradation between wild type and *mel-43&mpar-1/2(RNAi)* embryos indicated that *mel-43* and its paralogues were not likely involved in ubiquitin-mediated degradation by regulating the APC or CUL-2/ZYG-11.

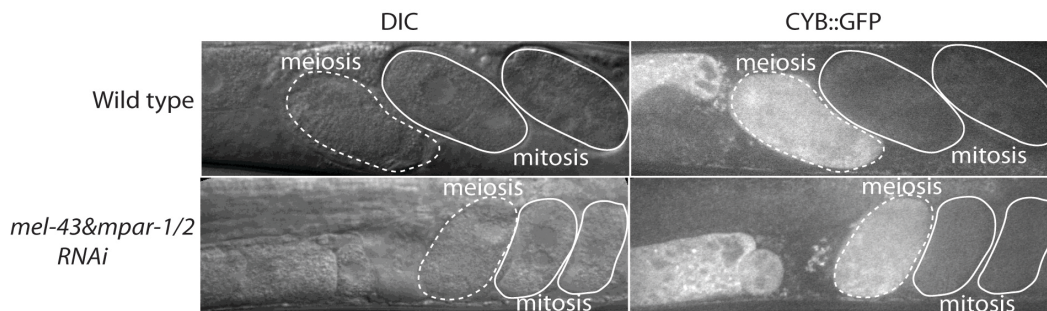


Figure 3-21: Cyclin B1 degradation in wild-type and *mel-43&mpar-1/2* (RNAi) embryos. Selected frame from a time-lapse movie of wild-type and *mel-43&mpar-1/2*(RNAi) embryos expressing GFP::CYB-1 with a single stack of DIC for showing the stages of the embryos in the gonad. GFP signal can be detected in oocytes and the meiotic embryos. Meiotic embryos are shown with dashed line and mitotic embryos with solid lines.

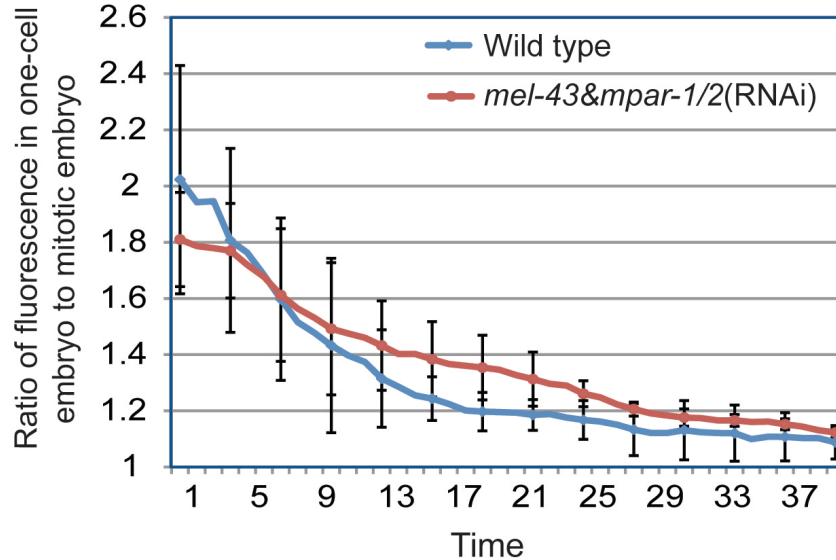


Figure 3-22: Measurement of the CYB- 1::GFP fluorescence intensity over time. Time 0 refers to spermatheca exit. Integrated intensity was calculated from the embryo of interest as well as for a multicellular embryo already in the uterus, to account for photobleaching. The ratio of fluorescence intensity was calculated and plotted.

3.5.2 Katanin degradation in *mel-43&mpar-1/2(RNAi)* embryos

The *mel-43&mpar-1/2(RNAi)* embryos enter mitosis without meiosis II spindle assembly. These embryos do not exhibit a lengthy delay or arrest in meiosis, arguing that the cell cycle machinery is functional. To further evaluate the mitotic cellular environment, the localization and degradation of a meiosis-specific factor was assessed. The MEI-1 protein is the catalytic subunit of *C. elegans* katanin, which localizes to the meiosis I and II spindles (with concentration at kinetochores and poles) and it is essential for proper meiotic spindle function (Srayko et al., 2000). CUL-3 ubiquitin ligase targets MEI-1 for ubiquitin-mediated proteolysis after meiosis (Furukawa et al., 2003; Pintard et al., 2003b). The MEL-26 protein

is the substrate-specific adaptor for MEI-1 degradation, and if MEL-26 is removed, MEI-1 persists into mitosis, localizing to centrosomes and kinetochores, causing mitotic spindle assembly defects (Pintard et al., 2003b). In order to determine if MEI-1 is degraded in *mel-43&mpar-1/2(RNAi)* embryos, *in utero* imaging of a MEI-1::GFP fluorescent strain was performed. In contrast to the *mel-26(RNAi)* positive control, the *mel-43&mpar-1/2(RNAi)* embryos behaved as wild type, with MEI-1 localizing to meiotic spindles but not to mitotic spindles (Figure 3-23).

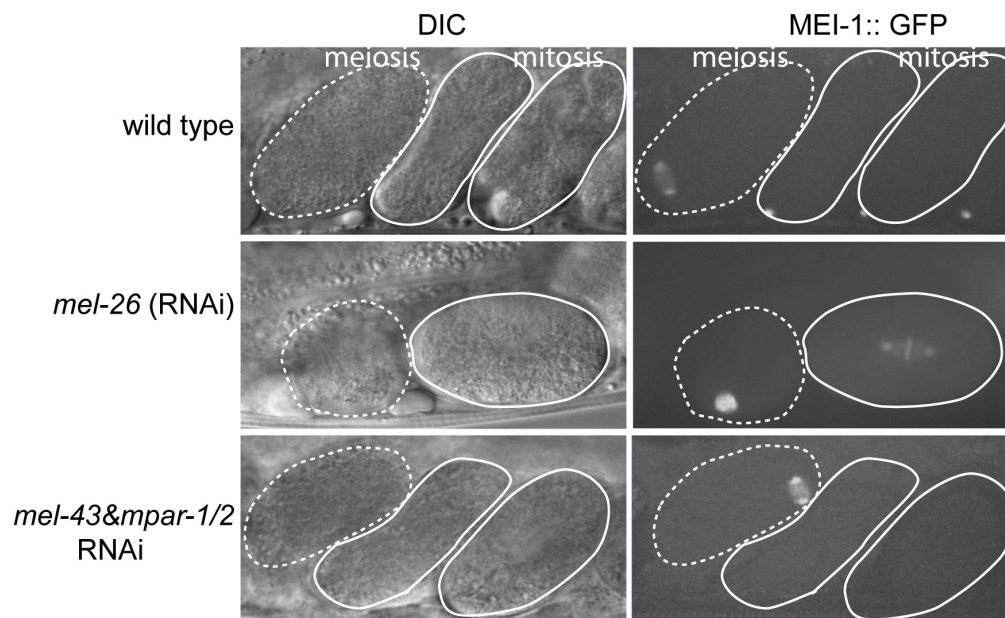


Figure 3-23: MEI-1 degradation in wild-type and *mel-43&mpar-1/2 (RNAi)* embryos. Stacks of wild-type, *mel-26(RNAi)* and *mel-43&mpar-1/2(RNAi)* embryos expressing GFP::MEI-1 with a single stack of DIC for showing the stages of the embryos in the gonad. Meiotic embryos are shown with dashed line and mitotic embryos with solid lines.

3.5.3 Investigation of the APC and cullin-based E3 ligase complex on MEL-43 degradation

Since MEL-43 is a cytoplasmic protein, which degrades at the end of meiosis, there is a possibility that MEL-43 is an uncharacterized substrate of ubiquitin-mediated proteolysis. In order to test whether the decline in MEL-43 protein levels observed in the one-cell embryo was affected by loss of a known proteolysis pathway, I performed RNAi feeding experiments to inactivate each of these two complexes separately, and then measure MEL-43 levels by indirect immunofluorescence *in vivo*.

mat-2 encodes one of the subunits of the anaphase-promoting complex (APC) and is required for chromosome segregation during meiosis I. *mat-3* encodes a conserved regulatory subunit of the APC and both of these genes are required for targeting proteins for degradation during the meiosis I metaphase-to-anaphase transition (Golden et al., 2000; Stein et al., 2007). Immunostaining was performed to compare the MEL-43 signal in meiosis I and mitosis of the wild-type and RNAi embryos. Although inactivation of these genes causes a severe delay in meiosis I, eventually these embryos progress. This progression might be the result of redundant activity of the CUL-2 based E3 ligase complex in meiosis I for degradation of substrates such as cyclin B when APC is inactive (Sonneville and Gonczy, 2004). In both *mat-2(RNAi)* and *mat-3(RNAi)*, the MEL-43 signal decreased after meiosis, which proved that MEL-43 was degrading even without APC activity (Figures 3-24 and 3-25).

ZYG-11 functions as a substrate-specific adaptor of the cullin-based E3 ligase complex, therefore knock-down of this protein interferes with the function of the complex (Liu et al., 2004; Sonnevile and Gonczy, 2004). Using immunostaining, *zyg-11(RNAi)* revealed a high signal for MEL-43 in mitosis which indicates a failure in MEL-43 degradation (Figures 3-24 and 3-25). This observation confirmed that the cullin-based E3 ligase complex is required for the observed reduction of cytoplasmic MEL-43 protein levels during the meiosis-to-mitosis transition.

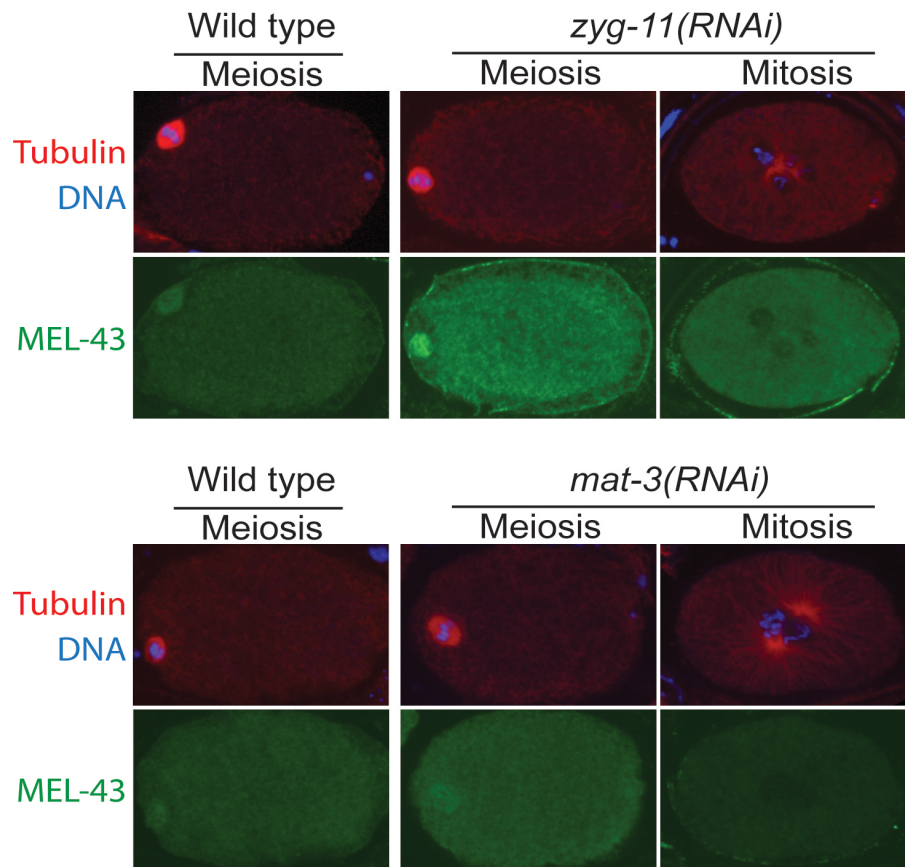


Figure 3-24: MEL-43 antibody staining of wild-type, *mat-3(RNAi)* and *zyg-11(RNAi)* embryos. Tubulin (red), DNA (blue) and MEL-43 (green). MEL-43 does not degrade in mitosis of *zyg-11(RNAi)* embryos. Decreased cytoplasmic signal of MEL-43 in mitosis is observed in both wild-type and *mat-3(RNAi)* embryos.

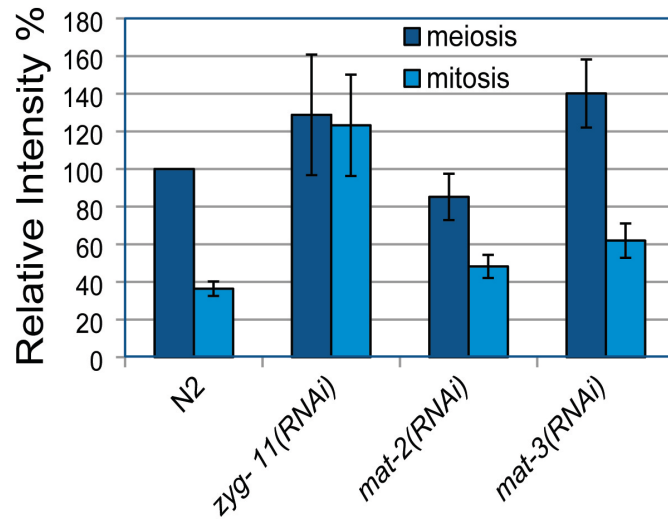


Figure 3-25: Quantification of cytoplasmic levels of MEL-43 in wild-type, *zyg-11(RNAi)*, *mat-2(RNAi)* and *mat-3(RNAi)*. High mitotic signal for *zyg-11(RNAi)* embryos indicates that ZYG-11 is required for post-meiotic reduction of MEL-43 levels.

3.6 Assessing REC-8 location in *mel-43(sb41)* mutants

The acentrosomal spindles in female meiosis facilitate the segregation of homologous chromosomes in meiosis I and sister chromatids in meiosis II. These two meiotic divisions are necessary to form a haploid set of female chromosomes. In order to segregate homologous chromosomes and sister chromatids properly, the physical associations between homologues and sister chromatids must be strictly controlled (Mito et al., 2003; de Carvalho et al., 2008). The cohesins, proteins that physically link homologues and sister chromatids, play an important role in controlling how chromosomes separate in the two meiotic divisions. During anaphase I, REC-8 cohesin is removed from

homologous chromosomes (Pasierbek et al., 2001). However, the sister chromatids remain associated during this process. At the end of this division the first polar body is extruded and the second meiotic spindle forms around the haploid set of sister chromatids. In anaphase II, REC-8 is removed to allow sister chromatid separation (Pasierbek et al., 2001) the second polar body is extruded and the meiotic division completes.

In *mel-43(sb41)* mutants, meiosis I occurs successfully and the embryos extrude their first polar body. However, after metaphase of meiosis II, chromatids are unable to segregate. Consistent with the *mel-43(sb41)* phenotype, persistence of REC-8 during meiosis II would prevent or delay sister chromatid separation. In order to test this hypothesis, anti-REC-8 antibody was obtained for immunostaining of the *mel-43(sb41)* mutants expressing GFP::tubulin.

In wild-type embryos, the REC-8 signal is high in metaphase I and it gets lower in metaphase II, however, the signal is not visible by anaphase II when sister chromatids separate (Figure 3-26). Since *mel-43(sb41)* embryos do not go through anaphase II, a way to separate the early metaphase II from the late metaphase II stage was required. As mentioned before, in *mel-43(sb41)* mutants, centrosomes eventually nucleate microtubules in the later stages of meiosis II. Therefore, the nucleation of the microtubules was used as a marker for late meiosis II metaphase. In 6/8 late-stage mutant embryos, REC-8 was observed on sister chromatids in meiosis II (Figure 3-26). However, in the embryos that

exhibited some separation of sister chromatids, REC-8 was not visible, 2/8 (Figure 3-26). Therefore, these observations suggest that the persistence of the REC-8/ kleisin on sister chromatids correlates with the failure of the anaphase II in *mel-43(sb41)* mutants. The embryos that exhibit some separation of sister chromatids still exhibit various defects such as abnormal polar body extrusion and cytokinesis failure in mitosis, therefore, *mel-43(sb41)* is likely perturbing multiple events required for the proper completion of meiosis II, including REC-8 removal and polar body formation.

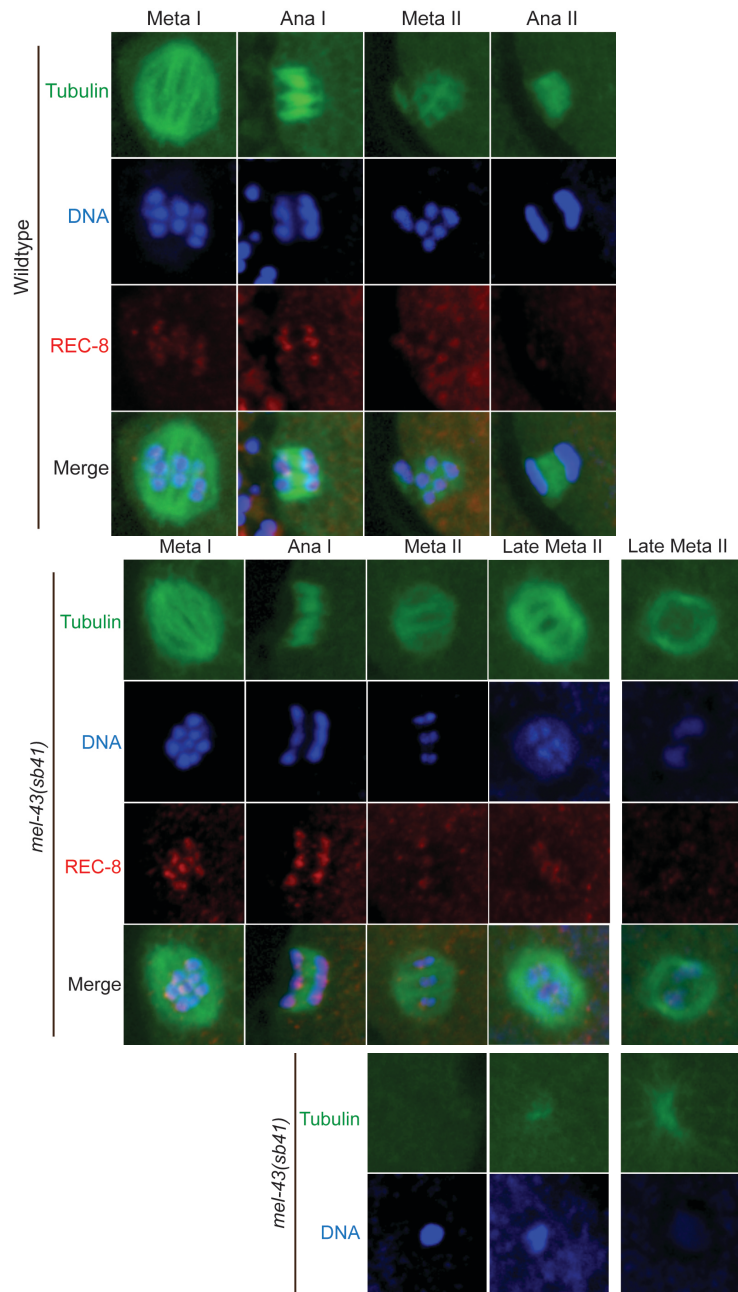


Figure 3-26: Immunofluorescence staining with anti-REC-8 antibody on wild-type and *mel-43(sb41)* embryos. Meiotic spindles are shown in metaphase I, anaphase I, metaphase II and anaphase II. REC-8 stains between the homologues in meiosis I and between sister chromatids in meiosis II. Late meta II (right) represents the mutant embryos that can segregate their chromatids (2/8). Late meta II (left) represents the mutants with failure in anaphase II (6/8). Metaphase and late metaphase are distinguished by the nucleation of the microtubules from the sperm centrosomes (shown below).

4. Discussion

4.1 *mel-43* is part of a novel protein family

mel-43 was originally mapped to chromosome IV between *unc-24* and *fem-3* (Mitenko et al., 1997), however in 2010, this gene was relocated four map units away from the originally-published location, likely near *dpy-13* (Pahara, 2010) Through genomic sequencing of the *mel-43(sb41)* mutant, I discovered a mutation within an uncharacterized gene, Y17G9B.9. The null mutation of Y17G9B.9 has no obvious phenotype, which suggests that it is functionally redundant. Consistent with this idea, database searches revealed two paralogues for this gene that exhibit almost 87% identity in the DNA sequence, termed *mpar-1* and *mpar-2*. There are no homologues outside of nematodes, but it is possible that proteins with diverged sequence perform a similar function in other animals. The RNAi directed against all three related genes resulted in 100% embryonic lethality at 25°C, which confirmed the functional redundancy of *mel-43*. The mutation in *mel-43(sb41)* is a change from proline to serine in amino acid number 75. Although it is difficult to predict the result of such an alteration to the MEL-43 protein, the change does not significantly alter the levels or the mobility of the protein through SDS PAGE. Proline has a unique structure, which makes its confirmation and the confirmation of the residue preceding it limited. Therefore the change from proline to serine in *mel-43(sb41)* mutants might change the

secondary structure of the MEL-43 protein and change its function and/or its interaction with other proteins such as MPAR-1 and MPAR-2.

Since *mel-43(sb41)* mutation is dominant, it could be a gain-of-function mutation. Indeed, chromosomal duplication analysis revealed that *mel-43(sb41)* is hypermorphic. This behavior can be the result of an increase in normal gene activity, for example via increased mRNA and/or protein levels, or a rise in protein activity. However, immunostaining and Western blot analysis revealed that the protein levels are not obviously altered in this mutant strain. Another possibility is that the MEL-43(*sb41*) protein might not respond to some inhibitory signal. In this way, the proline-to-serine mutation might cause inappropriate persistence of MEL-43 and/or paralogue activity, possibly by modulating MEL-43 binding capability.

4.2 *mel-43* is required for the meiosis II program

Deletion mutants of either *mel-43* or any single paralogue revealed no obvious phenotypes, however, RNA-mediated knock-down of all three paralogues resulted in 100% embryonic lethality. Although *mel-43(sb41)* mutants (at 25°C) and *mel-43&mpar-1/2(RNAi)* result in complete embryonic lethality, over the course of this thesis I found that the specific cellular defects associated with these conditions are distinct.

In *mel-43(sb41)* embryos, all aspects of female meiosis I appeared normal, from spindle assembly, homologue segregation, and polar body

extrusion. During a significantly delayed meiosis II, *mel-43(sb41)* embryos exhibited normal spindle assembly but chromosomes usually did not segregate and polar bodies were not extruded (Figure 3-1). Normally, the sperm-derived centrosomes nucleate microtubules only after the completion of meiosis II. However, in *sb41*, the centrosomes initiated microtubule formation despite the presence of a meiosis II spindle in the cytoplasm. This resulted in an embryo that contained three MTOCs within the same cytoplasm, and often the two centrosomes migrated towards the meiotic chromatin, and collided. Surprisingly, mitotic spindles eventually assembled after a brief period of dissolution of all microtubule organization. The mitotic chromosomes segregated in anaphase, but the embryos failed to complete cytokinesis.

In contrast, in *mel-43&mpar-1/2(RNAi)* embryos, homologous chromosomes segregated normally in anaphase I but the first polar body was not extruded and cytokinesis did not occur (Figure 3-13). These embryos never formed a meiosis II spindle, but instead proceeded into mitosis. This was inferred by the decondensation of the sperm DNA, the appearance of nuclear envelopes and centrosomal microtubules. As with *mel-43(sb41)*, mitotic chromosomes segregated during anaphase, but cytokinesis failed (Figure 3-13).

The *mel-43&mpar-1/2(RNAi)* embryos skip meiosis II but progress into mitosis, suggesting that the cell cycle regulatory pathways are working and that these genes are involved in a specific mechanism used to

distinguish between the end of meiosis I vs. the end of meiosis II. *mel-43* and paralogues might normally prevent entry into mitosis after meiosis I, and at the same time, they might also activate meiosis II spindle assembly. In *mel-43(sb41)* mutants, this putative signal to form a meiosis II spindle is normal since they do not reveal any defects prior to anaphase II. However, the *sb41* hypermorphic mutation could reveal a separate function for MEL-43 and paralogues in providing a signal that prevents mitosis after meiosis I. The mutant phenotypes could be explained if this mutation results in a persistent signal whereby, even after meiosis II spindle assembly, cell cycle progression into mitosis is inhibited.

The immunostaining of the wild-type embryos with anti-MEL-43 antibody, which recognizes all paralogues, revealed a strong cytoplasmic signal in meiosis I but a weaker cytoplasmic signal in meiosis II embryos. Interestingly, a fibrous staining pattern was observed at the midzone of meiosis I and II spindles (Figure 3-18). This location suggests a primary role for MEL-43 proteins in spindle function. This would explain the observed defects in chromosome segregation and polar body extrusion/cytokinesis in the mutants and RNAi embryos.

The quantification of the cytoplasmic signal revealed that the protein levels drop considerably by the start of mitosis. *mel-43(sb41)* embryos exhibited a variable cytoplasmic signal that might be a result of meiosis delays in these embryos (Figure 3-19). Therefore, this mutation might not interfere with the normal program of MEL-43 protein degradation,

but that the delay might simply allow more time for the degradation to occur during meiosis, creating more variation to the levels measured during meiosis. Deletion data suggests that the paralogues are functionally redundant and that worms need at least one for survival, therefore lowering the amount of these proteins individually or pair-wise is expected to be negligible, since each of them are capable of doing all the jobs, at least partially. In contrast, failure to degrade these proteins at the right time might interfere with the transition from meiosis to mitosis. Although *mel-43(sb41)* embryos did not result in obvious persistence of the MEL-43 proteins into mitosis, many of the phenotypes observed in *cul-2(RNAi)* embryos were similar to *mel-43(sb41)*, suggesting that at least a subset of the roles of this E3 ubiquitin ligase could involve the *mel-43* pathway.

4.3 MEL-43 and pathways of post-meiotic protein degradation

C. elegans uses two different complexes to regulate meiosis I and meiosis II divisions. Meiosis I requires the anaphase-promoting complex (APC) (Golden et al., 2000; Davis et al., 2002) and meiosis II is regulated by an E3 ligase complex containing the cullin protein CUL-2 and a substrate-recognition subunit, ZYG-11 (Liu et al., 2004; Sonnevile and Gonczy, 2004). Both of these complexes target proteins such as cyclin B types for degradation, which results in the transition from metaphase to anaphase. Based on the similarity between *mel-43(sb41)* mutant phenotypes and phenotypes caused by knock out of these regulatory

complexes, MEL-43 might function in these regulatory pathways. Loss of *mel-43* and the paralogues did not result in any obvious change in cyclin B degradation (Figure 3-22). Therefore, *mel-43* and its paralogues are likely not required for ubiquitin-mediated degradation by regulating the APC or *cul-2/zyg-11* pathways. However, based on the phenotypes observed and the documented reduction in MEL-43 proteins through the meiosis-to-mitosis transition, MEL-43 proteins might be an uncharacterized substrate of ubiquitin-mediated proteolysis at this time.

Inactivation of the APC results in a severe delay in meiosis I, however eventually, some of the embryos are able to exit meiosis and enter mitosis. In those embryos the MEL-43 signal declines to levels similar to wild-type mitosis (Figure 3-25), which demonstrates that MEL-43 can be degraded even though the APC is not functional. This degradation of MEL-43 could be explained by the fact that CUL-2 exhibits a partial functional redundancy with APC during meiosis I (Sonneville and Gonczy, 2004), therefore the CUL-2/ZYG-11 complex might be involved in degrading MEL-43 during the meiosis-to-mitosis transition.

cul-2(RNAi) and *zyg-11(RNAi)* result in a severe delay in meiosis II metaphase, however the embryos eventually enter mitosis (Liu et al., 2004; Sonneville and Gonczy, 2004). If the APC complex is able to degrade MEL-43 at least partially in meiosis I, a slight decrease in the MEL-43 signal would be expected, even in *zyg-11(RNAi)* or *cul-2(RNAi)* embryos. However, *zyg-11(RNAi)* embryos exhibited a high MEL-43 signal

in mitosis, not statistically different from the high levels measured in meiosis (Figure 3-25). From these observations, it can be concluded that intracellular MEL-43 protein levels are sensitive to cullin-based E3 ligase activity, which likely acts during both meiosis I and meiosis II, to trigger the decline of MEL-43 protein levels throughout the transition from meiosis to mitosis.

4.4 *mel-43* and chromosome segregation

Most of the *mel-43(sb41)* embryos fail to segregate chromatids in anaphase and they exhibit a 30 minute delay from metaphase II to metaphase of mitosis. Because spindle assembly checkpoints can prevent the progression of the cell cycle when chromosomes are not properly aligned/attached to microtubules, it is possible that the cell-cycle delays observed in *mel-43(sb41)* embryos are a direct consequence of chromatid mis-attachment or other spindle malfunction.

Cohesin proteins are known to link the chromosomes physically and their removal allows the segregation of the chromosomes. REC-8 is a meiotic-specific cohesin, which localizes between the homologous chromosomes and sister chromatids and its proper removal is required for normal segregation in both meiosis I and II (Pasierbek et al., 2001). In order to have a correct segregation of chromatids in meiosis, removal of the REC-8 is strictly controlled. One of the members of the chromosomal passenger complex, Aurora B kinase (AIR-2), is a key player in this regulation (Rogers et al., 2002). Phosphorylation of REC-8 by AIR-2

allows the protease separase to remove REC-8 from the chromosomes. In meiosis I, LAB-1 localizes between the sister chromatids and prevents REC-8 phosphorylation by AIR-2 in that region (Figure 4-1-A). The PP1 phosphatase GSP-1/2 has also been implicated in counteracting AIR-1 phosphorylation of REC-8 at this time. In meiosis II, LAB-1 removal allows the phosphorylation of REC-8, which results in the segregation of sister chromatids (Rogers et al., 2002; de Carvalho et al., 2008) (Figure 4-1-A).

Immunostaining of *mel-43(sb41)* mutants with anti-REC-8 antibody showed the presence of REC-8 in the delayed meiosis II embryos (Figure 3-26). Therefore, it can be concluded that failure of anaphase II in *mel-43(sb41)* embryos correlates with the persistence of REC-8 on sister chromatid.

Removal of REC-8 from homologous chromosomes in meiosis I of *mel-43(sb41)* embryos confirmed that AIR-2 phosphorylation at this stage is likely occurring normally. The REC-8 persistence in the *mel-43(sb41)* embryos does not necessarily implicate MEL-43 in its regulation directly. However, if AIR-2 uses the same mechanism in both meiosis I and meiosis II, REC-8 persistence in *mel-43(sb41)* mutants might be due to failure to remove LAB-1 from sister chromatids (Figure 4-1-B). Another explanation is that MEL-43 might be downstream of LAB-1 and improper regulation of GSP-1/2 in *mel-43(sb41)* mutants could result in REC-8 persistence between sister chromatids. Determining the behavior of LAB-

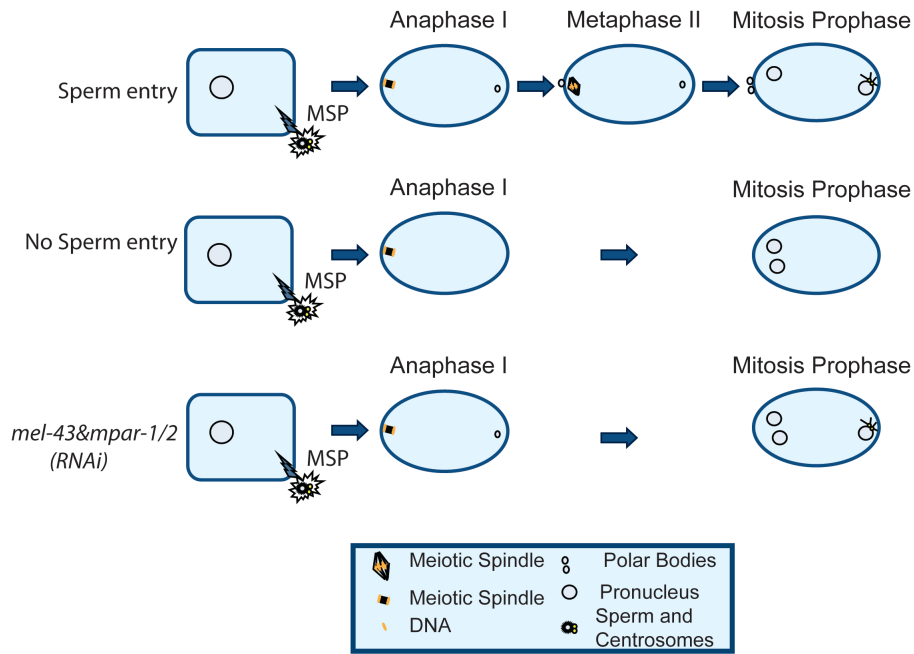
regulating different stages of meiosis and the processes used to differentiate between the end of meiosis I and meiosis II is limited, this work provides some possible mechanisms for regulating these processes.

In 2003, it was shown that a loss-of-function mutation in *cdc-27*, which encodes a putative subunit of the APC complex, resulted in a “skipped meiosis II” phenotype (Shakes, 2003), very similar to *mel-43¶logues(RNAi)* embryos. Therefore, one function for the APC might be to prevent MEL-43 degradation in meiosis I. In this case, the “skipped meiosis II” phenotype observed in the *cdc-27* mutants would result in the loss of MEL-43 protein. We know that the APC and *cul-2/zyg-11* pathways are functionally redundant in meiosis I. I also have shown that *cul-2/zyg-11* is either directly or indirectly responsible for reduced MEL-43 levels at the end of meiosis. Therefore the APC might inhibit at least some functions of *cul-2/zyg-11* activity in meiosis I, and CDC-27 could be directly involved in this pathway. For example, MEL-43 proteins could be protected from CUL-2-mediated degradation by CDC-27. Based on this hypothesis, in the *cdc-27(RNAi)* embryos, the APC would be unable to inhibit *cul-2/zyg-11*, causing premature degradation of MEL-43 and failure to begin the meiosis II program.

In 2005, the McNally lab used a mutant strain that produces non-functional sperm to show that sperm entry into the egg is required for completion of the female meiotic program. As with *mel-43¶logues(RNAi)*, these embryos have normal anaphase I but they

fail to extrude the first polar body and they appear to skip meiosis II (this is complicated because in unfertilized embryos, there are no sperm-derived centrosomes to produce a mitotic spindle) (McNally and McNally, 2005) (Figure 4-2-A). In their model, the sperm promotes the progression of the cell cycle past female meiotic prophase before sperm entry. In these embryos, the APC complex must be functional and independent of fertilization since these embryos are capable of partial degradation of cyclin B and transition from metaphase I to anaphase I. However, fertilization is required for events past anaphase I and the execution of the meiotic program. The nature of the sperm-derived signal has been a mystery, but this thesis presents strong evidence that the MEL-43 proteins are part of this signal. Furthermore, the shared loss-of-function phenotypes between *mel-43* and *cdc-27* suggest that there could be a functional link between the APC (largely responsible for the meiosis I transition) and the CUL-2 E3 ligase (largely responsible for the meiosis II transition) (Figure 4-2-B). Future work on these individual components should elucidate the molecular mechanism behind this interesting regulatory pathway.

A.



B.



Figure 4-2: Fertilization and meiosis II spindle assembly. A. On the top row, major sperm proteins activate the oocyte for meiosis I spindle assembly. Sperm entry is necessary for subsequent events such as extrusion of the first polar body and formation of the second meiotic spindle. On the second row, lack of sperm entry results in failure to extrude the first polar body, and the meiosis II program is skipped. On the last row, *mel-43&mpar-1/2(RNAi)* embryos also fail to extrude the first polar body and they skip the second meiosis. B. One possible pathway connecting a putative fertilization signal to the meiosis II program is suggested. This is based on previous work indicating a role for CDC-27 and sperm entry on promoting the meiosis II program. If fertilization activates CDC-27, then this could inhibit the cullin-based E3 ligase complex, which would prevent degradation of MEL-43 protein until after meiosis is completed. In this model, high levels of MEL-43 in meiosis I are required for meiosis II spindle assembly.

4.6 Mel-43 and cytokinesis

mel-43(sb41) and *mel-43&mpar-1/2(RNAi)* embryos exhibit cytokinesis failure in both meiosis and mitosis. *mel-43(sb41)* embryos have normal cytokinesis at the end of meiosis I, however in meiosis II and mitosis they fail in cytokinesis (Figure 3-1). *mel-43&mpar-1/2 (RNAi)* embryos were never observed to complete cytokinesis in meiosis or mitosis (Figure 3-13). Based on these observations, *mel-43* and the paralogous likely participate in cytokinesis mechanisms. One of the factors that is required for both meiosis and mitosis cytokinesis as well as the segregation of chromosomes is the chromosomal passenger protein Aurora kinase B (AIR-2). AIR-2 phosphorylates ZEN-4 and MKLP1 (proteins required for completion of cytokinesis and extrusion of polar bodies) to complete cytokinesis while phosphorylation of REC-8/kleisin by AIR-2 results in release of chromosomes in anaphase (Severson et al., 2000; Rogers et al., 2002; Guse et al., 2005). The phenotypes observed suggest that the loss of *mel-43* and paralogues might result in a block in Aurora B kinase activity. In addition, the *sb41* mutation would also be expected to interfere with Aurora B kinase activity, and this suggests a possible separation of function for this part of the MEL-43 protein. Further work on the *mel-43(sb41)* mutation and an investigation of the specific nature of the cytokinesis defects should shed more light on this particular pathway implicated in MEL-43 function.

4.7 Summary

The mechanisms involved in transition from meiosis to mitosis and controlling the formation of two types of spindles in one embryonic cytoplasm is not fully understood. Processes used to differentiate between the end of meiosis I and meiosis II as well as the role of the sperm in this process are not known. In this work, the MEL-43 protein family is introduced as a part of this mechanism through its involvement in directing meiosis II spindle assembly. Furthermore, the phenotypes observed suggest a possible functional link between the APC and the CUL-2 E3 ligase regulatory complexes. More experiments on the individual components of these complexes are required to determine the details behind these regulatory pathways. Interestingly, the novel MEL-43 family is also implicated in chromosome segregation and cytokinesis. Further investigation of the relationship between the MEL-43 family and AIR-2 kinase might reveal a new pathway that regulates these essential processes.

5. Bibliography

- Abrieu, A., Doree, M. and Fisher, D. (2001) 'The interplay between cyclin-B-Cdc2 kinase (MPF) and MAP kinase during maturation of oocytes', *J Cell Sci* 114(Pt 2): 257-67.
- Aceves, J., Erlij, D. and Martinez-Maranon, R. (1970) 'The mechanism of the paralyzing action of tetramisole on *Ascaris* somatic muscle', *Br J Pharmacol* 38(3): 602-7.
- Albertson, D. G. and Thomson, J. N. (1982) 'The kinetochores of *Caenorhabditis elegans*', *Chromosoma* 86(3): 409-28.
- Andrews, P. D., Knatko, E., Moore, W. J. and Swedlow, J. R. (2003) 'Mitotic mechanics: the auroras come into view', *Curr Opin Cell Biol* 15(6): 672-83.
- Askjaer, P., Galy, V., Hannak, E. and Mattaj, I. W. (2002) 'Ran GTPase cycle and importins alpha and beta are essential for spindle formation and nuclear envelope assembly in living *Caenorhabditis elegans* embryos', *Mol Biol Cell* 13(12): 4355-70.
- Azimzadeh, J. and Bornens, M. (2007) 'Structure and duplication of the centrosome', *J Cell Sci* 120(Pt 13): 2139-42.
- Bischoff, F. R. and Ponstingl, H. (1991) 'Catalysis of guanine nucleotide exchange on Ran by the mitotic regulator RCC1', *Nature* 354(6348): 80-2.
- Bobinnec, Y., Khodjakov, A., Mir, L. M., Rieder, C. L., Edde, B. and Bornens, M. (1998) 'Centriole disassembly in vivo and its effect on centrosome structure and function in vertebrate cells', *J Cell Biol* 143(6): 1575-89.
- Bornens, M. (2002) 'Centrosome composition and microtubule anchoring mechanisms', *Curr Opin Cell Biol* 14(1): 25-34.
- Boxem, M., Srinivasan, D. G. and van den Heuvel, S. (1999) 'The *Caenorhabditis elegans* gene *ncc-1* encodes a *cdc2*-related kinase required for M phase in meiotic and mitotic cell divisions, but not for S phase', *Development* 126(10): 2227-39.
- Brenner, S. (1974) 'The genetics of *Caenorhabditis elegans*', *Genetics* 77(1): 71-94.

- Buonomo, S. B., Clyne, R. K., Fuchs, J., Loidl, J., Uhlmann, F. and Nasmyth, K. (2000) 'Disjunction of homologous chromosomes in meiosis I depends on proteolytic cleavage of the meiotic cohesin Rec8 by separin', *Cell* 103(3): 387-98.
- Burrows, A. E., Scurman, B. K., Kosinski, M. E., Richie, C. T., Sadler, P. L., Schumacher, J. M. and Golden, A. (2006) 'The *C. elegans* Myt1 ortholog is required for the proper timing of oocyte maturation', *Development* 133(4): 697-709.
- Church, D. L., Guan, K. L. and Lambie, E. J. (1995) 'Three genes of the MAP kinase cascade, mek-2, mpk-1/sur-1 and let-60 ras, are required for meiotic cell cycle progression in *Caenorhabditis elegans*', *Development* 121(8): 2525-35.
- Clark-Maguire, S. and Mains, P. E. (1994) 'mei-1, a gene required for meiotic spindle formation in *Caenorhabditis elegans*, is a member of a family of ATPases', *Genetics* 136(2): 533-46.
- Dammermann, A., Muller-Reichert, T., Pelletier, L., Habermann, B., Desai, A. and Oegema, K. (2004) 'Centriole assembly requires both centriolar and pericentriolar material proteins', *Dev Cell* 7(6): 815-29.
- Davis, E. S., Wille, L., Chestnut, B. A., Sadler, P. L., Shakes, D. C. and Golden, A. (2002) 'Multiple subunits of the *Caenorhabditis elegans* anaphase-promoting complex are required for chromosome segregation during meiosis I', *Genetics* 160(2): 805-13.
- de Carvalho, C. E., Zaaier, S., Smolikov, S., Gu, Y., Schumacher, J. M. and Colaiacovo, M. P. (2008) 'LAB-1 antagonizes the Aurora B kinase in *C. elegans*', *Genes Dev* 22(20): 2869-85.
- Delattre, M., Leidel, S., Wani, K., Baumer, K., Bamat, J., Schnabel, H., Feichtinger, R., Schnabel, R. and Gonczy, P. (2004) 'Centriolar SAS-5 is required for centrosome duplication in *C. elegans*', *Nat Cell Biol* 6(7): 656-64.
- Doxsey, S., McCollum, D. and Theurkauf, W. (2005) 'Centrosomes in cellular regulation', *Annu Rev Cell Dev Biol* 21: 411-34.
- Drechsel, D. N. and Kirschner, M. W. (1994) 'The minimum GTP cap required to stabilize microtubules', *Curr Biol* 4(12): 1053-61.
- Ellefson, M. L. and McNally, F. J. (2009) 'Kinesin-1 and cytoplasmic dynein act sequentially to move the meiotic spindle to the oocyte cortex in *Caenorhabditis elegans*', *Mol Biol Cell* 20(11): 2722-30.

- Ellefson, M. L. and McNally, F. J. (2011) 'CDK-1 inhibits meiotic spindle shortening and dynein-dependent spindle rotation in *C. elegans*', *J Cell Biol* 193(7): 1229-44.
- Frokjaer-Jensen, C., Davis, M. W., Hopkins, C. E., Newman, B. J., Thummel, J. M., Olesen, S. P., Grunnet, M. and Jorgensen, E. M. (2008) 'Single-copy insertion of transgenes in *Caenorhabditis elegans*', *Nat Genet* 40(11): 1375-83.
- Furukawa, M., He, Y. J., Borchers, C. and Xiong, Y. (2003) 'Targeting of protein ubiquitination by BTB-Cullin 3-Roc1 ubiquitin ligases', *Nat Cell Biol* 5(11): 1001-7.
- Furuta, T., Baillie, D. L. and Schumacher, J. M. (2002) '*Caenorhabditis elegans* Aurora A kinase AIR-1 is required for postembryonic cell divisions and germline development', *Genesis* 34(4): 244-50.
- Glover, D. M., Leibowitz, M. H., McLean, D. A. and Parry, H. (1995) 'Mutations in aurora prevent centrosome separation leading to the formation of monopolar spindles', *Cell* 81(1): 95-105.
- Golden, A., Sadler, P. L., Wallenfang, M. R., Schumacher, J. M., Hamill, D. R., Bates, G., Bowerman, B., Seydoux, G. and Shakes, D. C. (2000) 'Metaphase to anaphase (mat) transition-defective mutants in *Caenorhabditis elegans*', *J Cell Biol* 151(7): 1469-82.
- Gopalan, G., Chan, C. S. and Donovan, P. J. (1997) 'A novel mammalian, mitotic spindle-associated kinase is related to yeast and fly chromosome segregation regulators', *J Cell Biol* 138(3): 643-56.
- Govindan, J. A., Nadarajan, S., Kim, S., Starich, T. A. and Greenstein, D. (2009) 'Somatic cAMP signaling regulates MSP-dependent oocyte growth and meiotic maturation in *C. elegans*', *Development* 136(13): 2211-21.
- Guse, A., Mishima, M. and Glotzer, M. (2005) 'Phosphorylation of ZEN-4/MKLP1 by aurora B regulates completion of cytokinesis', *Curr Biol* 15(8): 778-86.
- Hannak, E., Kirkham, M., Hyman, A. A. and Oegema, K. (2001) 'Aurora-A kinase is required for centrosome maturation in *Caenorhabditis elegans*', *J Cell Biol* 155(7): 1109-16.
- Hannak, E., Oegema, K., Kirkham, M., Gonczy, P., Habermann, B. and Hyman, A. A. (2002) 'The kinetically dominant assembly pathway for

- centrosomal asters in *Caenorhabditis elegans* is gamma-tubulin dependent', *J Cell Biol* 157(4): 591-602.
- Harris, J. E., Govindan, J. A., Yamamoto, I., Schwartz, J., Kaverina, I. and Greenstein, D. (2006) 'Major sperm protein signaling promotes oocyte microtubule reorganization prior to fertilization in *Caenorhabditis elegans*', *Dev Biol* 299(1): 105-21.
- Hassold, T. and Hunt, P. (2001) 'To err (meiotically) is human: the genesis of human aneuploidy', *Nat Rev Genet* 2(4): 280-91.
- Hill, D. P., Shakes, D. C., Ward, S. and Strome, S. (1989) 'A sperm-supplied product essential for initiation of normal embryogenesis in *Caenorhabditis elegans* is encoded by the paternal-effect embryonic-lethal gene, *spe-11*', *Dev Biol* 136(1): 154-66.
- Hornig, N. C. and Uhlmann, F. (2004) 'Preferential cleavage of chromatin-bound cohesin after targeted phosphorylation by Polo-like kinase', *EMBO J* 23(15): 3144-53.
- Horvitz, H. R., Brenner, S., Hodgkin, J. and Herman, R. K. (1979) 'A uniform genetic nomenclature for the nematode *Caenorhabditis elegans*', *Mol Gen Genet* 175(2): 129-33.
- Howe, M., McDonald, K. L., Albertson, D. G. and Meyer, B. J. (2001) 'HIM-10 is required for kinetochore structure and function on *Caenorhabditis elegans* holocentric chromosomes', *J Cell Biol* 153(6): 1227-38.
- Hyman, A. A., Salser, S., Drechsel, D. N., Unwin, N. and Mitchison, T. J. (1992) 'Role of GTP hydrolysis in microtubule dynamics: information from a slowly hydrolyzable analogue, GMPCPP', *Mol Biol Cell* 3(10): 1155-67.
- Johnston, W. L., Krizus, A. and Dennis, J. W. (2006) 'The eggshell is required for meiotic fidelity, polar-body extrusion and polarization of the *C. elegans* embryo', *BMC Biol* 4: 35.
- Kaitna, S., Mendoza, M., Jantsch-Plunger, V. and Glotzer, M. (2000) 'Incep and an aurora-like kinase form a complex essential for chromosome segregation and efficient completion of cytokinesis', *Curr Biol* 10(19): 1172-81.
- Kalab, P. and Heald, R. (2008) 'The RanGTP gradient - a GPS for the mitotic spindle', *J Cell Sci* 121(Pt 10): 1577-86.

- Kamath, R. S. and Ahringer, J. (2003) 'Genome-wide RNAi screening in *Caenorhabditis elegans*', *Methods* 30(4): 313-21.
- Kemp, C. A., Kopish, K. R., Zipperlen, P., Ahringer, J. and O'Connell, K. F. (2004) 'Centrosome maturation and duplication in *C. elegans* require the coiled-coil protein SPD-2', *Dev Cell* 6(4): 511-23.
- Kim, D. Y. and Roy, R. (2006) 'Cell cycle regulators control centrosome elimination during oogenesis in *Caenorhabditis elegans*', *J Cell Biol* 174(6): 751-7.
- Kimble, J. E. and White, J. G. (1981) 'On the control of germ cell development in *Caenorhabditis elegans*', *Dev Biol* 81(2): 208-19.
- Kirschner, M. W. and Mitchison, T. (1986) 'Microtubule dynamics', *Nature* 324(6098): 621.
- Kishimoto, T. (1998) 'Cell cycle arrest and release in starfish oocytes and eggs', *Semin Cell Dev Biol* 9(5): 549-57.
- Kops, G. J., Weaver, B. A. and Cleveland, D. W. (2005) 'On the road to cancer: aneuploidy and the mitotic checkpoint', *Nat Rev Cancer* 5(10): 773-85.
- Lee, M. H., Ohmachi, M., Arur, S., Nayak, S., Francis, R., Church, D., Lambie, E. and Schedl, T. (2007) 'Multiple functions and dynamic activation of MPK-1 extracellular signal-regulated kinase signaling in *Caenorhabditis elegans* germline development', *Genetics* 177(4): 2039-62.
- Leggett, D. S., Jones, D. and Candido, E. P. (1995) '*Caenorhabditis elegans* UBC-1, a ubiquitin-conjugating enzyme homologous to yeast RAD6/UBC2, contains a novel carboxy-terminal extension that is conserved in nematodes', *DNA Cell Biol* 14(10): 883-91.
- Leidel, S., Delattre, M., Cerutti, L., Baumer, K. and Gonczy, P. (2005) 'SAS-6 defines a protein family required for centrosome duplication in *C. elegans* and in human cells', *Nat Cell Biol* 7(2): 115-25.
- Leidel, S. and Gonczy, P. (2003) 'SAS-4 is essential for centrosome duplication in *C. elegans* and is recruited to daughter centrioles once per cell cycle', *Dev Cell* 4(3): 431-9.
- Liu, J., Vasudevan, S. and Kipreos, E. T. (2004) 'CUL-2 and ZYG-11 promote meiotic anaphase II and the proper placement of the anterior-posterior axis in *C. elegans*', *Development* 131(15): 3513-25.

- Luders, J. and Stearns, T. (2007) 'Microtubule-organizing centres: a re-evaluation', *Nat Rev Mol Cell Biol* 8(2): 161-7.
- Maduro, M. and Pilgrim, D. (1995) 'Identification and cloning of unc-119, a gene expressed in the *Caenorhabditis elegans* nervous system', *Genetics* 141(3): 977-88.
- Manneville, J. B. and Etienne-Manneville, S. (2006) 'Positioning centrosomes and spindle poles: looking at the periphery to find the centre', *Biol Cell* 98(9): 557-65.
- Maruyama, R., Velarde, N. V., Klancer, R., Gordon, S., Kadandale, P., Parry, J. M., Hang, J. S., Rubin, J., Stewart-Michaelis, A., Schweinsberg, P. et al. (2007) 'EGG-3 regulates cell-surface and cortex rearrangements during egg activation in *Caenorhabditis elegans*', *Curr Biol* 17(18): 1555-60.
- McCarter, J., Bartlett, B., Dang, T. and Schedl, T. (1999) 'On the control of oocyte meiotic maturation and ovulation in *Caenorhabditis elegans*', *Dev Biol* 205(1): 111-28.
- McNally, F. J. and Vale, R. D. (1993) 'Identification of katanin, an ATPase that severs and disassembles stable microtubules', *Cell* 75(3): 419-29.
- McNally, K., Audhya, A., Oegema, K. and McNally, F. J. (2006) 'Katanin controls mitotic and meiotic spindle length', *J Cell Biol* 175(6): 881-91.
- McNally, K. L., Martin, J. L., Ellefson, M. and McNally, F. J. (2010) 'Kinesin-dependent transport results in polarized migration of the nucleus in oocytes and inward movement of yolk granules in meiotic embryos', *Dev Biol* 339(1): 126-40.
- McNally, K. L. and McNally, F. J. (2005) 'Fertilization initiates the transition from anaphase I to metaphase II during female meiosis in *C. elegans*', *Dev Biol* 282(1): 218-30.
- Mello, C. and Fire, A. (1995) 'DNA transformation', *Methods Cell Biol* 48: 451-82.
- Mello, C. C., Kramer, J. M., Stinchcomb, D. and Ambros, V. (1991) 'Efficient gene transfer in *C. elegans*: extrachromosomal maintenance and integration of transforming sequences', *EMBO J* 10(12): 3959-70.
- Michaelis, C., Ciosk, R. and Nasmyth, K. (1997) 'Cohesins: chromosomal proteins that prevent premature separation of sister chromatids', *Cell* 91(1): 35-45.

- Mikeladze-Dvali, T., von Tobel, L., Strnad, P., Knott, G., Leonhardt, H., Schermelleh, L. and Gonczy, P. (2012) 'Analysis of centriole elimination during *C. elegans* oogenesis', *Development* 139(9): 1670-9.
- Miller, M. A., Nguyen, V. Q., Lee, M. H., Kosinski, M., Schedl, T., Caprioli, R. M. and Greenstein, D. (2001) 'A sperm cytoskeletal protein that signals oocyte meiotic maturation and ovulation', *Science* 291(5511): 2144-7.
- Mitchison, T. and Kirschner, M. (1984) 'Dynamic instability of microtubule growth', *Nature* 312(5991): 237-42.
- Mitenko, N. L., Eisner, J. R., Swiston, J. R. and Mains, P. E. (1997) 'A limited number of *Caenorhabditis elegans* genes are readily mutable to dominant, temperature-sensitive maternal-effect embryonic lethality', *Genetics* 147(4): 1665-74.
- Mito, Y., Sugimoto, A. and Yamamoto, M. (2003) 'Distinct developmental function of two *Caenorhabditis elegans* homologs of the cohesin subunit Scc1/Rad21', *Mol Biol Cell* 14(6): 2399-409.
- Nasmyth, K. and Haering, C. H. (2005) 'The structure and function of SMC and kleisin complexes', *Annu Rev Biochem* 74: 595-648.
- Nixon, V. L., Levasseur, M., McDougall, A. and Jones, K. T. (2002) 'Ca²⁺ oscillations promote APC/C-dependent cyclin B1 degradation during metaphase arrest and completion of meiosis in fertilizing mouse eggs', *Curr Biol* 12(9): 746-50.
- O'Connell, K. F. (2000) 'The centrosome of the early *C. elegans* embryo: inheritance, assembly, replication, and developmental roles', *Curr Top Dev Biol* 49: 365-84.
- O'Connell, K. F., Caron, C., Kopish, K. R., Hurd, D. D., Kempfues, K. J., Li, Y. and White, J. G. (2001) 'The *C. elegans* zyg-1 gene encodes a regulator of centrosome duplication with distinct maternal and paternal roles in the embryo', *Cell* 105(4): 547-58.
- O'Toole, E., Greenan, G., Lange, K. I., Srayko, M. and Muller-Reichert, T. (2012) 'The role of gamma-tubulin in centrosomal microtubule organization', *PLoS One* 7(1): e29795.
- Ozlu, N., Srayko, M., Kinoshita, K., Habermann, B., O'Toole E, T., Muller-Reichert, T., Schmalz, N., Desai, A. and Hyman, A. A. (2005) 'An

- essential function of the *C. elegans* ortholog of TPX2 is to localize activated aurora A kinase to mitotic spindles', *Dev Cell* 9(2): 237-48.
- Pahara, D. C. (2010) 'Mapping and characterization of mel-43(sb41), a gene required for early embryonic viability in *C. elegans*', *MS.c thesis*.
- Parry, J. M., Velarde, N. V., Lefkovith, A. J., Zegarek, M. H., Hang, J. S., Ohm, J., Klancer, R., Maruyama, R., Druzhinina, M. K., Grant, B. D. et al. (2009) 'EGG-4 and EGG-5 Link Events of the Oocyte-to-Embryo Transition with Meiotic Progression in *C. elegans*', *Curr Biol* 19(20): 1752-7.
- Pasierbek, P., Jantsch, M., Melcher, M., Schleiffer, A., Schweizer, D. and Loidl, J. (2001) 'A *Caenorhabditis elegans* cohesion protein with functions in meiotic chromosome pairing and disjunction', *Genes Dev* 15(11): 1349-60.
- Pelletier, L., Ozlu, N., Hannak, E., Cowan, C., Habermann, B., Ruer, M., Muller-Reichert, T. and Hyman, A. A. (2004) 'The *Caenorhabditis elegans* centrosomal protein SPD-2 is required for both pericentriolar material recruitment and centriole duplication', *Curr Biol* 14(10): 863-73.
- Pickart, C. M. (2001) 'Mechanisms underlying ubiquitination', *Annu Rev Biochem* 70: 503-33.
- Piel, M., Nordberg, J., Euteneuer, U. and Bornens, M. (2001) 'Centrosome-dependent exit of cytokinesis in animal cells', *Science* 291(5508): 1550-3.
- Pintard, L., Kurz, T., Glaser, S., Willis, J. H., Peter, M. and Bowerman, B. (2003a) 'Neddylolation and deneddylation of CUL-3 is required to target MEL-1/Katanin for degradation at the meiosis-to-mitosis transition in *C. elegans*', *Curr Biol* 13(11): 911-21.
- Pintard, L., Willis, J. H., Willems, A., Johnson, J. L., Srayko, M., Kurz, T., Glaser, S., Mains, P. E., Tyers, M., Bowerman, B. et al. (2003b) 'The BTB protein MEL-26 is a substrate-specific adaptor of the CUL-3 ubiquitin-ligase', *Nature* 425(6955): 311-6.
- Portier, N., Audhya, A., Maddox, P. S., Green, R. A., Dammermann, A., Desai, A. and Oegema, K. (2007) 'A microtubule-independent role for centrosomes and aurora a in nuclear envelope breakdown', *Dev Cell* 12(4): 515-29.

- Praitis, V., Casey, E., Collar, D. and Austin, J. (2001) 'Creation of low-copy integrated transgenic lines in *Caenorhabditis elegans*', *Genetics* 157(3): 1217-26.
- Rogers, E., Bishop, J. D., Waddle, J. A., Schumacher, J. M. and Lin, R. (2002) 'The aurora kinase AIR-2 functions in the release of chromosome cohesion in *Caenorhabditis elegans* meiosis', *J Cell Biol* 157(2): 219-29.
- Ruchaud, S., Carmena, M. and Earnshaw, W. C. (2007) 'Chromosomal passengers: conducting cell division', *Nat Rev Mol Cell Biol* 8(10): 798-812.
- Schlaitz, A. L., Srayko, M., Dammermann, A., Quintin, S., Wielsch, N., MacLeod, I., de Robillard, Q., Zinke, A., Yates, J. R., 3rd, Muller-Reichert, T. et al. (2007) 'The *C. elegans* RSA complex localizes protein phosphatase 2A to centrosomes and regulates mitotic spindle assembly', *Cell* 128(1): 115-27.
- Schumacher, J. M., Ashcroft, N., Donovan, P. J. and Golden, A. (1998a) 'A highly conserved centrosomal kinase, AIR-1, is required for accurate cell cycle progression and segregation of developmental factors in *Caenorhabditis elegans* embryos', *Development* 125(22): 4391-402.
- Schumacher, J. M., Golden, A. and Donovan, P. J. (1998b) 'AIR-2: An Aurora/Ipl1-related protein kinase associated with chromosomes and midbody microtubules is required for polar body extrusion and cytokinesis in *Caenorhabditis elegans* embryos', *J Cell Biol* 143(6): 1635-46.
- Severson, A. F., Hamill, D. R., Carter, J. C., Schumacher, J. and Bowerman, B. (2000) 'The aurora-related kinase AIR-2 recruits ZEN-4/CeMKLP1 to the mitotic spindle at metaphase and is required for cytokinesis', *Curr Biol* 10(19): 1162-71.
- Severson, A. F., Ling, L., van Zuylen, V. and Meyer, B. J. (2009) 'The axial element protein HTP-3 promotes cohesin loading and meiotic axis assembly in *C. elegans* to implement the meiotic program of chromosome segregation', *Genes Dev* 23(15): 1763-78.
- Shakes, D. C. (2003) 'Developmental defects observed in hypomorphic anaphase-promoting complex mutants are linked to cell cycle abnormalities', *Development* 130(8): 1605-1620.

- Sonneville, R. and Gonczy, P. (2004) 'Zyg-11 and cul-2 regulate progression through meiosis II and polarity establishment in *C. elegans*', *Development* 131(15): 3527-43.
- Srayko, M., Buster, D. W., Bazirgan, O. A., McNally, F. J. and Mains, P. E. (2000) 'MEI-1/MEI-2 katanin-like microtubule severing activity is required for *Caenorhabditis elegans* meiosis', *Genes Dev* 14(9): 1072-84.
- Srayko, M., Kaya, A., Stamford, J. and Hyman, A. A. (2005) 'Identification and characterization of factors required for microtubule growth and nucleation in the early *C. elegans* embryo', *Dev Cell* 9(2): 223-36.
- Srayko, M., O'Toole E, T., Hyman, A. A. and Muller-Reichert, T. (2006) 'Katanin disrupts the microtubule lattice and increases polymer number in *C. elegans* meiosis', *Curr Biol* 16(19): 1944-9.
- Srayko, M., Quintin, S., Schwager, A. and Hyman, A. A. (2003) '*Caenorhabditis elegans* TAC-1 and ZYG-9 form a complex that is essential for long astral and spindle microtubules', *Curr Biol* 13(17): 1506-11.
- Stein, K. K., Davis, E. S., Hays, T. and Golden, A. (2007) 'Components of the spindle assembly checkpoint regulate the anaphase-promoting complex during meiosis in *Caenorhabditis elegans*', *Genetics* 175(1): 107-23.
- Strome, S., Powers, J., Dunn, M., Reese, K., Malone, C. J., White, J., Seydoux, G. and Saxton, W. (2001) 'Spindle dynamics and the role of gamma-tubulin in early *Caenorhabditis elegans* embryos', *Mol Biol Cell* 12(6): 1751-64.
- Sumara, I., Vorlaufer, E., Stukenberg, P. T., Kelm, O., Redemann, N., Nigg, E. A. and Peters, J. M. (2002) 'The dissociation of cohesin from chromosomes in prophase is regulated by Polo-like kinase', *Mol Cell* 9(3): 515-25.
- Timmons, L., Court, D. L. and Fire, A. (2001) 'Ingestion of bacterially expressed dsRNAs can produce specific and potent genetic interference in *Caenorhabditis elegans*', *Gene* 263(1-2): 103-12.
- Timmons, L. and Fire, A. (1998) 'Specific interference by ingested dsRNA', *Nature* 395(6705): 854.

- Tunquist, B. J. and Maller, J. L. (2003) 'Under arrest: cytosstatic factor (CSF)-mediated metaphase arrest in vertebrate eggs', *Genes Dev* 17(6): 683-710.
- Uhlmann, F., Lottspeich, F. and Nasmyth, K. (1999) 'Sister-chromatid separation at anaphase onset is promoted by cleavage of the cohesin subunit Scc1', *Nature* 400(6739): 37-42.
- Vale, R. D. (1991) 'Severing of stable microtubules by a mitotically activated protein in *Xenopus* egg extracts', *Cell* 64(4): 827-39.
- van der Voet, M., Berends, C. W., Perreault, A., Nguyen-Ngoc, T., Gonczy, P., Vidal, M., Boxem, M. and van den Heuvel, S. (2009) 'NuMA-related LIN-5, ASPM-1, calmodulin and dynein promote meiotic spindle rotation independently of cortical LIN-5/GPR/Galpha', *Nat Cell Biol* 11(3): 269-77.
- Vasudevan, S., Starostina, N. G. and Kipreos, E. T. (2007) 'The *Caenorhabditis elegans* cell-cycle regulator ZYG-11 defines a conserved family of CUL-2 complex components', *EMBO Rep* 8(3): 279-86.
- Watanabe, Y. and Nurse, P. (1999) 'Cohesin Rec8 is required for reductional chromosome segregation at meiosis', *Nature* 400(6743): 461-4.
- Yang, H. Y., Mains, P. E. and McNally, F. J. (2005) 'Kinesin-1 mediates translocation of the meiotic spindle to the oocyte cortex through KCA-1, a novel cargo adapter', *J Cell Biol* 169(3): 447-57.
- Yang, H. Y., McNally, K. and McNally, F. J. (2003) 'MEI-1/katanin is required for translocation of the meiosis I spindle to the oocyte cortex in *C. elegans*', *Dev Biol* 260(1): 245-59.
- Zeiser, E., Frokjaer-Jensen, C., Jorgensen, E. and Ahringer, J. (2011) 'MosSCI and gateway compatible plasmid toolkit for constitutive and inducible expression of transgenes in the *C. elegans* germline', *PLoS One* 6(5): e20082.
- Zhou, K., Rolls, M. M., Hall, D. H., Malone, C. J. and Hanna-Rose, W. (2009) 'A ZYG-12-dynein interaction at the nuclear envelope defines cytoskeletal architecture in the *C. elegans* gonad', *J Cell Biol* 186(2): 229-41.